OPTIMIZATION OF INTERNAL TAGGING OF INHIBITORY G-PROTEINS FOR INVESTIGATING THEIR INTERACTIONS WITH DOPAMINE RECEPTOR D2 VIA FRET METHOD

A THESIS SUBMITTED TO
THE GRADUATE SCHOOL OF NATURAL AND APPLIED SCIENCES
OF
MIDDLE EAST TECHNICAL UNIVERSITY

BY

GİZEM ÖZCAN

IN PARTIAL FULFILLMENT OF THE REQUIREMENTS
FOR
THE DEGREE OF MASTER OF SCIENCE
IN
BIOCHEMISTRY

DECEMBER 2016

Approval of the thesis:

OPTIMIZATION OF INTERNAL TAGGING OF INHIBITORY G-PROTEINS FOR INVESTIGATING THEIR INTERACTIONS WITH DOPAMINE RECEPTOR D2 VIA FRET METHOD

submitted by **GİZEM ÖZCAN** in partial fulfillment of the requirements for the degree of **Master of Science in Biochemistry Department, Middle East Technical University** by,

Prof. Dr.Gülbin Dural Ünver
Dean, Graduate School of **Natural and Applied Sciences** __________________

Assoc. Prof. Dr. Bülent İçgen
Head of Department, **Biochemistry** __________________

Assoc. Prof. Dr. Çağdaş Devrim Son
Supervisor, **Biology Dept., METU** __________________

Assist. Prof. Dr. Salih Özçubukçu
Co-Supervisor, **Chemistry Dept., METU** __________________

Examining Committee Members:

Prof. Dr. Ufuk Gündüz __________________
Biology Dept., METU

Assoc. Prof. Dr. Çağdaş Devrim Son __________________
Biology Dept., METU

Assoc. Prof. Dr. Can Özen __________________
Biotechnology Dept., METU

Assoc. Prof. Dr. Tülin Yanık __________________
Biology Dept., METU

Prof. Dr. İhsan Gürsel __________________
Molecular Biology and Genetics Dept., Bilkent University

Date: 06.12.2016

I hereby declare that all information in this document has been obtained and presented in accordance with academic rules and ethical conduct. I also declare that, as required by these rules and conduct, I have fully cited and referenced all material and results that are not original to this work.

Name, Last name: Gizem Özcan

Signature :

ABSTRACT

OPTIMIZATION OF INTERNAL TAGGING OF INHIBITORY G-PROTEINS FOR INVESTIGATING THEIR INTERACTIONS WITH DOPAMINE RECEPTOR D2 VIA FRET METHOD

Özcan, Gizem
M.S., Department of Biochemistry
Supervisor: Assoc. Prof. Dr. Çağdaş Devrim Son
Co-supervisor: Assist. Prof. Dr. Salih Özçubukçu

December 2016, 103 pages

G-Protein Coupled Receptors (GPCRs) constitute a large family of receptors which act by sensing the molecules outside the cell and start a signal transduction inside the cell through interacting with their associated G-proteins. This interaction results in activation or repression of related signaling pathways via associated secondary messengers. Dopamine receptor D2 (D2R) is a member of D2-like Dopamine Receptor group, which also belongs to the GPCR family. It is known that D2R has critical roles in emotion and behavior related pathways.

G-proteins take their name from their ability to bind to guanine nucleotide. They are key molecules for activation or deactivation for their related signaling pathways. D2R acts through inhibitory G-proteins which in turn reduces adenylyl cyclase activity. Deregulation of the dopaminergic signaling is shown to be related to many neurologic diseases including schizophrenia and Parkinson's disease.

Förster resonance energy transfer (FRET) technique is used for investigating distances between molecules. Energy transfer between two molecules is possible only when they are very close to each other, making it possible to conclude that these molecules are actually interacting when this transfer occurs.

The purpose of the present study was to optimize labeling of inhibitory G-protein α subunits GNAO1 (Go1) and GNAI3 (Gi3) with fluorophores for the first time in the literature to be able to investigate their interactions with D2R *via* FRET method. To achieve this, D2R was labeled with Enhanced Green Fluorescent Protein (EGFP) from its C-terminus and G proteins were labeled with mCherry from three different internal locations. Co-transfections of all of the labeled proteins to *Mus musculus* Neuroblastoma-2a (N2a) cells were done and interactions were investigated *via* spinning disc confocal microscopy. Selected constructs were expressed in embyronic kidney (HEK293) cells to compare different cellular environment's effects on their interaction. Results presented in this study are highlighting a possible starting point to investigate these subunits' interactions with their receptors and other downstream molecules *via* FRET which adds a value to the GPCR targeted study grounds.

Keywords: Förster Resonance Energy Transfer (FRET), Dopamine D2R, G-Protein Coupled Receptors, G-Protein, GNAO1, GNAI3

ÖZ

İNHİBİTÖR G PROTEİNLERİNİN DOPAMİN RESEPTRÖRÜ D2 İLE ETKİLEŞİMİNİN FRET METODUYLA İNCELENMESİ İÇİN İNTERNAL İŞARETLENMELERİNİN OPTİMİZASYONU

Özcan, Gizem
Yüksek Lisans, Biyokimya Bölümü
Tez Yöneticisi: Doç. Dr. Çağdaş Devrim Son
Ortak Tez Yöneticisi: Yrd. Doç. Dr. Salih Özçubukçu

Aralık 2016, 103 sayfa

G-Protein Kenetli Reseptörler (GPKR) hücre dışında algıladıkları moleküllerle aktif hale gelerek kendilerine bağlanan G-proteinler aracılığıyla hücre içerisinde sinyal yolaklarını başlatan geniş bir reseptör ailesidir. Bu aktivasyon etkilediği ikincil moleküller ile GKPR'nin bağlı olduğu sinyal yolağının indüklenmesi ya da deaktivasyonuyla sonuçlanır. Dopamin reseptörü D2 (D2R), GKPR ailesine dahil olan D2-benzeri dopamin reseptörleri grubunun bir üyesidir. D2R'nin duygu ve davranış bağlantılı yolaklarında kritik rollere sahip olduğu bilinmektedir. G-proteinler adlarını Guanin nükleotidine bağlanabilmelerinden almışlardır. G-proteinler bağlı oldukları sinyal yolaklarının aktivasyon ve/veya deaktivasyonunda anahtar roller üstlenirler. D2R, inhibitör G-proteinlerle etkileşime girerek adenilil siklaz aktivitesini düşürür. Dopaminerjik sistemdeki aksamalar şizofreni ve Parkinson hastalığı da dahil olmak üzere birçok nörolojik hastalıkta rol almaktadır.

Förster rezonans enerji transferi (FRET) yöntemi canlı hücrelerde moleküller arası uzaklığı hassas bir şekilde incelemek amacıyla kullanılmaktadır. Yöntemdeki enerji transferi çok düşük uzaklıklarda gerçekleştiğinden bu transfer gerçekleştiğinde söz konusu moleküllerim etkileştiği yorumu yapılabilmektedir.

Sunulan çalışmanın amacı inhibitör G proteinlerin α birimleri olan GNAO1 (Go1) ve GNAI3 (Gi3) moleküllerinin florofor moleküllerle literatürde ilk defa işaretlenmesi ve D2R ile olan ilişkilerinin FRET yöntemiyle incelenebilmesi için kullanılan metodların optimizasyonudur. Bunun için, D2R "enhanced green fluroescent protein" (EGFP) ile karboksi ucundan, G-proteinler ise mCherry ile üç farklı internal lokasyondan işaretlenmiştir. İşaretli proteinlerin ko-transfeksiyonları *Mus musculus* Neuroblastoma-2a (N2a) hücrelerinde yapılmış ve etkileşimleri konfokal floresan mikroskopla incelenmiştir. Hazırlanan proteinlerin bir kısmı değişen hücresel ortamların etkileşim üzerindeki etkilerini görmek üzere İnsan Embriyonik Böbrek (HEK293) hücrelerine transfekte edilmiştir. Bu çalışmada elde edilen sonuçlar bu altbirimlerin reseptörleri ve diğer moleküllerle olan ilişkilerinin FRET ile incelenmesi için bir başlangıç noktası sunmakta ve GPCR odaklı çalışmalara yeni bir değer katmaktadır.

Anahtar Kelimeler: Förster Rezonans Enerji Transfer (FRET), Dopamin D2R, G-Protein Kenetli Reseptörler, G-Protein, GNAI3, GNAO1

Micro- for the mind
Macro- for the spirit
Moto- for the heart

To the *micro-scope* of life

ACKNOWLEDGEMENTS

I would like to thank my advisor, Assoc. Prof. Dr. Çağdaş Devrim Son for his endless financial, academic, and personal support -without his excellent personality and mentorship, I would never be able to learn this much about molecular biology and biochemistry, as this thesis would never be complete without him; my co-supervisor Assist. Prof. Dr. Salih Özçubukçu for his supports for this interdisciplinary project; my mother Ayşe Ataoğlu not only for her support in my academic life and master of science studies but also for her endless friendship, guidance in my life and unlimited understanding; my father Nazif Özcan for being such an amazing father and for bringing me a definitely unique point of view for my life; my lab mates Cansu Bayraktaroğlu, Hüseyin Evci, Gökberk Kaya, Özge Atay, Dihar Koçak, and Orkun Cevheroğlu for their support and help; Hasan Hüseyin Kazan and everyone I know in the department for their friendship and technical support. TÜBİTAK was supporting the project 113Z639; and I am quite thankful by heart to my thesis examining committee for spending their time and attention to examine this thesis and make suggestions on it. My riding friends in parallel with METU Riders, Ceren Gülcan, Coşkun Çifci, Engin Kurgan, Kürşat Çoban, Murat Erkoşan, Musab Çağrı Uğurlu, Sinan Özgün Demir, Tansel Fıratlı, and Tayfun Efe Ertop were amazing supporters and motivators during my studies. I would also thank my housemate Gözde Eşan for her guidance, sincere support for this thesis and being a heartwarming person in all ways; Doğem Çelik, Suna Onay, and Ekin Şanlı just for being who they are; and finally to Derhan Asega Nassur Ahmad for being an ubervisor beyond boundaries for this thesis and downshifting my heart's gearbox to bring me an instant and huge motivation.

TABLE OF CONTENTS

ABSTRACT v

ÖZ vii

ACKNOWLEDGEMENTS x

TABLE OF CONTENTS xi

LIST OF TABLES xv

LIST OF FIGURES xvi

CHAPTERS

1. INTRODUCTION 1

  1.1. G-Protein Coupled Receptors 1

    1.1.1. Dopamine Signaling and Dopamine D2 Receptor 3

  1.2. G – Proteins 6

    1.2.1. Inhibitory G-Proteins and Subtypes G_{o1} and G_{i3} 9

  1.3. Methods for Detection of Interactions of GPCRs and G-Proteins 10

  1.3.1. Förster Resonance Energy Transfer 12

  1.4. Aim of the Study 15

2. MATERIALS AND METHODS 17

  2.1. Materials 17

    2.1.1. Mammalian Cell Line and Maintenance 17

      2.1.1.1. Neuro 2a Cells 17

      2.1.1.2. HEK293 Cells 18

    2.1.2. Bacterial Cell Culture 19

    2.1.3. Plasmids, Primers, and Sequencing 19

2.1.4. Other Chemicals and Materials 20

2.2. Methods 21

2.2.1. G-Protein Plasmid Screening, Primer Designs, Insertion and Cloning 21

2.2.1.1. G-Protein Plasmid Screening 21

2.2.1.2. Primer Design for Cloning the Products 22

2.2.1.3. Primer Design for Insertion of Fluorophores 22

2.2.1.4. PCR Amplifications 25

2.2.1.5. Agarose Gel Electrophoresis 26

2.2.1.6. Agarose Gel DNA Isolation 26

2.2.1.7. PCR Integration Method 26

2.2.1.8. PCR Purification 28

2.2.1.9. Restriction Enzyme Digestion 28

2.2.1.10. DNA Concentration Determination 28

2.2.1.11. Ligation 29

2.2.1.12. Preparation of Competent Cells 29

2.2.1.13. Transformation of Competent Cells 30

2.2.1.14. Plasmid Isolation 30

2.2.2. Mammalian Cell Maintenance, Transfection and Imaging 30

2.2.2.1. N2a Cell Maintenance 30

2.2.2.2. Hek293 Cell Maintenance 31

2.2.2.3. Transfection of Cells 32

2.2.2.4 Imaging with Confocal Microscope 33

2.2.2.5. Image Analysis with PixFRET 34

2.2.3. Functionality Tests of D2R with Constructed G-Proteins 35

2.2.3.1. cAMP-Glo™ Assay 35

3. RESULTS AND DISCUSSION 39

3.1. Cloning and Labeling Studies 39

    - 3.1.1. Cloning GNAO1 and GNAI3 cDNAs to Mammalian Expression Vector pcDNA3.1(-) 39
    - 3.1.2. Tagging GNAO1 gene with mCherry from A122, R113, and E94 via PCR Integration Method 41
    - 3.1.3. Tagging GNAI3 gene with mCherry from E122, L91, and G60 via PCR Integration Method 43
    - 3.1.4. Tagging D2 Receptor gene with EGFP from Carboxyl-Terminus via PCR Integration Method 45
  - 3.2. Imaging Studies 47
    - 3.2.1. GNAO1 Constructs in N2a Cells 48
      - 3.2.1.1. Validations of Signals for Single Transfections 48
      - 3.2.1.2. Co-localization and FRET studies of GNAO1 Constructs with D2R EGFP in N2a Cells 49
    - 3.2.2. GNAI3 Constructs in N2a Cells 53
      - 3.2.2.1. Validations of Signals for Single Transfections 53
      - 3.2.2.2. Double Transfection and FRET studies of GNAI3 Constructs with D2R EGFP in N2a Cells 54
    - 3.2.3. GNAO1 and GNAI3 Constructs in HEK293 Cells 57
      - 3.2.3.1. Double Transfection and FRET studies of G Protein Constructs with D2R EGFP in HEK293 Cells 57
  - 3.3. Functionality Assays 61
    - 3.3.1. Functionality Assays of 122nd Position Labeling of GNAI3 and GNAO1 with mCherry 61
- 4. CONCLUSION AND FUTURE PERSPECTIVE 63
- REFERENCES 67

APPENDICES

  - A. MEDIUMS, SOLUTIONS and BUFFERS 75
  - B. PLASMIDS AND PRIMERS 79
  - C. pcDNA3.1(-) MCS, GNAO1 and GNAI3 CUT SITES 83

D. SIMILARITY SCORES OF GNAO1 AND GNAI3 GENES 85
E. FILTERS USED IN CONFOCAL MICROSCOPY 87
F. SEQUENCES OF THE PROTEINS AND CONSTRUCTS 89
G. CROSS-TALK and BACKGROUND ELIMINATION 99
H. FURTHER RESULTS OF FUNCTIONALITY ASSAYS 103

LIST OF TABLES

TABLES

Table 1.1 Summary of G-protein alpha parts and their effectors 9

Table 2.1 Template based 3D model Identities 23

Table 2.2 Optimized PCR Protocol for gene amplification 25

Table 2.3 Optimized PCR Conditions for second step of PCR Integration 27

Table A.1 D-MEM high glucose with L-glutamine 75

Table A.2 1X Phosphate Buffered Saline (PBS) Solution 76

Table A.3 Luria Bertani (LB) Medium 76

Table A.4 Composition of TFBI and TFBII 78

Table B.1 Primer Sequences and Descriptions 79

Table C.1 pcDNA3.1(-) MCS and GNAO1-GNAI3 gene cut sites 83

LIST OF FIGURES

FIGURES

Figure 1.1 Representation of structural GPCR classification requirements.............. 2

Figure 1.2 Dopamine and Dopamine Receptor demonstration... 4

Figure 1.3 Demonstration of GPCR and G-protein interactions 6

Figure 1.4 Representation of Gα subtypes and their effectors. 8

Figure 1.5 Fluorescence spectra of EGFP and mCherry 14

Figure 2.1. Demonstration of PCR Integration Method.. 27

Figure 2.2 Spinning disk technology schematically explained 33

Figure 2.3 Demonstration of cAMP-Glo™ Assay working principle 36

Figure 3.1 Agarose gel electrophoresis image of amplified GNAI3 and GNAO1 genes with EcoRI and KpnI cut sites 40

Figure 3.2 Agarose gel electrophoresis images of pcDNA3.1(-) and GNAI3 and GNAO1 genes double digested with EcoRI and KpnI enzymes 41

Figure 3.3 Agarose gel electrophoresis image of double digested pcDNA3.1(-) plasmids carrying GNAO1 genes labeled with mCherry either from 122nd, 94th, or 113th aminoacids.. 42

Figure 3.4 Agarose gel electrophoresis image of double digested pcDNA3.1(-) plasmids carrying GNAI3 genes labeled with mCherry either from 122nd, or 91st and 60th aminoacids. 44

Figure 3.5 Agarose gel electrophoresis image of double digested pcDNA3.1(-) plasmids carrying D2R genes labeled with EGFP from its carboxyl terminus....... 46

Figure 3.6 Confocal fluorescent microscopy images of N2a cells transfected with GNAO1 labeled with mCherry from its 122nd, 113th, and 94th aminoacid............. 48

Figure 3.7 FRET images of N2a cells co-transfected with D2R labeled with EGFP and GNAO1 labeled with mCherry from 122nd aminoacid..................................... 50

Figure 3.8 FRET images of N2a cells co-transfected with D2R labeled with EGFP and GNAO1 labeled with mCherry from 113th aminoacid 51

Figure 3.9 FRET images of N2a cells co-transfected with D2R labeled with EGFP and GNAO1 labeled with mCherry from 94th aminoacid 52

Figure 3.10 FRET images of N2a cells transfected with GNAI3 labeled with mCherry from its 122nd, 91st, and 60th aminoacid 53

Figure 3.11 FRET images of N2a cells co-transfected with D2R labeled with EGFP and GNAI3 labeled with mCherry from its 122nd aminoacid 54

Figure 3.12 FRET images of N2a cells co-transfected with D2R labeled with EGFP and GNAI3 labeled with mCherry from 91st aminoacid.. 55

Figure 3.13 FRET images of N2a cells co-transfected with D2R labeled with EGFP and GNAI3 labeled with mCherry from 60th aminoacid....................................... 56

Figure 3.14 FRET images of HEK293 cells transfected with D2R labeled with EGFP and GNAI3 labeled with mCherry from its 122nd aminoacid 58

Figure 3.15 FRET images of HEK293 cells co-transfected with D2R labeled with EGFP and GNAO1 labeled with mCherry from 113th aminoacid 59

Figure 3.16 FRET images of HEK293 cells co-transfected with D2R labeled with EGFP and GNAO1 labeled with mCherry from 94th aminoacid 60

Figure 3.17 cAMP levels of N2a cells after transfecting or co-transfecting them with GNAI3, D2R, GNAI3 Labeled from 122nd position 62

Figure B.1 pcDNA3.1(-) specifications 79

Figure D.1 Similarity Scores of GNAO1 Gene 85

Figure D.2 Similarity Scores of GNAI3 Gene 85

Figure D.3 Philogenetic Tree Generated for GNAO1 and GNAI3 genes 86

Figure E.1 Excitation and emission ranges of EGFP filter used in Leica DMI4000 B with Andor DSD2 Confocal device 87

Figure E.2 Excitation and emission ranges of mCherry filter used in Leica DMI4000 B with Andor DSD2 Confocal device 88

Figure E.3 Excitation and emission ranges of FRET configuration (EGFP excitation, mCherry emission) used in Leica DMI4000 B with Andor DSD2 Confocal device 88

Figure G.1 A Sample FRET Set-Up for Cross-Talk Elimination 99

Figure H.1 cAMP levels of N2a cells after transfecting or co-transfecting them with GNAI3, GNAO1 and D2R groups 103

Figure H.2 cAMP levels of N2a cells after transfecting or co-transfecting them with GNAO1 and D2R groups 103

CHAPTER 1

INTRODUCTION

1.1 G-Protein Coupled Receptors

In eukaryotes, G-Protein Coupled Receptors (GPCRs) constitute a wide family of cell surface receptors, which sense a vast variety of molecules outside cell (Kobilka, 2013). Cells' interaction with the outside world is mostly covered by GPCRs, which are encoded by more than 800 genes in the human genome (Fredriksson *et al.*, 2003). As GPCRs interact with signals coming from cell's outer space, they also start a variety of signaling pathways via associated secondary messengers depending on the type of the GPCR and pathway they are included (Lin, 2013).

GPCRs consist of seven transmembrane alpha-helices with their amino-end outside the cell and carboxyl end in intracellular matrix (Venkatakrishnan *et al.*, 2013). The loops between these helices vary in their lengths and composition to interact with different ligands; loops at the extracellular matrix and amino terminus interact with ligands whereas parts inside the cell interact with other proteins via alterations in their conformation to start signaling (Figure 1.1) (Trzaskowski *et al.*, 2012).

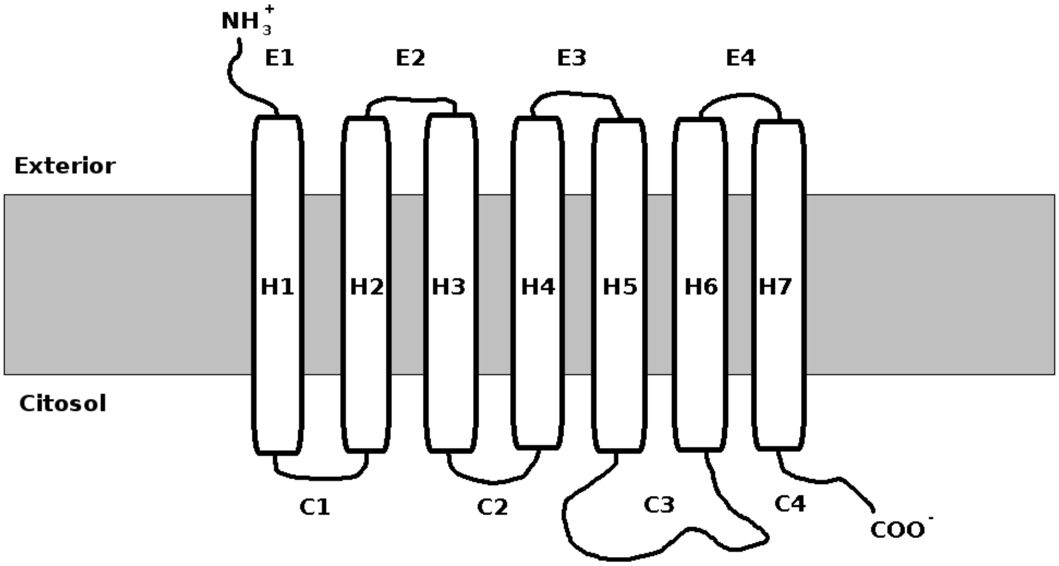

Figure 1.1 Representation of structural GPCR classification requirements. Seven transmembrane domains, amino and carboxyl ends, extracellular and intracellular loops (taken from The Trenches of Discovery, 2012).

As one of the widest family of receptors encoded by genes of mammalians, GPCRs constitute a vast variety of ligands (Gentry *et al.* 2015). These ligands can be ions, proteins, lipids, light energy, taste, odor, neurotransmitters, glycoproteins, and protons (Fredriksson *et al.*, 2003; Kobilka, 2013).

GPCR family is divided into Glutamate, Rhodopsin, Adhesion, Frizzles/Taste2, and Secretin subgroups according to their sequential alignments (Trzaskowski *et al.*, 2012).

To be classified as a GPCR, one receptor must have seven transmembrane domains and interact with G-proteins which in turn bind to secondary messengers in the cell to activate or deactivate the pathway they are included (Fredriksson *et al.,* 2003).

There are various types of G-proteins and GPCRs can interact with many subtypes of G-proteins (Wettschureck & Offermanns, 2005).

Approximately half of the drugs at the market are targeting GPCRs, and top selling drugs are found to be ligands for these receptors (Fredriksson *et al.,* 2003). More than 46 GPCRs are directly targeted by modern drugs, and more than 800 GPCR genes encoded by human genome (Lagerstrom, 2008; Fredriksson *et al.,* 2003; Kobilka, 2007).

There are many diseases both inherited and caused by somatic mutations on GPCRs, or by malfunctions in their signaling; such as, nephrogenic diabetes insipidus (NDI), bilateral frontoparietal polymicrogyria (BFPP), depression, bipolar disorder and schizophrenia (Shöneberg *et al.,* 2008; Catapano & Manji, 2007).

1.1.1. Dopamine Signaling and Dopamine D2 Receptor

Dopamine is a neurotransmitter from catecholamine family, involved in modulating cognition, emotion, food intake and reward behavior (Missale *et al.,* 1998; Schultz, 2007). Dopamine takes action through binding dopamine receptors which are GPCRs. Dopamine receptors divided into two subgroups, namely D1-like (D1 and D5 receptors) and D2-like (D2, D3, and D4 receptors) receptor families (Neve *et al.,* 2004).

This division is rooted from this two groups' opposite effect on the cAMP levels through nervous system which D1 and D2 receptors are abundantly found. D1-like receptors interact with stimulatory G proteins to activate adenylyl cyclase, thus increase cAMP levels; whereas D2-like receptors are interacting with inhibitory G-proteins to decrease adenylyl cyclic activity. D1-like receptors are coded without introns in the genome; however, D2-like receptors undergo alternative splicing for they have introns leaving them with the capability of raising multiple combinations (Missale *et al.*, 1998).

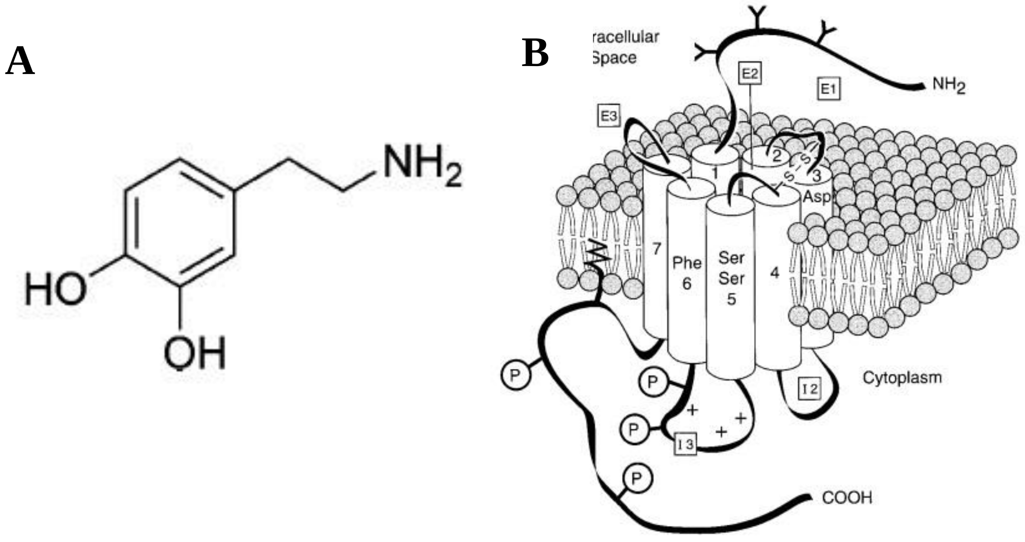

Figure 1.2 (A) Dopamine and (B) Dopamine Receptor demonstration. (taken from Missale *et al.*, 1998)

Dopamine receptors' interactions with G-proteins rely on their GPCR structure's intracellular loops and C-tails. The third intracellular loop of D2-like receptors is long and their carboxy-terminus is relatively short when compared to D1-like receptors (Civelli *et al.*, 1993). As short third intracellular loop and long C-tail presence is characterized to give the protein the ability to bind stimulatory G-proteins, D1-like receptors bind to stimulatory G-proteins; whereas D2-like receptors couple to inhibitory G-proteins (Missale *et al.*, 1998; Neve *et al.*, 2004).

D1-Like receptors stimulate adenylate cyclase through stimulatory G protein activity which in turn interacts with protein kinase A (PKA) in the neostriatum resulting in decrease of Na^+ and K^+ ions via affecting ion channels. They are also involved in phospholipase C (PLC) controlled calcium level modulation by affecting Ca^{2+} channels. They are also found to be diversely affecting glutamate and GABA receptors. On the other hand, D2-like receptors interact with inhibitory G-proteins, thus, they decrease the intracellular cAMP levels through PKA dependent pathway. Likewise, D2-like receptors are also interacting with GABA, NMDA receptors and ion channels to yield various effects in the cell. Moreover, they also regulate many pathways through $G_{\beta\gamma}$ dependent pathways including proteins such as K^+ channels, Ca^{2+} channels, MAP kinases, and phospholipases (Neve *et al.,* 2004).

Dopamine receptor anomalies results in a variety of diseases related to movement, hormonal regulation, and cardiovascular disorders. Deregulation of dopamine receptor related signaling pathways results in many neurological diseases such as Parkinson's disease, schizophrenia, Huntington's disease, and attention deficit hyperactivity disorder. Making this family of GPCR's an outstanding target for drug development (Beaulieu & Gainetdinov, 2011).

DRD2 gene, coding for dopamine D2 receptor (D2R), is located on chromosome 11q23 and expressed in the brain and pituitary. Receptor is found to inhibit adenylyl cyclic activity. D2R has two alternative forms differing in the length of their third intracellular loops. These two forms are the result of alternative splicing, causing 29-amino acid change (Civelli *et al.,* 1993). Long form is found to be expressed more than the short form (Neve *et al.,* 1991). D2R mRNA is found most abundantly in the striatum, substantia nigra, nucleus accumbens, and olfactory tubercle (O'Dowd, 1993). D2R signaling is shown to be affecting prolactin secretion, aldosterone secretion, symphatetic tone and deregulation of the neurologic pathways which result in many neurologic disorders such as Parkinson's disease and schizophrenia (Beaulieu & Gainetdinov, 2011).

1.2. G – Proteins

GPCR - G – protein complex’s structure was crystalized at 2011 for the first time (Rasmussen *et al.*, 2011). Heterotrimeric G-proteins are trimeric proteins inside the cell which are consisting of α, β, and γ subunits.

G-proteins take their name from their ability to bind and hydrolyze guanosine triphosphate (GTP) to yield guanosine diphosphate (GDP). When bound to GTP, they are stimulating the pathway they are included, whereas hydrolyzing GTP to GDP results in deactivation of the pathway (Bouvier, 2001). Upon activation of a GPCR, G-protein is activated by replacing GDP with GTP and G-protein α (Gα) subunit dissociates from G-protein βγ (Gβγ) subunits to start a signaling cascade via various secondary messengers, whereas Gβγ complex’s major role was thought to downregulate Gα’s activity by decreasing its affinity to GTP via changing Gα’s conformational shape, it is found that they are activating other pathways by interacting ion channels, kinases, and phospholipases (Brandt & Ross, 1985; Dorsam & Gutkind, 2007). A demonstration of GPCR and G-protein interaction is shown at Figure 1.3.

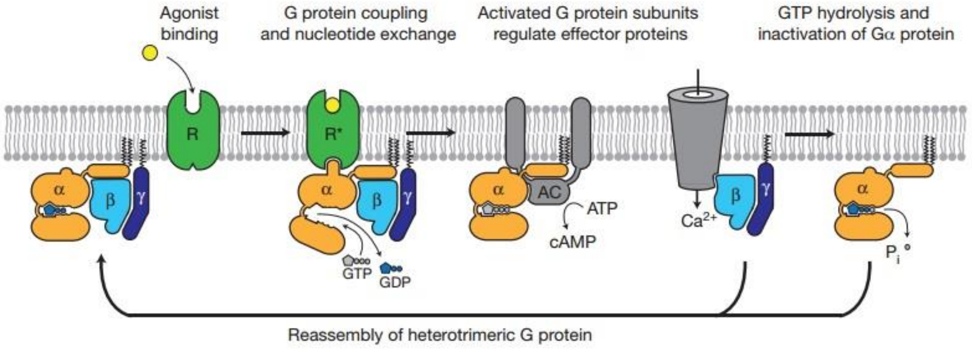
Agonist binding
G protein coupling and nucleotide exchange
Activated G protein subunits regulate effector proteins
GTP hydrolysis and inactivation of Gα protein
R
R*
α
β
γ
AC
ATP
cAMP
Ca2+
GTP
GDP
Pi
Reassembly of heterotrimeric G protein

Figure 1.3 Demonstration of GPCR and G-protein interactions. Upon activation by ligand binding GDP exchanged by GTP and Gβγ complex dissociates from Gα (taken from Rasmussen *et al.*, 2011).

Some of the secondary messengers and effectors involved in signal transduction of G-proteins involve phospholipase C (PLC), diacylglycerol (DAG), inositol triphosphate (IP_3), and cyclic adenosine monophosphate (cAMP) (Tewson *et al.*, 2013, Dorsam & Gutkind, 2007).

In the ligand-GPCR-G-protein bound state complex, it is found that G-protein has higher affinity for GTP than GDP and GPCR has multiple times more affinity to its ligand, pointing out that the structural changes in the complex units are ongoing upon complex formation (Rasmussen *et al.*, 2011). These changes include extracellular loops for they bind to ligands, intracellular ends for they interact with G-proteins of GPCRs, and G-protein's sites for receptor binding and GDP binding (Kobilka, 2007; Chung *et al.*, 2011).

$G\alpha$parts of G-proteins are classified into four main groups, namely $G\alpha_s$, $G\alpha_i$, $G\alpha_q$, and $G\alpha_{12}$. In short; $G\alpha_s$ is stimulatory, $G\alpha_i$ is inhibitory, $G\alpha_q$ is interacting with PLC, and $G\alpha_{12}$ is involved in Rho family GTPase signaling (Figure 1.4) (Dorsam & Gutkind, 2007).

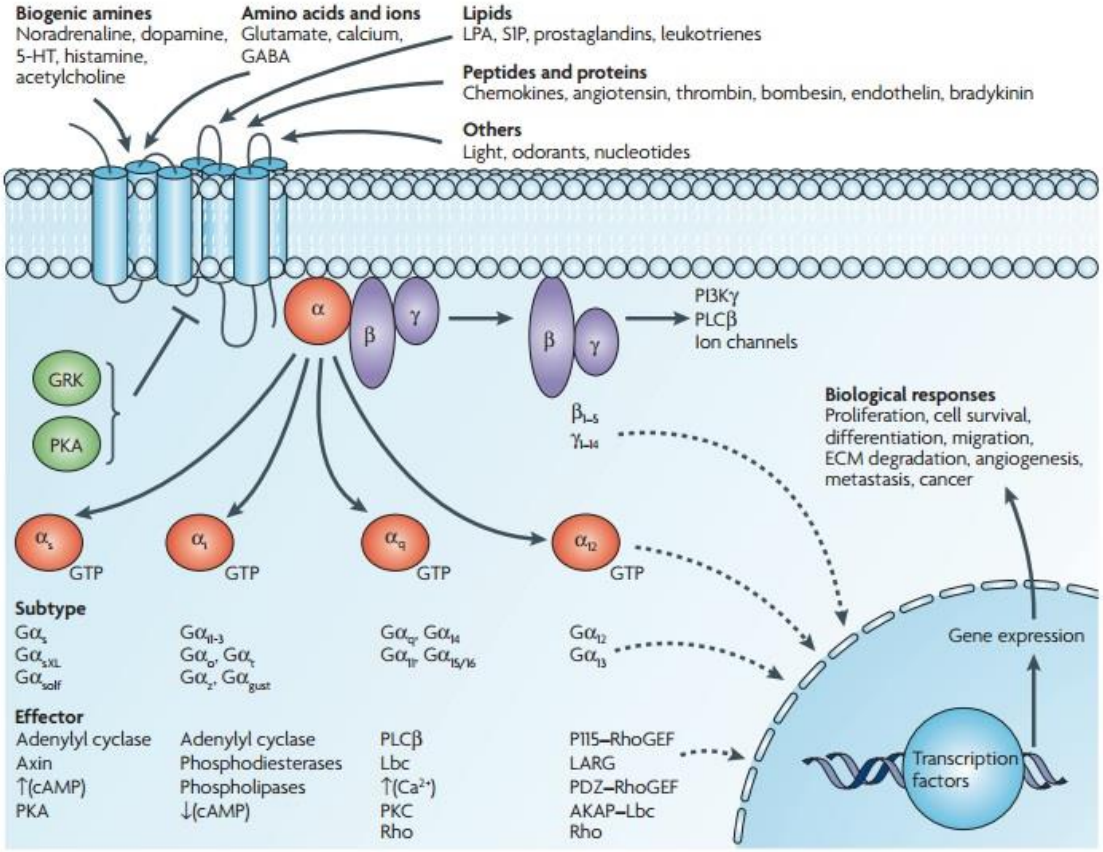
Biogenic amines
Noradrenaline, dopamine, 5-HT, histamine, acetylcholine
Amino acids and ions
Glutamate, calcium, GABA
Lipids
LPA, S1P, prostaglandins, leukotrienes
Peptides and proteins
Chemokines, angiotensin, thrombin, bombesin, endothelin, bradykinin
Others
Light, odorants, nucleotides
α
β
γ
β
γ
PI3Kγ
PLCβ
Ion channels
GRK
PKA
β_{1-5}
γ_{1-14}
Biological responses
Proliferation, cell survival, differentiation, migration, ECM degradation, angiogenesis, metastasis, cancer
α_s
GTP
α_i
GTP
α_q
GTP
α_{12}
GTP
Subtype
$G\alpha_s$
$G\alpha_{sXL}$
$G\alpha_{solf}$
$G\alpha_{i1-3}$
$G\alpha_o$, $G\alpha_t$
$G\alpha_z$, $G\alpha_{gust}$
$G\alpha_q$, $G\alpha_{14}$
$G\alpha_{11}$, $G\alpha_{15/16}$
$G\alpha_{12}$
$G\alpha_{13}$
Effector
Adenylyl cyclase
Axin
↑(cAMP)
PKA
Adenylyl cyclase
Phosphodiesterases
Phospholipases
↓(cAMP)
PLCβ
Lbc
↑(Ca^{2+})
PKC
Rho
P115–RhoGEF
LARG
PDZ–RhoGEF
AKAP–Lbc
Rho
Gene expression
Transcription factors

Figure 1.4 Representation of Gα subtypes and their effectors (taken from Dorsam & Gutkind, 2007).

These groups are also divided into subtypes depending on their alignments and effector types, in which main signal cascades are started or deactivated by, upon response to a ligand binding to a GPCR outside the cell, and resulting in cell's biological responses (Dorsam & Gutkind, 2007). Table 1.1 represents known G-protein alpha parts.

Table 1.1 Summary of G-protein alpha parts and their effectors. (adapted from Malbon, 2005)

Name	Effector
$G\alpha_{i1}$	Inhibition of adenylyl cyclase
$G\alpha_{i2}$	Inhibition of adenylyl cyclase
$G\alpha_{i3}$	Inhibition of adenylyl cyclase
$G\alpha_{oA,B}$	Inhibition of adenylyl cyclase
$G\alpha_{z}$	Inhibition of adenylyl cyclase
$G\alpha_{t1}$	Activation of visual rod
$G\alpha_{t2}$	Activation of visual cone
$G\alpha_{gust}$	Activation of taste
$G\alpha_{s}$	Stimulation of adenylyl cyclase
$G\alpha_{olf}$	Stimulation of adenylyl cyclase
$G\alpha_{sXL}$	Stimulation of adenylyl cyclase
$G\alpha_{q}$	Stimulation of PLCβ
$G\alpha_{11}$	Stimulation of PLCβ
$G\alpha_{14-16}$	Stimulation of PLCβ
$G\alpha_{12}$	Stimulation of Rho guanine-exchange factors
$G\alpha_{13}$	Stimulation of Rho guanine-exchange factors

1.2.1. Inhibitory G-Proteins and Subtypes G_{o1} and G_{i3}

Inhibitory G protein subtype (G_i) alters cAMP levels inside the cell negatively by inhibiting adenylyl cyclic activity through interacting with ion channels rather than adenylyl cyclases (Alberts *et al.*, 2002). G_i subfamily includes G-proteins G_{i1}, G_{i2},

G_{i3}, G_{o1}, G_{o2}, and G_z (Kimple *et al.,* 2014). This family of proteins is highly expressed; therefore, their activation is resulting in high levels of Gβγ complexes released from their Gα, which means inhibitory G-protein family also plays a triggering role in the Gβγ dependent signaling pathways (Wettschureck & Offermanns, 2005).

G_i family is mostly found in nervous system and also affected by *Pertussis toxin,* which leaves inhibitory G proteins incapable of binding to their receptors (Wettschureck & Offermanns, 2005; Alberts *et al.*, 2002). Also, since cAMP levels are related to insulin release, this family is also related to obesity and diabetes (Kimple, 2014).

Coded by *GNAO1* gene, alpha part of the trimeric G_{o1} protein is located on chromosome 16q12.2 and expressed abundantly in brain tissue. Mutations in its gene are shown to cause oncogenic features and epileptic encephalopathy by affecting the structure of the protein (Kulkarni *et al.*, 2015).

GNAI3 gene is coding for alpha part of inhibitory G_{i3} protein and is located on 17q22-24. *GNAI3* is shown to affect cytokinesis, proliferation, migration, invasion and apoptosis (Chen *et al.,* 2015). Variants of G-protein subtype I3 (G_{i3}), namely c.118G>C and c.141C>A, are found to be related to auriculocondylar syndrome (ACS) (Tavares *et al.*, 2015).

1.3. Methods for Detection of Interactions of GPCRs and G-Proteins

Understanding of how this large family of GPCRs signal outside and inside the cell and interact with its ligands and counterparts is a quite important step to unravel mechanisms behind to improve drug development systems, correct targeting when medication is introduced, and beyond all, to understand a key signaling mechanism in many organisms to gain a strong insight about life. Within the scope of this aim, several experimental approaches have been developed to understand structures of these proteins. To decipher GPCR structure, construction of prediction models via sequence analysis showed that extracellular loops of these proteins are the least conserved regions whereas intracellular loops are highly conserved with the discovery of lengths of these loops varies suggesting an importance over interaction mechanisms of these receptors inside the cell (Ballesteros *et al.*, 2001; Mirzadegan *et al.*, 2003; Shacham *et al.*, 2001).

Crystal structure of a GPCR was discovered for the first time in 2000 (Palczewski *et al.*, 2000), GPCR and its ligand at 2007 (Cherezov *et al.*, 2007) and with a G-protein complex at 2011 (Rasmussen *et al.*, 2011). After these discoveries more dynamic studies to determine the interactions were established since the behavior of these proteins under cellular conditions and discovery of interactions with other possible proteins remained unknown.

Mass spectrometry is one of the methods used to characterize how G-proteins are activated upon GPCR coupling. Using the data gathered from X-ray crystallography studies, nucleotide exchange mechanism of G_s upon coupling is provided via mass-spectrometry, particularly hydrogen-deuterium exchange mass spectrometry (HDXMS) (Chung *et al.*, 2011). While using HDXMS reveals more dynamic information about GPCR-G-protein interaction, studies in live cells are required to fully understand the characteristics.

Site-directed mutagenesis and coimmunoprecipitation (CoIP) studies are also widely used to determine interactions of GPCRs with G-proteins (Kristiansen, 2004; Holz *et al.*, 1989). While these approaches are significantly helping over determining structural areas of interaction and the unknown proteins in the interaction complexes, they are still insufficient to shed a light on the mechanisms of interactions in live cells.

In vitro studies has limitations of being unnatural, proteins developed and investigated outside the cell do not behave exactly as in their natural environment. Another limitation is that the complexity of the behavior of the GPCRs and G-proteins, it is known that a particular GPCR can act through more than one G-protein subtype and each coupling changes the outcome rapidly and significantly (Giulietti *et al.*, 2014). Therefore, live cell studies are preferred over *in vitro* studies to fully understand the mechanisms of signaling of these proteins.

The most commonly used methods to track interactions of GPCRs and G-proteins in live cells are Förster Resonance Energy Transfer (FRET) and Bioluminescent Resonance Energy Transfer (BRET). The most outstanding advantage of these methods is that they are applicable to live cell systems without interfering with the functionality. Second, energy transfer depends on the distance between molecules and this distance must be dramatically low for transfer to occur, this requirement brings enormous accuracy for tracking interactions between molecules. FRET relies on energy transfer between two fluorophores, whereas BRET uses an enzymatic donor. It is also possible to follow cAMP levels in live cells by using FRET and/or BRET methods via tracking conformational changes in the strategically placed biosensors (Denis *et al.*, 2012). FRET's advantage over BRET is that it allows tracking the events happening inside the cell, whereas, it is important to carefully pick the fluorophores used in FRET, for their spectra should be eligible to each other and for photobleaching, background noise due to autofluorescence of fluorophores may affect the studies (Boute *et al.*, 2002).

1.3.1. Förster Resonance Energy Transfer

With the discovery of green fluorescent protein (GFP) from *Victoria aequoira* at 1962 by Shimomura *et al.* new ways to track and investigate molecules rapidly emerged. One of the methods that GFP and its variants are used is Förster resonance energy transfer (FRET) method (Milligan & Bouvier, 2005).

FRET uses energy transfer between two fluorophores to determine the distance between these fluorophore containing structures and allows its users to process this information to gain information about interactions between molecules and conformational changes. For FRET to occur, it is necessary for the fluorophores to be in distance from 10 Å to 100 Å which allows users to investigate interactions dramatically accurate changes in the molecules (Clegg, 1995).

FRET occurs between an excited donor and an acceptor via intermolecular dipole-dipole coupling. Its requirements are the distance (10-100 Å), eligibility of spectra of donor and acceptor fluorophores (Figure 1.5), sufficient quantum yield of the molecules to be excitable and detectable, and correct orientation of fluorophores for this phenomenon to occur (Clegg, 1995).

The efficiency of this energy transfer decreases by 6th power of the distance between donor and acceptor molecules. FRET efficiency is described as follows (Förster, 1946):

$$k_T = \left(\frac{1}{\tau_D}\right) \times \left(\frac{R_0}{R}\right)^6$$

k_T: dipole-dipole coupling rate

τ_D fluorescence lifetime of the donor molecule

R: distance between donor and acceptor molecules

R_0: Förster distance where half maximum FRET efficiency is yielded

Advantages of FRET include its eligibility to work with living single cells and cell cultures where fluorophore-fused molecules can be visualized in their natural environment and being able to investigate both subcellular occasions and membrane-located ones (Sekar & Periasamy, 2003). Disadvantages include autofluorescence of the molecules and the noise generated because of them and limitations based on chosen fluorophore spectra (Clegg, 1995).

After discovery of GFP, mutants of it are generated giving rise to a variety of fluorophores with different emission wavelengths and also excited at different wavelengths. For example, cyan fluorescent protein (CFP) and yellow fluorescent protein (YFP) were widely used in the early years for their excitation/emission spectra eligibility (Milligan & Bouvier, 2005). Later, more variants were developed for better eligibility and one of the most fitted couple are mCherry as acceptor and enhanced green fluorescent protein (EGFP) as donor. Overlap of emission spectrum of EGFP and excitation spectrum of mCherry is sufficient for energy transfer as illustrated in Figure 1.5 and when the donor is excited, acceptor would not be excited too much, eliminating the noise from the crosstalk which is considered as an important limitation of FRET technique (Albertazzi *et al*, 2009).

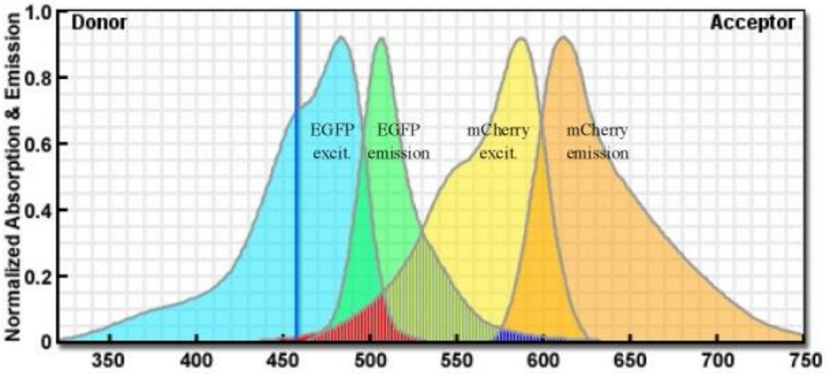

Figure 1.5 Fluorescence spectra of EGFP and mCherry (obtained from FRET for Fluorescence Proteins JAVA Tutorial, provided by MicroscopyU of Nikon®).

1.4. Aim of the Study

The purpose of the present study was to optimize the labeling of inhibitory G protein α subunits GNAO1 (Go_1) and GNAI3 (Gi_3) for the first time in literature in order to be able to detect and investigate molecular interactions between D2R and inhibitory G-proteins by labeling D2R with Enhanced Green Fluorescent Protein (EGFP) from its C-terminus and G proteins with mCherry from three internal locations; and subsequently transfecting them to *Mus musculus* Neuro-2a (N2a) and HEK293 cells to investigate their signals and possible interactions via spinning disc confocal microscopy.

The developed system can be used for analyzing interactions and behavior of various GPCRs with G-proteins. In addition, drug candidates and different agonists/antagonists can be applied to see the alterations in the behavior of the molecules.

CHAPTER 2

MATERIALS AND METHODS

2.1. Materials

2.1.1. Mammalian Cell Line and Maintenance

2.1.1.1. Neuro 2a Cells

To express and visualize fluorescently tagged proteins D2R, G_{i3} and G_{o1} in live cells, one of the chosen cell lines was mouse neuroblastoma cell line Neuro 2a (N2a) since D2R protein was abundantly expressed in neurons. These cells were supplied by ŞAP Institute, Ankara, TURKEY.

The growth media required for maintenance of N2a cells is a mixture of volume-wise 44,5% Dulbecco's Modified Eagle Medium (D-MEM) high glucose with L-glutamine (see Appendix A) (Invitrogen, Cat#41966-029), 44,5% OptiMEM®I Reduced Serum Medium with L-glutamine (Invitrogen, Cat#31985-047), 10% Fetal Bovine Serum (FBS) (Invitrogen, Cat#26140-079) and 1% Penicillin/Streptomycin solution (Invitrogen, Cat#15140-122); filtered via Millipore Stericup® Filter Unit for sterilization.

When cells were to be subcultured, they were washed with Phosphate Buffered Saline (PBS) Solution (See Appendix A). Dissociation of the cells from the flask was done with Trypsin-like solution, TrypLE™ Express with Phenol Red (Invitrogen, Cat#12605-028) Incubation conditions were 37°C and 5% CO_2. Nüve EC 160 CO_2 Incubator was used for incubation and for cell culture Nüve MN 090 Microbiological Safety cabinet was used.

For stocking the cells for long-term, freezing medium was prepared by mixing the following volume-wise: 35% D-MEM, 35% OptiMEM®I, 20% glycerol and 10% FBS.

2.1.1.2. HEK293 Cells

HEK293 cells were derived from human embryonic kidney cells and widely used for expression studies because of their ease in maintenance, growth and transfection. For this study, they were chosen to express tagged proteins in a non-neuronal environment to keep tagged proteins away from coupling with wild-type untagged G-proteins and D2Rs for they would have affected fluorescence signal efficiency. These cells were supplied by ATCC and gifted by Assist. Prof. Dr. Md. Ebru Erbay, Bilkent University, Ankara, TURKEY.

The complete growth media required to culture and maintain HEK293 cell line included (v/v) 90% D-MEM high glucose with L-glutamine (see Appendix A), 10% FBS, and 1% Penicillin/Streptomycin solution; filtered via Millipore Stericup® Filter Unit for sterilization. Rinsing of the cells were done with D-MEM, detachment was achieved via Trypsin. Incubation conditions are 37°C and 5% CO_2. Nüve EC 160 CO_2 Incubator was used for incubation and for cell culture Nüve MN 090 Microbiological Safety cabinet was used.

For cryopreservation, freezing medium was complete growth medium supplemented with 5% (v/v) DMSO.

2.1.2 Bacterial Cell Culture

Escherichia coli XL1 Blue strain was used for plasmid amplification. Strain was grown in Luria Bertani (LB) Solution or in its solidified form with the required antibiotics (Ampicillin 100 mg/mL, Kanamycin 50 mg/mL) (see Appendix A). Solution was sterilized at 121°C for 20 minutes by use of Nüve OT 40L autoclave.

Cells were grown in solidified LB are incubated at 37°C incubator for 16 hours. For liquid LB, cells were shaken at 200 rpm for 16 hours at 37°C. The orbital shaker incubator used for liquid media was ZHWY-200B by Zhicheng Instruments.

2.1.3. Plasmids, Primers, and Sequencing

Complementary DNA (cDNA) sequence of D2R in pDONR221 vector (Accession Number: NM_000795), GNAO1 in pDONR221 vector (Accession Number: HsCD00296446), and GNAI3 in PDNR-Dual vector (Accession Number: HsCD00000990) were obtained from PlasmID, Harvard Medical School (MA, USA). cDNA of EGFP in pEGFP-N1 vector (Accession Number: AAB02574) and mCherry in pCS2-mCherry vector (Accession Number: ACO48282) were gifted by Prof. Dr. Henry Lester, California Institute of Technology (CA, USA). For mammalian expression, all of the cDNA sequences were cloned into pcDNA3.1(-) (Appendix B) which was gifted by Assoc. Prof. Dr. Ayşe Elif Erson Bensan, Middle East Technical University, Turkey.

Primers designed to sequence the clones, to clone the cDNA sequences into pcDNA3.1(-), and to amplify EGFP and mCherry sequences with overhangs to insert them into desired regions of the proteins (Appendix B) were purchased from Sentegen (Ankara, Turkey) and Integrated DNA Technologies (IDT) (IO, USA). Sequencing of the generated clones were done by Molecular Cloning Laboratories (MCLAB) (CA, USA).

2.1.4. Other Chemicals and Materials

All of the chemicals were supplied by Sigma-Aldrich (NY, USA).

DNA Polymerases, T4 Ligases, GeneRuler 100bp plus (#SM0321) and GeneRuler 1kb (#SM0313) DNA ladders used in the procedures were obtained from Thermo Scientific (MA, USA). Restriction enzymes were supplied by New England BioLabs Inc. (MA, USA).

QIAquick® Gel Extraction Kits (#280706) were obtained from QIAGEN (Hilden, Germany). GeneJET PCR Purification Kits (#K0702) and Plasmid Miniprep Kit (#K0503) for plasmid isolation were supplied by Thermo Scientific (MA, USA). Transfection Kits used in the procedures was Lipofectamine® LTX and Plus™ Reagent (#15338-100) by Invitrogen (CA, ABD). T-25 cell culture flasks are supplied by Greiner-Bio (Frankfurt, Germany). Glass bottom dishes were supplied by In Vitro Scientific (CA, USA). Functionality assay cAMP-Glo™ Assay (#V1502) was purchased from Promega (WI, USA).

Fluorescent live cell imaging was done by Leica Microsystems CMS GmBH's DMI4000B confocal microscope with Andor DSD2 spinning differential disc confocal device.

Image Analysis was done via PixFRET, a plug-in for ImageJ.

2.2. Methods

2.2.1. G-Protein Plasmid Screening, Primer Designs, Insertion, and Cloning

2.2.1.1. G-Protein Plasmid Screening

Plasmids containing GNAO1 (354aa) (Accession Number: HsCD00296446) and GNAI3 (354aa) (Accession Number: HsCD00000990) genes were obtained from PlasmID, Harvard Medical School (MA, USA). Database screening was done with the priority of sequence identity of the plasmid containing desired insert with the original protein sequence. To assess this, ExPASy Translate Tool was used for obtaining the plasmids' protein sequences. Then, EMBOSS Needle Tool was used for seeing pair-wise protein sequence alignment. Another important aspect of choosing the plasmid was to control if it contains any known mutations or not. Since they were going to be used for expression, they must not have contained any morphologic or functional deficiency-creating mutations. Closed plasmids (with a stop codon at their end) were known not to carry any mutations. However, if the plasmid was in the fusion format (meaning that they lack the stop codon at the end of their coding sequence), their mutation statuses were not known and must be checked via DNA sequencing after all modifications and transfections were done.

Obtained plasmid specifications were:

- GNAO1: HsCD00296446, 97% similar to wild-type sequence, closed, 1065 bp, kanamycin resistant, in pDONR221
- GNAI3: HsCD00000990, 100% similar to wild-type sequence, closed, 1065 bp, ampicillin resistant, in pDNR-Dual

GNAO1's low identity was investigated by obtaining coding sequence and mutation information from Ensembl and it was found that the mutations were synonymous meaning that they were not going to interfere with the protein's function.

2.2.1.2. Primer Design for Cloning the Products into pcDNA3.1(-)

Fluorescent proteins were inserted to the strategic points of these genes and these fusion genes were cloned into mammalian expression vector pcDNA3.1(-). To achieve cloning part, restriction enzyme cut sites compatible with the multiple cloning site (MCS) of the pcDNA3.1(-) were introduced to these genes via polymerase chain reaction (PCR). In order to avoid cutting internal sites of the genes, unique cut sites must have been introduced. Sequences of the G-protein genes were analyzed for their cut sites via NEBcutter Tool, and common cut sites inside the genes with the expression vector were eliminated while designing cloning primers (Appendix C). Also, 6 bases of linker regions were added to increase restriction enzyme efficiency (Appendix B).

2.2.1.3. Primer Design for Insertion of Fluorescent Proteins

In order not to interfere with the functionality of the G-proteins, fluorescent protein insertion should have been done strategically. To achieve this, literature screening was done and phylogenetic, functional and structural similarities of the GNAO1 and GNAI3 genes were determined and compared with previously tagged G-proteins. By use of GeneCard's GenesLikeMe tool, similarity scores of GNAO1 and GNAI3 genes were determined; and a phylogenetic tree was generated by use of EMBL's ClustalW2-Phylogeny tool (Appendix C). Results showed that these two genes were closely related to GNAI1 gene, which was previously tagged successfully from a variety of locations. The most validated positions were E122-L123, corresponding to between alpha helices αB and αC; L91-K92, corresponding to between alpha helices αA and αB; and G60-Y61, corresponding to linker between helix and GTPase domain of G protein α right after αA helix for GNAI1 (Gales *et al.*, 2006; Gibson *et al.*, 2006).

Template based similar 3D structures of GNAO1 and GNAI3 were found via SWISS-MODEL, a tool which analyzes sequences of the proteins and puts the most similar known 3D model out (Table 2.1).

Table 2.1 Template based 3D model Identities

	Template and PDB ID	**Sequence Identity**
GNAO1	Mouse GNAO1 3C7K	98%
GNAI3	Human GNAI3 4G5O	100%

After obtaining the reference templates, the templates and the GNAI1's 3D structures were compared via PDB Comparison Tool. GNAI1's PDB ID in use was 1GG2 and was obtained from Gales *et al.*'s paper as their reference protein when tagging their human G proteins. Correlating positions in GNAO1 and GNAI3for E122-L123, L91-K92, G60-Y61 points on GNAI1 which were corresponding to between alpha helices αB and αC, between alpha helices αA and αB, and to the linker between helical and GTPase domain of G protein α right after αA helix respectively, were found to be A122-E123, R113-M114, E94-Y95 for GNAO1 and

E122-L123, L91-K92, G60-Y61 for GNAI3 considering identity, and the actual physical positions on the model.

Corresponding DNA sequences for the amino acid positions on the G-protein genes were found in frame via EMBOSS-Sixpack tool. A frequently used linker SGGGS was added to both ends of the fluorescent protein on the primer sequence, the sequence of the linker was determined by using Codon Usage Database in order to find the most frequently used codons by *Mus musculus* and humans as the host organism for Neuro2a and HEK293 cells in which the proteins would be expressed for imaging. Detailed list of the primers were given in Appendix B.

D2R gene was cloned into pcDNA3.1(-) in its naïve form previously, it was sent to sequencing in order to inspect if it contains any mutations and to find out its exact location on pcDNA3.1(-). After determining that there was no mutation on the sequence of D2R, EGFP insertion primers were designed as forward primer covering the last nucleotides of D2R and first nucleotides of EGFP, reverse primer covering the last nucleotides of EGFP and the region of pcDNA3.1(-) immediately after where D2R was located (Appendix B). Sequence of D2R in pcDNA3.1(-) was given in the Appendix F.

These insertion primers were to be used for amplifying fluorescent protein genes with overhangs compatible with the corresponding protein's DNA sequence. These products were to be used in the PCR Integration method for a second PCR (Gibson, 2011).

2.2.1.4. PCR Amplifications

Fluorescent protein genes EGFP and mCherry were amplified with overhangs to be used later in a second PCR step to fuse them into their target proteins. Targeting was achieved with compatible overhangs at the ends of fluorescent protein sequences. Also for cloning of the constructs to the mammalian expression plasmid pcDNA3.1(-), constructs should have been amplified with particular restriction enzyme sites. Optimized PCR protocol was given in Table 2.2.

Table 2.2. Optimized PCR Protocol for gene amplification

1. Pre-Denaturation	95°C	90 sec	
2. Denaturation	98°C	5 sec	35 cycles
3. Annealing	55°C	5 sec	
4. Extension	72°C	28 sec	
5. Final Extension	72°C	1 min	

5x PhireII Reaction Buffer	10 µl
$MgCl_2$ (25 mM)	1 µl
dNTPs (10mM)	2 µl
Forward Primer (20 pmol)	1 µl
Reverse Primer (20 pmol)	1 µl
Phire II HS Polymerase	1 µl
Template (EGFP/mCherry in pcDNA3.1(-))	100 ng
Nuclease-free water	Complete to 50 µl

2.2.1.5. Agarose Gel Electrophoresis

In order to separate DNA fragments and see their sizes, agarose gel electrophoresis with 1% weight to volume ratio agarose gel was performed. Gel was prepared by dissolving required amount of agarose in 1X TAE (Appendix A). DNA samples were loaded to gel with by mixing them with 6x loading dye (Thermo Scientific, #R0611) with 1x final loading dye concentration. The samples were run for 45 minutes at 90-100V in 1X TAE Buffer. Separated DNA fragments' sizes were determined with loading proper DNA ladders, and/or they were processed further.

2.2.1.6. Agarose Gel DNA Isolation

Separated and size confirmed DNA fragments were extracted from agarose gel by use of QIAquick® Gel Extraction Kits (#280706) by QIAGEN.

2.2.1.7. PCR Integration Method

Fluorescent protein genes mCherry and EGFP were amplified with overhangs compatible with the sequences of the proteins that they were intended to be inserted. In this study, mCherry sequence was inserted between A122-E123, R113-M114, E94-Y95 in GNAO1 and E122-L123, L91-K92, G60-Y61 in GNAI3 genes. Whereas, EGFP sequence was added to carboxyl terminus of D2R sequence. These products were then used as primer sets for a second set of PCR, in which DNA of the target protein in plasmid used as template (Gibson, 2011). These two steps of PCR are called PCR Integration method which is demonstrated in Figure2.1.

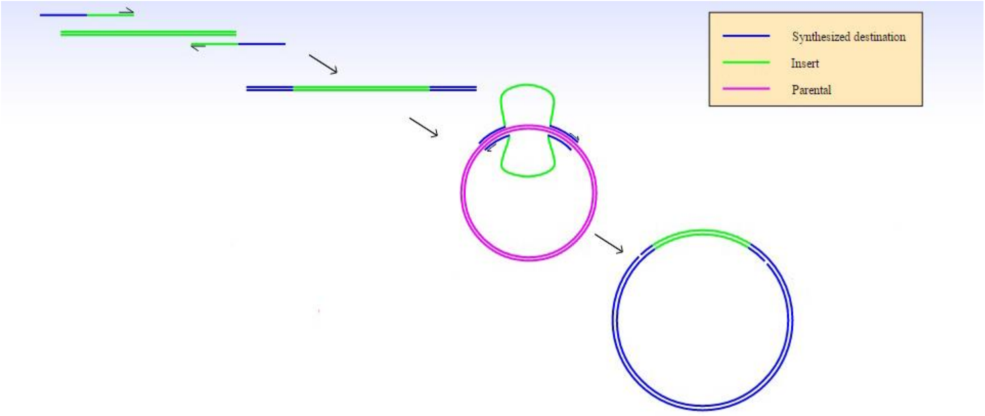

Figure 2.1. Demonstration of PCR Integration Method (adapted from http://rf-cloning.org/QandA.php)

Optimized second step conditions are given in Table 2.3.

Table 2.3 Optimized PCR Conditions for second step of PCR Integration

5x Phusion HF Buffer	10 µl
$MgCl_2$ (25 mM)	1 µl
dNTPs (10mM)	3 µl
1st PCR Product	50 x molar ratio
Phusion HF HS Polymerase	1 µl
Template	x molar ratio
Nuclease-free water	Completed to 50 µl

1. Pre-Denaturation	98°C	3 min	
2. Denaturation	98°C	30 sec	18 cycles
3. Annealing	55°C	1 min	
4. Extension	72°C	14 min	
5. Final Extension	72°C	15 min	

Another key point of this method was to eliminate parent vectors before transformation of PCR products to bacterial cells since they also contain antibiotics resistance gene but do not contain the desired insert. To achieve this, DpnI enzyme by Thermo Scientific (#ER1702) treatment was done according to supplier's manual. DpnI is an enzyme which cuts the methylated GATC sites, which this time the parent plasmids isolated from *E. coli* cells contain. Since PCR products do not contain any methylation, they remain not digested by DpnI.

2.2.1.8. PCR Purification

To remove PCR components after PCR was completed, PCR purification was done via Thermo Scientific GeneJET PCR Purification Kit (#K0702) in order not to affect restriction enzyme efficiency negatively. Procedure was applied according to instruction manual of the kit.

2.2.1.9. Restriction Enzyme Digestion

In order to cut the host plasmid pcDNA3.1(-) and fusion proteins from desired locations, double restriction enzyme digestions were done according to supplier's protocol (New England Biolabs).

2.2.1.10. DNA Concentration Determination

To determine the amount and concentration of DNA containing samples, Thermo Scientific NanoDrop 2000 spectrophotometer was used.

2.2.1.11. Ligation

After restriction enzyme digestion of the host plasmid and fusion protein DNA sequences, ligation reactions were utilized in 1:5 vector:insert molar ratio via T4 DNA ligase (New England Biolabs). Procedure was applied according to supplier's manual.

2.2.1.12. Preparation of Competent *E. coli* Cells by RbCl Method

Single colony from XL1 Blue strain on LB plate was inoculated into 4 mL LB medium without antibiotics. Inoculum was shaken for 16 hours at 37°C at 200 rpm. Suspension was subcultured in 1:100 ratio to LB medium. 20 mM $MgSO_4$ was added. Cells were grown until OD_{590} had reached to 0.4-0.6, which took 3-4 hours. After desired OD_{590} value was reached, mixture was centrifuged at 4000 rpm for 5 minutes at pre-cooled 4°C centrifuge. Supernatant was discarded. Pellet was resuspended in pre-chilled 0.4x original subculture volume Transformation Buffer I (TFBI) (Appendix A) and incubated on ice for 5 minutes. After this step, all of the procedure was performed on ice and the pipettes, tubes, flasks and solutions were pre-chilled. Mixture was centrifuged at 5000 rpm for 5 minutes at pre-cooled 4°C centrifuge. Supernatant was discarded and pellet was resuspended in 0.04x original subculture volume pre-chilled Transformation Buffer II (TFBII) (Appendix A). Mixture was incubated on ice for 45 minutes then aliquoted 100 µl/tube and quick froze in liquid nitrogen. Aliquots were kept at -80°C for long-period storage.

2.2.1.13. Transformation of Competent Cells

All of the steps were carried under Bunsen-Burner fire. Previously aliquoted 100 µl of competent cells were chilled on ice for 15 minutes. 10% volume of plasmid / ligation / PCR product was added to the tube. Mixture was incubated on ice for 30 minutes. Cells were heat-shocked at 42°C for 30 seconds. Mixture was incubated on ice for 5 minutes. Volume was completed to 1 mL with sterile LB. Cells were shaken at 37°C for 1 hour, at 200 rpm. Mixture was centrifuged at 3000 rpm for 3 minutes. 800 µl of supernatant was removed; pellet was gently resuspended in the remaining supernatant and plated on agar with required antibiotics. Cells were grown for 16 hours at 37°C.

2.2.1.14. Plasmid Isolation

Single colony was inoculated into 4 mL of LB medium with the required antibiotics. Tube was incubated by shaking them at 37°C for 16 hours at 200 rpm. Plasmid isolation was done via Thermo Scientific’s GeneJET Plasmid Miniprep Kit (#K0503) instructions for use.

2.2.2. Mammalian Cell Maintenance, Transfection, and Imaging

2.2.2.1. N2a Cell Maintenance

N2a cells were grown in their medium at 37°C with 5% CO_2 until their confluency reaches 90%, which takes 3-4 days in T25 flasks with 8 ml of growth medium.

After this point their waste and population density starts to intoxicate them and they need to be passaged. Passaging includes removal of growth medium, washing gently with 2 ml PBS, incubation with 1 ml of TrypLE™ Express with Phenol Red (Invitrogen, Cat#12605-028) for 5 minutes at 37°C to detach them from the flask surface, diluting TrypLE™ at 1:10 ratio with growth medium, and passaging 10% of the mixture to a new T25 flask containing fresh 37°C growth medium.

For long term stocking, 10^7 cells were centrifuged at 1000 rpm for 5 minutes, supernatant was removed, and pellet was resuspended in N2a freezing medium and transferred to cryovials which were stored at -80°C for 24 hours. After that, they were moved to liquid nitrogen tank. To revive the cells, cryovial was thawed at 37°C and thawed cells were transferred to 9 ml 37°C growth medium. Mixture was centrifuged at 1000 rpm for 5 minutes. Supernatant was removed; pellet was resuspended in 1 ml 37°C growth medium. They were then transferred to 8 ml 37°C growth medium containing 25 cm^3 flasks.

2.2.2.2. HEK293 Cell Maintenance

HEK293 cells were grown in complete growth medium at 37°C with 5% CO_2 until cell concentration reached $6\text{-}7x10^4$ cells/cm^2, which takes 2-3 days. Subculturing involves removal of culture medium, rinsing the cells with 1 mL of D-MEM high glucose with L-glutamine to remove all toxic remnants and trypsin inhibitors, incubation with 1 mL of 0.25% (w/v) Trypsin-0.53 mM EDTA for 5 minutes at 37°C to detach cells from flask, dilution of trypsin via addition of 9 mL of complete growth medium, addition of 9 mL of fresh complete growth medium to a new 25 cm^3 flask, and finally addition of 1 mL liquid from previously detached and diluted flask to the new one to achieve 1:10 subcultivation ratio.

For cryopreservation, 10^7 cells were centrifuged at 1000 rpm for 5 minutes, supernatant was removed, and pellet was resuspended in HEK293 freezing medium and transferred to cryovials which were stored at -80°C for 24 hours. After that, they were moved to liquid nitrogen tank. To revive the cells, cryovial was thawed at 37°C and thawed cells were transferred to 9 ml 37°C complete growth medium. Mixture was centrifuged at 1000 rpm for 5 minutes. Supernatant was removed; pellet was resuspended in 1 ml 37°C complete growth medium. They were then transferred to 9 ml 37°C complete growth medium containing 25 cm^3 flasks.

2.2.2.3. Transfection of Cells

60000 N2a or HEK293 cells were counted via hematocytometer and they were seeded on a 2 ml growth medium containing 35mm glass bottom dish. The cells were grown for 24 hours. 500 ng of the desired construct was diluted in 100 µl of OptiMEM®I. 4 µl of Plus™ Reagent was added and the mixture was incubated for 15 minutes at room temperature. 4 µl of Lipofectamine LTX was diluted in 100 µl of OptiMEM®I and added to the plasmid containing mixture at the end of incubation. Final mixture was incubated at room temperature for 15 minutes. During this incubation, media in the 35mm glass bottom dish was removed and the plate was washed with 1 ml of 1X PBS and 1 ml of OptiMEM®I was added to dish. After the incubation time was over, final mixture was added to the dish. Cells were incubated at 37°C with 5% CO_2 for 3 hours, and then 2 ml of 37°C growth medium was added. Dish was incubated at 37°C with 5% CO_2 for 24 hours, then the media was removed and fresh 2 ml of 37°C growth medium was added. Cells were grown at 37°C incubator with 5% CO_2 for two days before imaging.

2.2.2.4. Imaging with Spinning Disc Confocal Microscope

After transfection of cells and growing for 2 days, expression of the constructs was completed and the cells are imaged by Leica DMI4000 B with Andor DSD2 Confocal device with a 63x oil immersion objective lens.

DSD2 is using differential spinning disc technology and has an excitation range of 370 – 700 nm and an emission range of 410 – 750 nm with a maximum of 22 frames per second frame rate. Differential spinning disc is an optical design that effectively and fastly rejects non-focused light via its many rotating holes to pass the correctly focused light to the sample; therefore, resulting in sharper and more detailed images.(Browne, 2010).

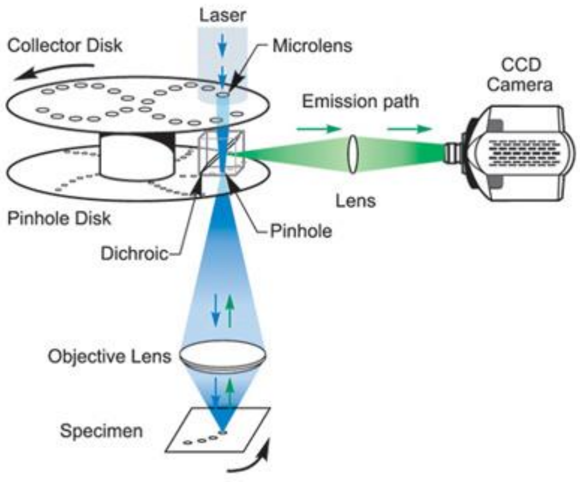
Laser
Collector Disk
Microlens
CCD Camera
Emission path
Lens
Pinhole Disk
Pinhole
Dichroic
Objective Lens
Specimen

Figure 2.2 Spinning disk technology schematically explained. (Adapted from LMCF, Duke University)

Cells were kept alive in dishes with a 37˚C heated CO_2 stage. Green signal from EGFP was obtained by exciting cells with 482 nm wavelength and obtaining their emissions at 525 nm wavelength. Red signal from mCherry was obtained via exciting cells with 583 nm, and obtaining their emissions at 631 nm. For FRET signal, cells were excited from the donor channel (EGFP) with 482 nm, and emissions were collected from acceptor channel (mCherry), at 631 nm. Information about filters used was given in Appendix E.

2.2.2.5. Image Analysis with PixFRET

PixFRET is an ImageJ plug-in which processes images provided by the user pixel by pixel to determine the location and amount of FRET sensitively. In order to eliminate spectral bleed-through (SBT) caused by the donor or the acceptor molecule spectral overlap, it uses stacks of images generated by user via taking images from three channels; FRET channel, donor channel, and acceptor channel. SBT occurs when acceptor is excited at the donor excitation interval and when donor emits light in the acceptor spectra. PixFRET eliminates these false-positives in order to reduce the noise. The system PixFRET uses is as follows:

Firstly, to calculate donor SBT, only donor-labeled proteins are transfected to cells and images are taken from two channels. One is FRET channel, meaning excitation with donor wavelength and collecting signals from acceptor emission spectra. Second is donor channel, meaning excitation from donor wavelength and collecting signals from donor spectra.

Secondly, to calculate acceptor SBT, only acceptor-labeled proteins are transfected to cells and images are taken from two channels. One is FRET channel, meaning excitation with donor wavelength and collecting signals from acceptor emission spectra. Second is acceptor channel, meaning excitation from acceptor wavelength and collecting signals from acceptor spectra.

Final set up is for FRET signal. Cells are transfected both with donor- and acceptor-labeled proteins and the images are taken from three channels. One is FRET channel, meaning excitation with donor wavelength and collecting signals from acceptor emission spectra. Second is donor channel, meaning excitation from donor wavelength and collecting signals from donor spectra. Final image is from acceptor channel, meaning excitation from acceptor wavelength and collecting signals from acceptor spectra.

These images are used by PixFRET algorithm for noise cancellation by eliminating SBTs and FRET efficiency calculation via pixel-count (Feige *et al.,* 2005). An example to demonstrate the used images for calculation efficiency was presented at Appendix G.

2.2.3. Functionality Test of D2R with Constructed G-Proteins

To test whether modifications done to D2R, GNAO1 and GNAI3 G-Protein α subunits affect their functionality on their related pathways, a functional assay based on determining changing levels of cAMP in the cells via ATP and luciferase reaction had been applied.

2.2.3.1. cAMP-Glo™ Assay

Developed by Promega (WI, USA), this assay designed specifically for cAMP modulating GPCR expressing cells. Assay measures cAMP levels in the cells via monitoring remaining ATP levels at the end of a specific signaling cascade. After activation or deactivation of adenylate cyclase (AC) by a GPCR, AC modulates cAMP levels in the cell accordingly. cAMP molecule activates Protein Kinase A (PKA) which in return phosphorylates its substrate by the use of ATP. Remaining ATP levels are then determined by presence of luciferase which consumes ATP to produce luminescence (Figure 2.6).

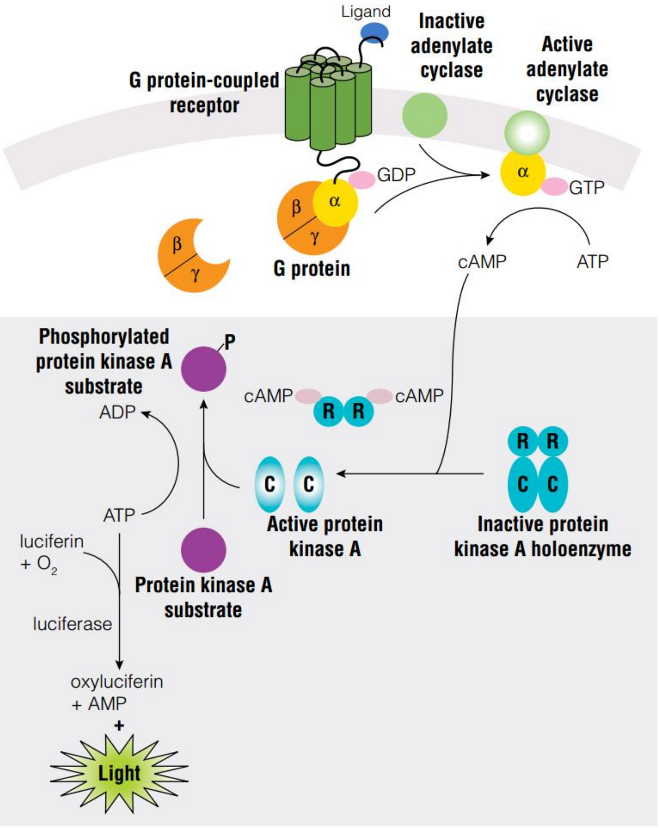
Ligand
Inactive adenylate cyclase
Active adenylate cyclase
G protein-coupled receptor
GDP
α
GTP
β
α
γ
β
γ
G protein
cAMP
ATP
Phosphorylated protein kinase A substrate
P
ADP
cAMP
R
R
cAMP
R
R
C
C
C
C
Active protein kinase A
Inactive protein kinase A holoenzyme
ATP
luciferin
+ O2
Protein kinase A substrate
luciferase
oxyluciferin
+ AMP
+
Light

Figure 2.3 Demonstration of cAMP-Glo™ Assay working principle. GPCR is activated upon ligand binding, activates or deactivates adenylate cyclase depending on its G-protein subtype, modulates cAMP levels. cAMP in return activates protein kinase A, which will phosphorylate its substrate by the use of ATP. Remaining ATP will be consumed by luciferase presented by the assay to produce luminescence (taken from www.promega.com).

Since more cAMP levels would lead to more active PKA to consume ATP, assay's principle relates cAMP levels and luminescence reciprocally. As D2R was found to be interacting with inhibitory G-proteins, D2R activation would lead lower cAMP levels in the cell when compared to non-D2R-expressing lines (Missale *et al.*, 1998).

To assess this assay over inhibitory D2R activation, forskolin (Sigma – Aldrich) was used to increase cAMP levels up to a certain level. Quinpirole (Sigma - Aldrich) was used as agonist of D2R.

10.000 N2a cells were seeded to each of the wells to be used of the poly-D-Lysine coated 96-well plate. After 24 hours of incubation in 37˚C 5% CO_2 incubator, the cells were transfected with the desired constructs. Amount of DNA, volume of the medium used, and all of the chemicals were decreased proportional to the number of the cells in the wells. After 48 hours of incubation in 37˚C 5% CO_2 incubator, 20 µl of 10 µM of forskolin in induction buffer was applied to the wells to be tested for 15 minutes 37˚C 5% CO_2 incubator in order for cAMP levels to rise. Then 20 µl of D2R ligand quinpirole was introduced to the same wells at 10 µM concentration in induction buffer. Wells were incubated for 15 minutes in 37˚C 5% CO_2 incubator. Then assay's protocol was applied according to the supplier's manual.

CHAPTER 3

RESULTS AND DISCUSSION

3.1. Cloning and Labeling Studies

3.1.1. Cloning GNAO1 and GNAI3 cDNAs to Mammalian Expression Vector pcDNA3.1(-)

Genes obtained from Harvard PlasmID came in their native plasmids, and they needed to be cloned into a mammalian expression vector, which should also be viable in bacteria, in order to be expressed in N2a and HEK293 cells.

To clone GNAO1 gene from pDONR221 vector and GNAI3 gene from pDNR-Dual vector to pcDNA3.1(-) vector, the inserted genes were amplified with specific cut-site containing regions. These primers were given in Appendix B. A small amount from the amplified genes were run on 1% agarose gel and genes' amplifications were confirmed (Figure 3.1).

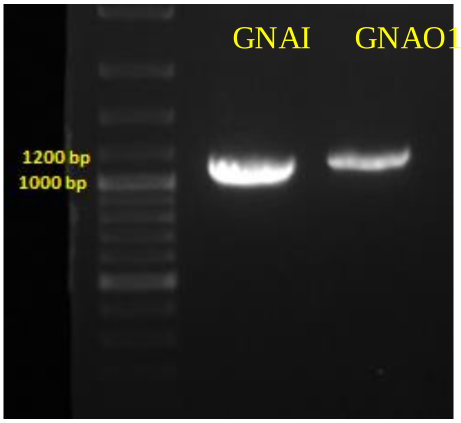

Figure 3.1 Agarose gel electrophoresis image of amplified GNAI3 and GNAO1 genes with EcoRI and KpnI cut sites. Thermo Scientific GeneRuler 100 bp Plus DNA Ladder (Cat. Num. #SM0321) is used.

GNAO1 and GNAI3 genes were both 1065 bp long, and EcoRI and KpnI cut sites together with their linkers were giving an additional 24 base pairs to each of the genes. The bands in the gel were on the expected area.

Amplified GNAO1 and GNAI3 genes were PCR purified and put in double digestion reactions together with pcDNA3.1(-). The products of restriction were run on gel (Figure 3.2) and extracted from the gel.

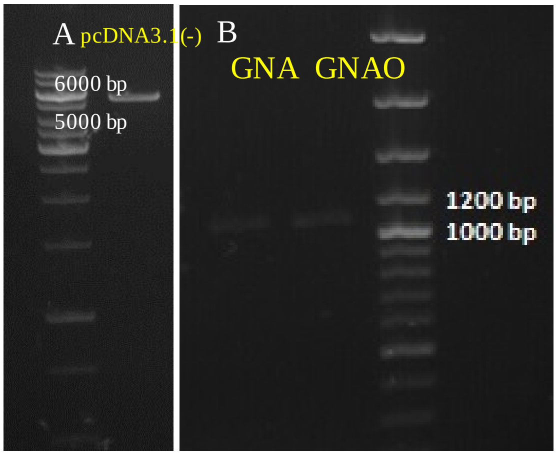

Figure 3.2 Agarose gel electrophoresis images of (A) pcDNA3.1(-) and (B) GNAI3 and GNAO1 genes double digested with EcoRI and KpnI enzymes. On (A) Thermo Scientific GeneRuler 1 kb DNA Ladder (Cat. Num. #SM0311), on (B) 100 bp Plus DNA Ladder (Cat. Num. #SM0321) is used.

Restricted pcDNA3.1(-), around 5428 bp; GNAI3 and GNAO1 around 1100 bp were at the expected regions on the gel. Extracted products were put in ligation reactions in 1:10 molar ratio. Ligated products were directly transformed to competent XL-1 Blue strain of *E. coli* and the day after colonies were observed.

3.1.2. Tagging GNAO1 gene with mCherry from A122, R113, and E94 via PCR Integration Method

mCherry gene was amplified with flanking ends specific for the positions A122-E123, R113-M114, and E94-Y95 on GNAO1 protein. Primers used in these amplifications were given in Appendix B.

These products were then used as primer sets for PCR integration. Template for the reactions is GNAO1 gene located in pcDNA3.1(-). Products were treated with

DpnI, and they were transformed to competent XL-1 Blue bacteria. The day after, colonies were observed for all three of the constructs.

Three of the colonies were chosen randomly from each of the constructs and their plasmids were isolated and double digested with KpnI and EcoRI restriction enzymes. To see if the inserts were tagged with mCherry, digested plasmids were run on agarose gel.

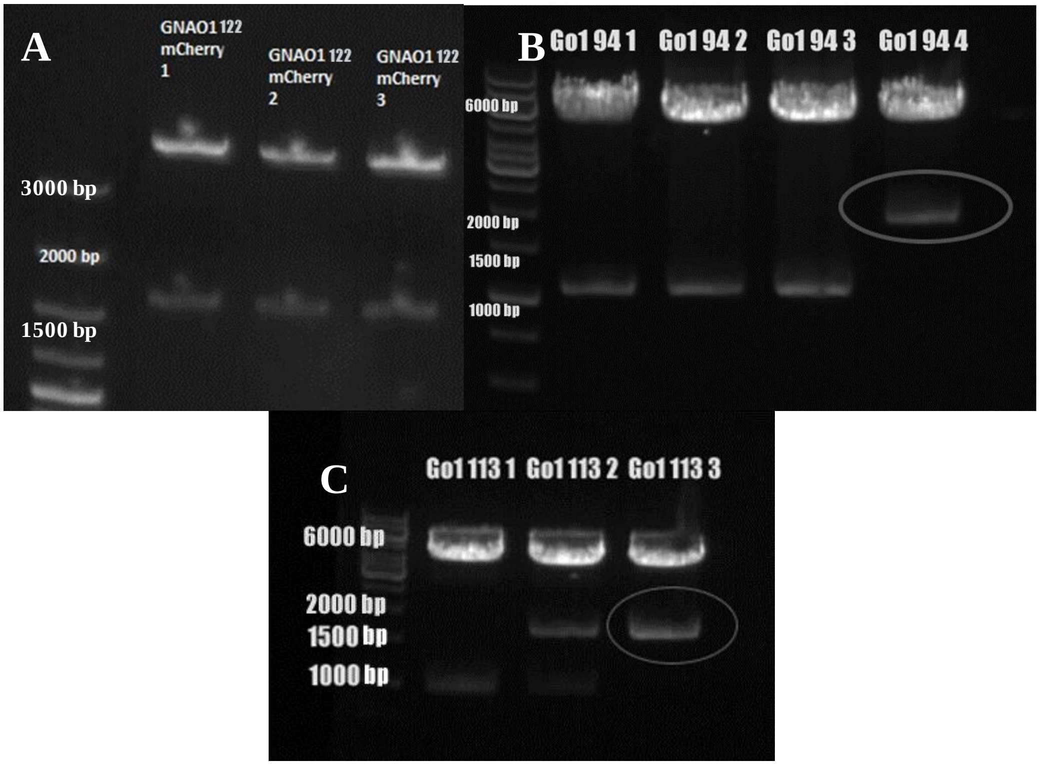
A
GNAO1 122 mCherry 1
GNAO1 122 mCherry 2
GNAO1 122 mCherry 3
3000 bp
2000 bp
1500 bp
B
Go1 94 1
Go1 94 2
Go1 94 3
Go1 94 4
6000 bp
2000 bp
1500 bp
1000 bp
C
Go1 113 1
Go1 113 2
Go1 113 3
6000 bp
2000 bp
1500 bp
1000 bp

Figure 3.3 Agarose gel electrophoresis image of double digested pcDNA3.1(-) plasmids carryingGNAO1 genes labeled with mCherry either from (A) 122nd, (B) 94th, or (C) 113th aminoacids. On (A) 100 bp Plus DNA Ladder (Cat. Num. #SM0321), on (B) and (C) Thermo Scientific GeneRuler 1 kb DNA Ladder (Cat. Num. #SM0311) was used.

Since pcDNA3.1(-) is 5428 bp, mCherry is 720 bp and GNAO1 is 1065 bp, all of the 122nd position constructs, Go1 94 “4”, and Go1 113 “3” were in their expected area as seen on Figure 3.3. Further validations were done via sequencing. Coding sequences of mentioned plasmids were given in Appendix F.

3.1.3. Tagging GNAI3 gene with mCherry from E122, L91, and G60 via PCR Integration Method

mCherry gene was amplified with flanking ends specific for the positions E122-L123, L91-K92, and G60-Y61 on GNAI3 protein. Primers used in these amplifications were given in Appendix B.

These amplified genes with flanking ends were used as primer sets for PCR integration. GNAI3 gene located in pcDNA3.1(-) was used as the template for this reaction. Products were treated with DpnI, and transformed to competent XL-1 Blue bacteria. The other day colonies were observed for all of the constructs.

Three of the colonies’ plasmids were isolated and double digested with KpnI and EcoRI restriction enzymes. Digested plasmids are run on agarose gel to confirm that they carry mCherry gene.

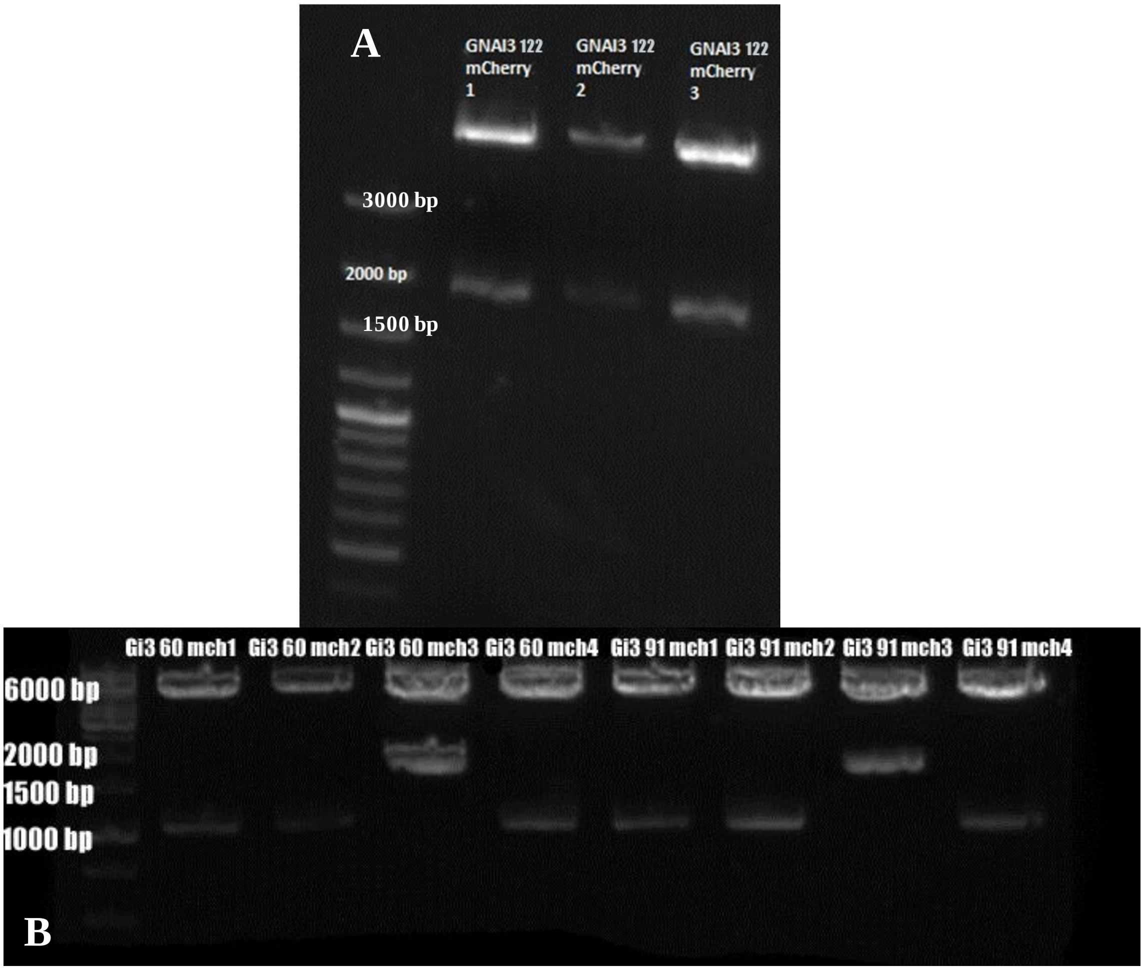
A
GNAI3 122 mCherry 1
GNAI3 122 mCherry 2
GNAI3 122 mCherry 3
3000 bp
2000 bp
1500 bp
Gi3 60 mch1
Gi3 60 mch2
Gi3 60 mch3
Gi3 60 mch4
Gi3 91 mch1
Gi3 91 mch2
Gi3 91 mch3
Gi3 91 mch4
6000 bp
2000 bp
1500 bp
1000 bp
B

Figure 3.4 Agarose gel electrophoresis image of double digested pcDNA3.1(-) plasmids carrying GNAI3 genes labeled with mCherry either from (A) 122nd, or (B) 91st and 60th aminoacids. On (A) 100 bp Plus DNA Ladder (Cat. Num. #SM0321), on (B) Thermo Scientific GeneRuler 1 kb DNA Ladder (Cat. Num. #SM0311) was used.

Since pcDNA3.1(-) is 5428 bp, mCherry is 720 bp and GNAI3 is 1065 bp, all of 122nd position constructs, GI3 60 mch3, and GI3 91 mch3 were in their expected area as seen on Figure 3.4. Further validations were done via sequencing. Coding sequences of mentioned plasmids were given in Appendix F.

3.1.4. Tagging D2 Receptor gene with EGFP from Carboxyl-Terminus via PCR Integration Method

EGFP gene was amplified with flanking ends specific for the end of the D2R coding sequence and right after its position in the pcDNA3.1(-). The position of D2R gene was determined by sequencing which was given in Appendix F. Primers were also designed based on this sequence information and were given in Appendix B.

This product was the primer set for PCR integration method. D2R gene in pcDNA3.1(-) was used as the template. Product of PCR integration was treated with DpnI, and immediately after this treatment, product was transformed to competent XL-1 Blue bacteria. The day after colonies observed on the selective LB plate.

Three of the colonies were chosen randomly from the plate and their plasmids were isolated and double digested with SalI and AflII restriction enzymes. To see if the inserts were tagged with EGFP, digested plasmids were run on agarose gel.

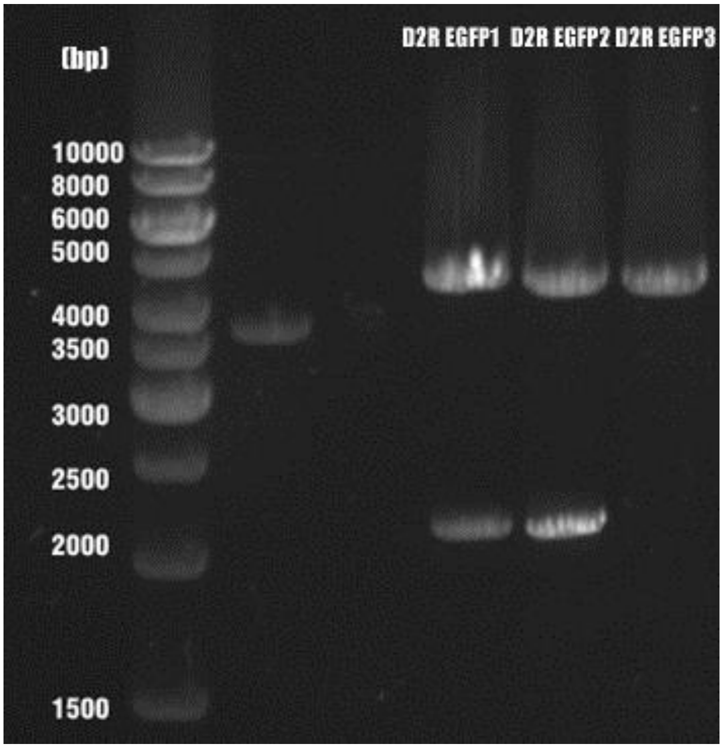
(bp)
10000
8000
6000
5000
4000
3500
3000
2500
2000
1500
D2R EGFP1
D2R EGFP2
D2R EGFP3

Figure 3.5 Agarose gel electrophoresis image of double digested pcDNA3.1(-) plasmids carrying D2R genes labeled with EGFP from its carboxyl terminus. Thermo Scientific GeneRuler 1 kb DNA Ladder (Cat. Num. #SM0311) was used. Unlabeled wells belong to another study.

Since pcDNA3.1(-) is 5428 bp, EGFP is 720 bp and D2R is 1332 bp, D2R EGFP 1 and 2 were in their expected area as seen on Figure 3.5. Further validations were done via sequencing. Coding sequences of mentioned plasmids were given in Appendix F.

3.2. Imaging Studies

To see whether fluorescent labeling of G_αO1 and G_αI3 give signal, if present, observe their signals' positions on the cell, and consequently investigating if they were interacting with D2R or not, N2a cells were transfected alone with labeled G protein α subunits or co-transfected with G protein α subunits labeled with mCherry and D2R labeled with EGFP using Lipofectamine™ LTX with Plus reagent. Also, some of the constructs were transfected to HEK293 cells alone with labeled G protein α subunits or co-transfected with G protein α subunits labeled with mCherry and D2R labeled with EGFP.

Both N2a and HEK293 cell lines were mammalian and were chosen for comparison for two reasons. First, N2a line is derived from *Mus musculus* nerve cells and gives the correct environment for D2R and their G proteins. However, secondly, since they also contain internal D2Rs and G proteins, impairments in modified proteins' positioning and targeting may occur. Also, labeled proteins in this study may also couple with internal ones, resulting in decrease in FRET signal. HEK293 cells are derived from human embryonic kidney tissue and do not express D2R and their G proteins at their natural conditions.

After transfection, cells were incubated for two days and their signals were gathered via spinning disc confocal microscope with several different filter configurations. Co-transfected cells' FRET channel images were further processed via PixFRET plugin of Image J as described in methodology.

FRET channel images were processed to develop a final FRET efficiency image and they were artificially colored by PixFRET depending on their efficiency ranges. As referenced on the calibration bars on these images, blue pixels stand for the range of 1-10% FRET efficiency, green pixels are for 11-20%, yellow pixels are for 21-30%, red pixels are for 31-40%, and white pixels are for the range of 41-50% FRET efficiencies.

3.2.1. GNAO1 Constructs in N2a Cells

3.2.1.1. Validations of Signals for Single Transfections

GNAO1 labeled with mCherry from its 122nd, 113th, and 94th positions were transfected to N2a cells and then imaged with spinning disc confocal microscope to investigate their signals' existence, positions, and quality.

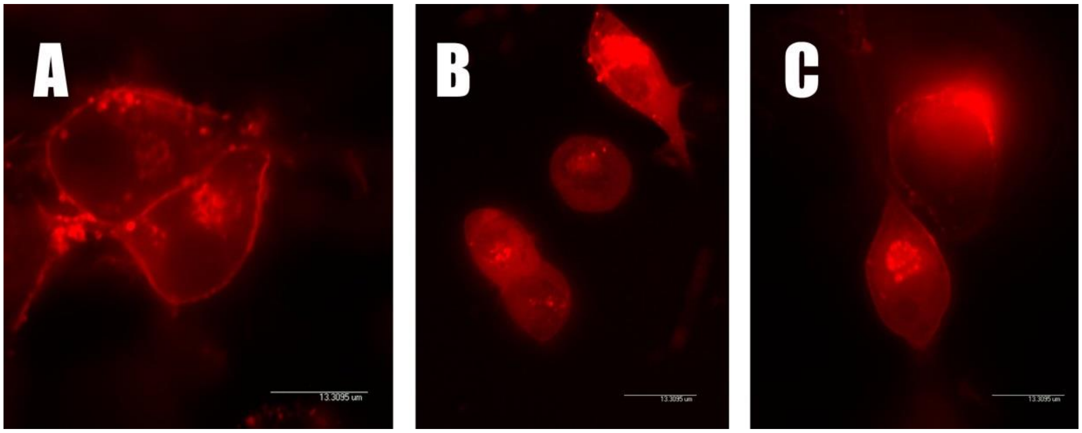

Figure 3.6 Spinning disc confocal fluorescent microscopy images of N2a cells transfected with 500 ng of (A) GNAO1 labeled with mCherry from its 122nd aminoacid, (B) GNAO1 labeled with mCherry from its 113th aminoacid, and (C) GNAO1 labeled with mCherry from its 94th aminoacid. Excitation is at 583 nm. 63x.

As seen on Figure 3.6, signals were present, but except for 122nd position of GNAO1, labeled proteins were expressed in the cytosol (B) and (C) of Figure 3.6, which was not expected and might imply that labeling GNAO1 from 113th and 94th positions were interfering with targeting of GNAO1 protein to the membrane. However, 94th position tagging expressed well on the membrane in addition to the cytosolic expression. On the other hand, as seen on (A), 122nd position labeling of GNAO1 is targeted mostly membrane and visible in vesicles of transportation.

3.2.1.2. Co-localization and FRET studies of GNAO1 Constructs with D2R EGFP in N2a Cells

GNAO1 constructs were co-transfected to N2a cells with D2R labeled with EGFP to see if they co-localize with each other and/or give FRET signal to show expected coupling of inhibitory GNAO1 protein with GPCR D2R.

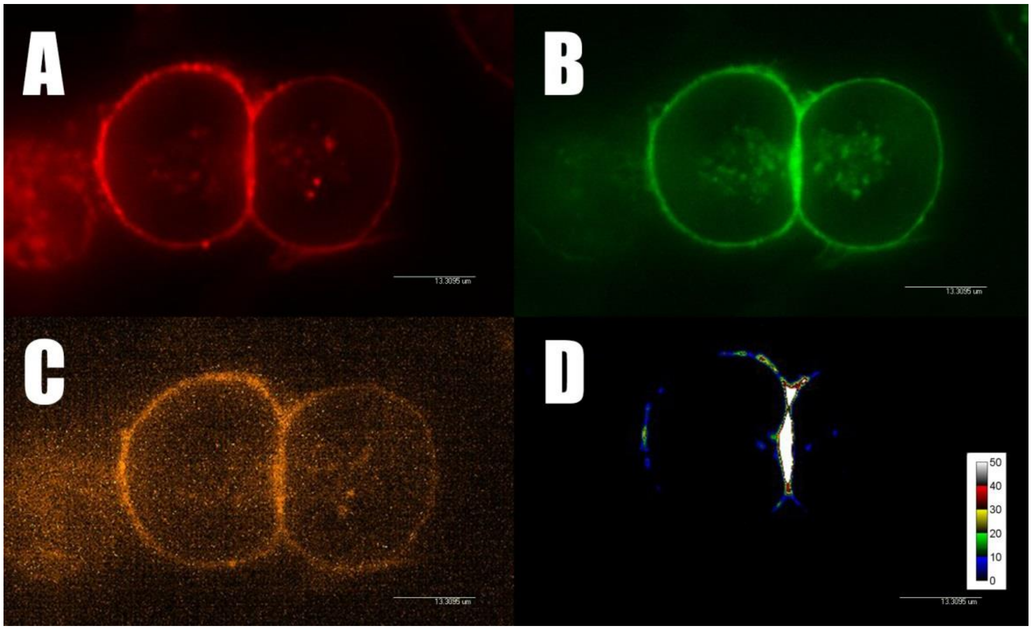

Figure 3.7 Spinning disc confocal fluorescent microscopy images of N2a cells co-transfected with 500 ng of D2R labeled with EGFP from its carboxyl end and GNAO1 labeled with mCherry from its 122nd aminoacid. (A) Demonstrates the localization of GNAO1 122 with mCherry channel excitation at 583 nm (B) Demonstrates the localization of D2R with EGFP channel excitation at 482 nm.. (C) FRET signal. (D) FRET signal efficiency. 63x. Color blue represents 0-10%, green 10-20%, yellow 20-30%, red 30-40%, and white 40-50% FRET efficiency.

Figure 3.7 shows successful labeling of D2R-EGFP, and GNAO1-122-mCherry as expected on the cell membrane as a thin line and on the cytoplasm in the vesicles. On (C) part of Figure 3.7, pixels where FRET occurs were seen being mostly on cell membrane and in the cytoplasm near to the nuclei where synthesized proteins' transportation and final modifications were done in ER and Golgi apparatus. On (D) FRET signal efficiency was observable mostly on the membrane.

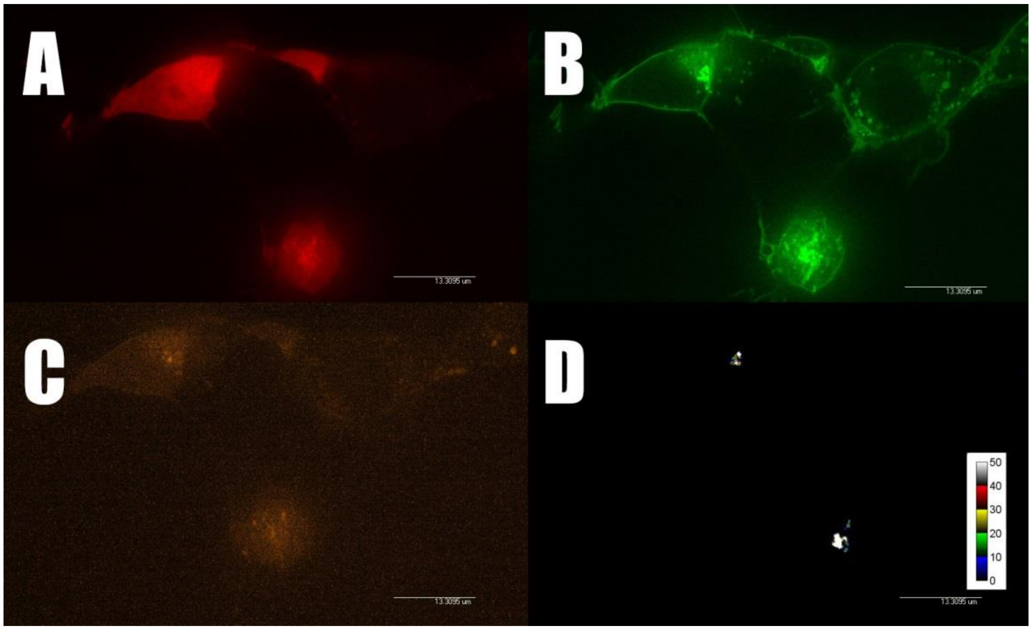

Figure 3.8 Spinning disc confocal fluorescent microscopy images of N2a cells co-transfected with 500 ng of D2R labeled with EGFP from its carboxyl end and GNAO1 labeled with mCherry from its 113th aminoacid. (A) Demonstrates the localization of GNAO1 113 with mCherry channel excitation at 583 nm. (B) Demonstrates the localization of D2R with EGFP channel excitation at 482 nm. (C) FRET signal. (D) FRET signal efficiency. 63x. Color blue represents 0-10%, green 10-20%, yellow 20-30%, red 30-40%, and white 40-50% FRET efficiency.

Figure 3.8 demonstrates labeling of D2R-EGFP, and GNAO1-113-mCherry. However, GNAO1-113-mCherry was highly expressed in the ER and Golgi apparatus and this was not expected as GNAO1 codes for a membrane protein. On (C) pixels where FRET occurs were seen mostly on the cytosol and on (D) FRET signal efficiency were seen on very small fraction of the cell with a quite low FRET efficiency level. This might be caused by improper positioning of mCherry within the protein causing prevention of targeting the protein and coupling with the D_2 receptor.

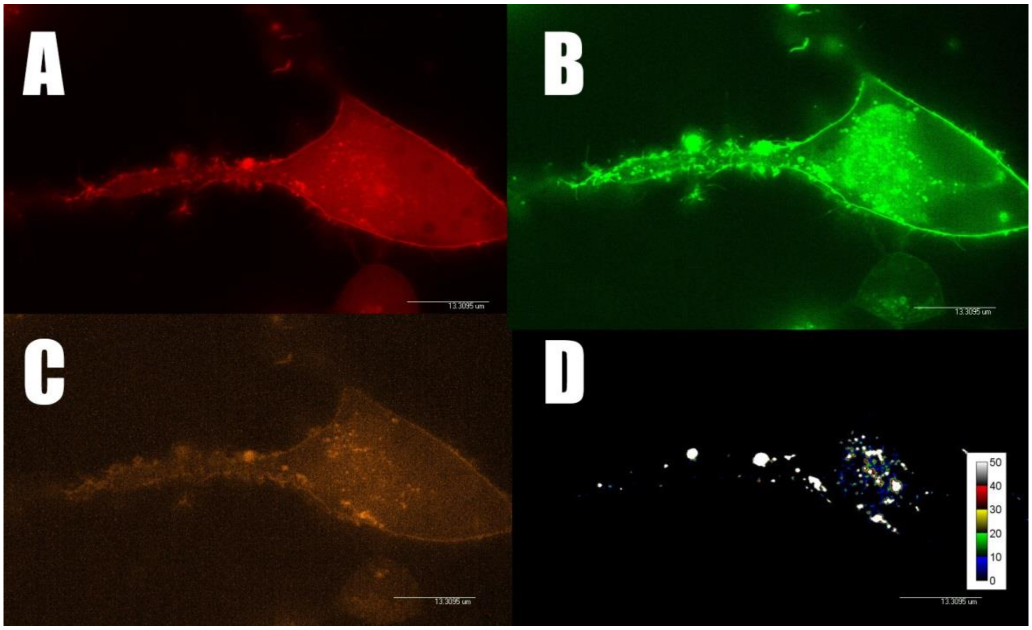

Figure 3.9 Spinning disc confocal fluorescent microscopy images of N2a cells co-transfected with 500 ng of D2R labeled with EGFP from its carboxyl end and GNAO1 labeled with mCherry from its 94th aminoacid. (A) Demonstrates the localization of GNAO1 94 with mCherry channel excitation at 583 nm. (B) Demonstrates the localization of D2R with EGFP channel excitation at 482 nm. (C) FRET signal. (D) FRET signal efficiency. 63x. Color blue represents 0-10%, green 10-20%, yellow 20-30%, red 30-40%, and white 40-50% FRET efficiency.

Figure 3.9 demonstrates labeling of D2R-EGFP, and GNAO1-94-mCherry. However, GNAO1-94-mCherry was also mostly expressed in the cytosol as well as membrane and this was not expected and could be caused by positioning of mCherry causing impairments in targeting. On (C) pixels where FRET occurs were seen both on the membrane and cytosol. However, as seen on (D), when FRET efficiency was calculated, most of the signal efficiency was seen at points where ER and Golgi apparatus might be present. This may imply early coupling of the expressed proteins. This unexpected result might be caused by positioning of mCherry within the protein causing impairments in labeled G proteins for coupling and targeting with the D_2 receptor.

3.2.2. GNAI3 Constructs in N2a Cells

3.2.2.1. Validations of Signals for Single Transfections

GNAI3 labeled with mCherry from its 122nd, 91st, and 60th positions were transfected to N2a cells and then imaged with spinning disc confocal microscope to investigate their signals' existence, positions, and quality.

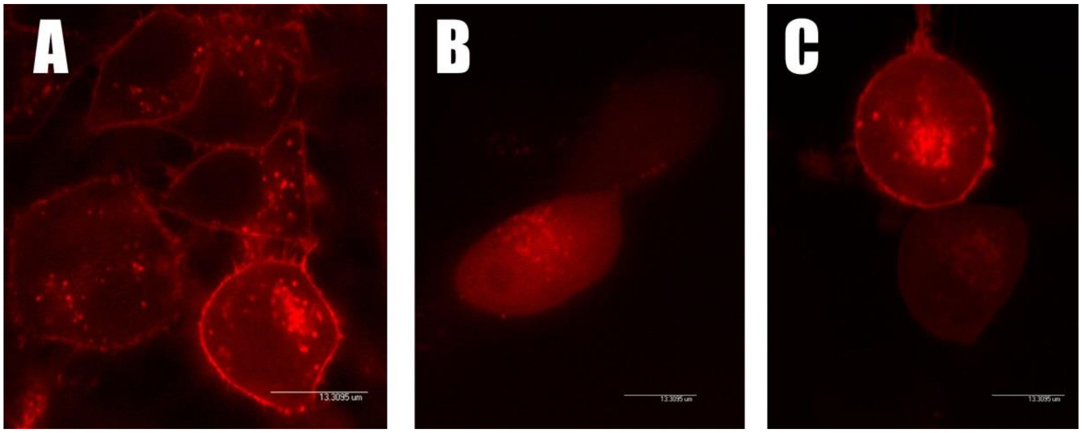

Figure 3.10 Spinning disc confocal fluorescent microscopy images of N2a cells transfected with 500 ng of (A) GNAI3 labeled with mCherry from its 122nd aminoacid, (B) GNAI3 labeled with mCherry from its 91st aminoacid, and (C) GNAI3 labeled with mCherry from its 60th aminoacid. Excitation is at 583 nm. 63x.

As seen on Figure 3.10 part (A), 122nd position labeling of GNAI3 formed a fine line on the cell membrane and signal was also present at vesicles. On part (B) cytosolic 91st position labeling expression was seen, and on (C) 60th position labeling formed a strong cell membrane signal whereas most of the signal was coming from vesicles and cytoplasm. Neither cytosolic expression, nor excess vesicle signal without membrane signal was not expected and this might imply that labeling GNAI3 from 91st and 60th positions were interfering with targeting of GNAI3 protein to the membrane.

3.2.2.2. Double Transfection and FRET studies of GNAI3 Constructs with D2R EGFP in N2a Cells

GNAI3 constructs were co-transfected to N2a cells with D2R labeled with EGFP to see if they co-localize with each other and/or give FRET signal to show expected coupling of inhibitory GNAI3 protein with GPCR D2R.

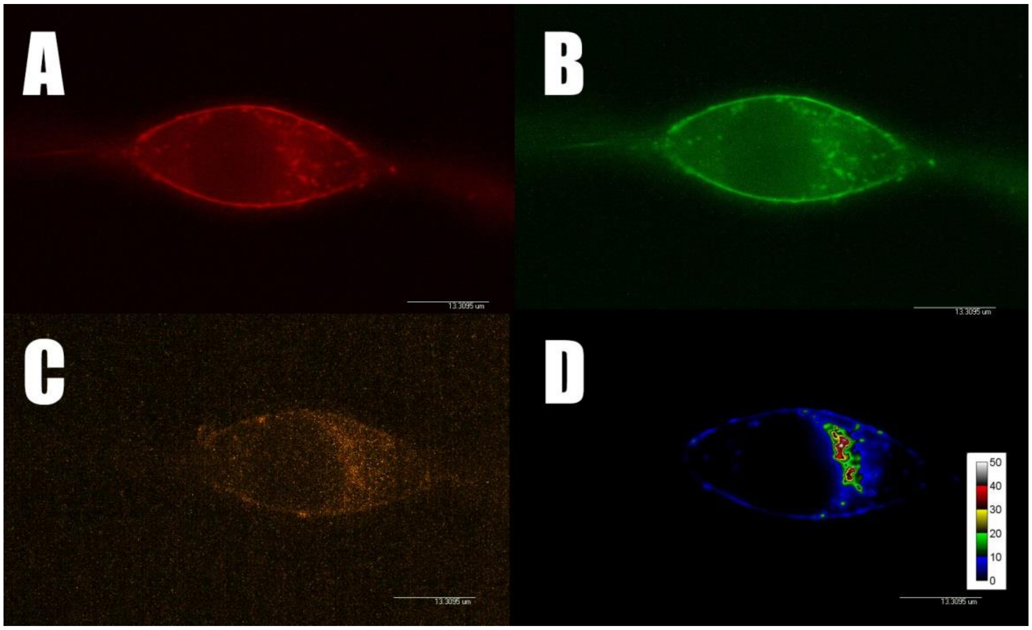

Figure 3.11 Spinning disc confocal fluorescent microscopy images of N2a cells co-transfected with 500 ng of D2R labeled with EGFP from its carboxyl end and GNAI3 labeled with mCherry from its 122nd amino acid. (A) Demonstrates the localization of GNAI3 122 with mCherry channel excitation at 583 nm. (B) Demonstrates the localization of D2R with EGFP channel excitation at 482 nm. (C) FRET signal. (D) FRET signal efficiency. 63x. Color blue represents 0-10%, green 10-20%, yellow 20-30%, red 30-40%, and white 40-50% FRET efficiency.

Figure 3.11 shows successful labeling of D2R-EGFP, and GNAI3-122-mCherry as expected on the cell membrane as a thin line and on the cytoplasm in the vesicles. On (C) part of Figure 3.11, pixels where FRET occurs were seen being mostly on cell membrane and in the cytoplasm near to the nuclei where synthesized proteins' transportation and final modifications were done in ER and Golgi apparatus. On (D) processed FRET efficiency image was presented and FRET signal efficiency was seen lower on the membrane and higher on the cytosolic elements, such as ER and Golgi apparatus which is a strong implication that these proteins might be coupling before targeting to the membrane was complete.

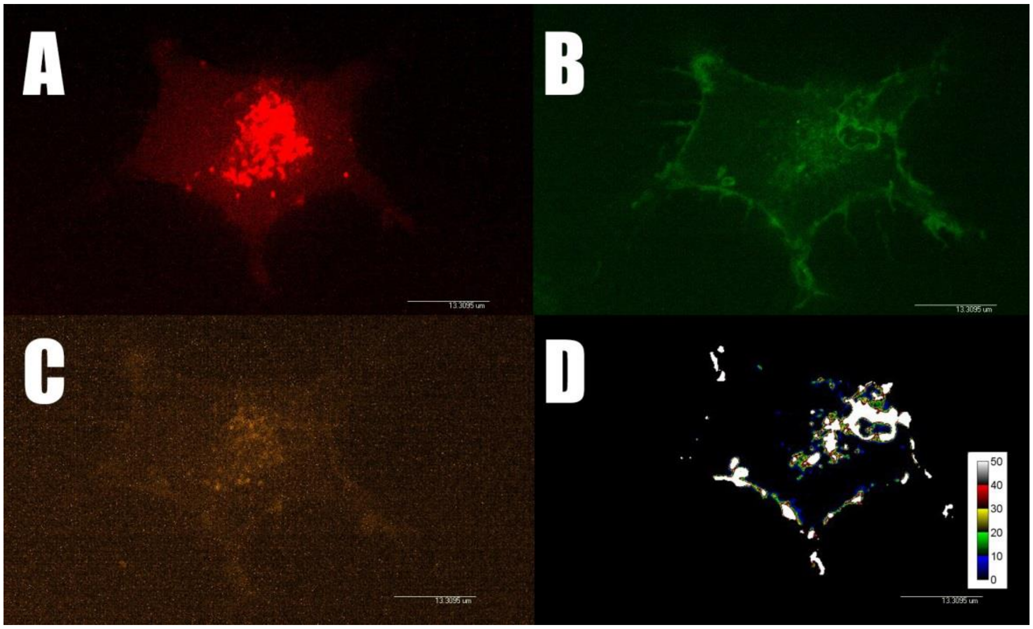

Figure 3.12 Spinning disc confocal fluorescent microscopy images of N2a cells co-transfected with 500 ng of D2R labeled with EGFP from its carboxyl end and GNAI3 labeled with mCherry from its 91st aminoacid. (A) Demonstrates the localization of GNAI3 91 with mCherry channel excitation at 583 nm. (B) Demonstrates the localization of D2R with EGFP channel excitation at 482 nm. (C) FRET signal. (D) FRET signal efficiency. 63x. Color blue represents 0-10%, green 10-20%, yellow 20-30%, red 30-40%, and white 40-50% FRET efficiency.

Figure 3.12 demonstrates labeling, co-localization sites and FRET signal efficiency of D2R-EGFP, and GNAI3-90-mCherry. GNAI3-90-mCherry was observed mostly expressed in vesicles and cytosol more than membrane which was not expected as G protein α I3 subunit was a membrane protein. On (C) pixels where FRET occurs were seen on the cytosol and membrane. On (D) processed FRET efficiency signal image was presented, most of the effective FRET seemed to be occurring on the membrane and vesicles. This might be caused by early coupling of Gi3 protein with the D_2 receptor.

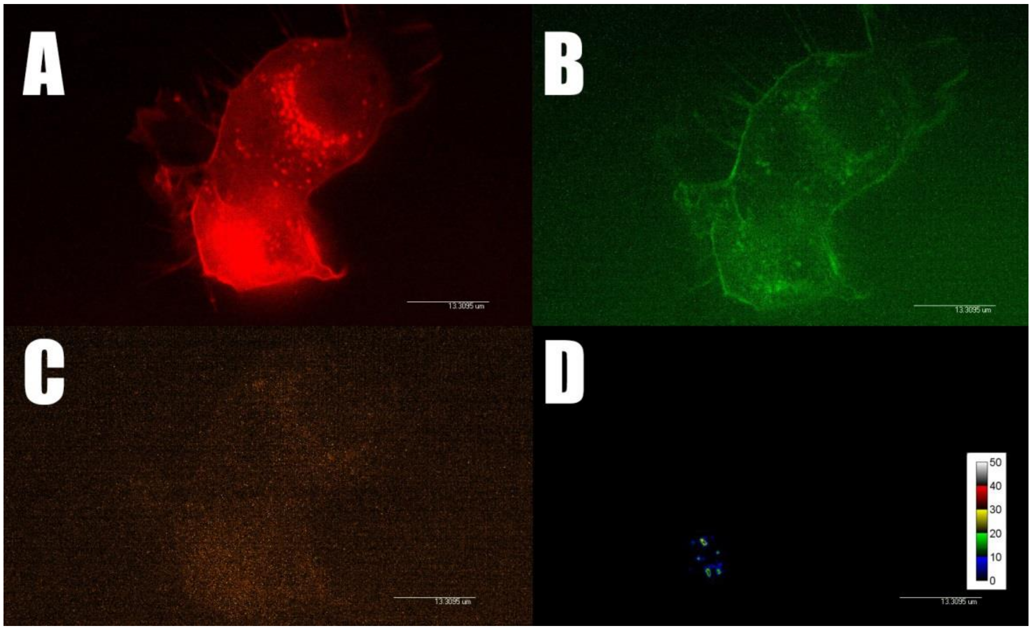

Figure 3.13 Spinning disc confocal fluorescent microscopy images of N2a cells co-transfected with 500 ng of D2R labeled with EGFP from its carboxyl end and GNAI3 labeled with mCherry from its 60th amino acid. (A) Demonstrates the localization of GNAI3 60 with mCherry channel excitation at 583 nm. (B) µDemonstrates the localization of D2R with EGFP channel excitation at 482 nm. (C) FRET signal. (D) FRET signal efficiency. 63x. Color blue represents 0-10%, green 10-20%, yellow 20-30%, red 30-40%, and white 40-50% FRET efficiency.

Figure 3.13 demonstrates labeling of D2R-EGFP, and GNAI3-60-mCherry. However, GNAI3-60-mCherry signal was coming mostly from vesicles and cytosol not only membrane and this was not expected and maybe caused by positioning of mCherry causing impairments in targeting. On (C) pixels where FRET occurs were seen and this imaged was processed to see the efficiency of FRET signal on (D) as they are within the 1-10% range which was very low. This might be caused by positioning of mCherry within the protein causing prevention of proper coupling with the D_2 receptor.

3.2.3. GNAO1 and GNAI3 Constructs in HEK293 Cells

To be able to observe the cytosolic environment's effects on the expressed proteins interactions and positioning, selected G protein constructs were co-transfected to HEK293 cells with D2R tagged with EGFP from its C-tail. They were then imaged and observed images were processed to gather their FRET efficiencies.

3.2.3.1. Double Transfection and FRET studies of G protein Constructs with D2R EGFP in HEK293 Cells

GNAI3 tagged from 122nd, GNAO1 tagged from 94th and 113th were co-transfected to HEK293 cells with D2R labeled with EGFP to see if they co-localize with each other and/or give FRET signal to show expected coupling of inhibitory GNAO1 and GNAI3 proteins with GPCR D2R.

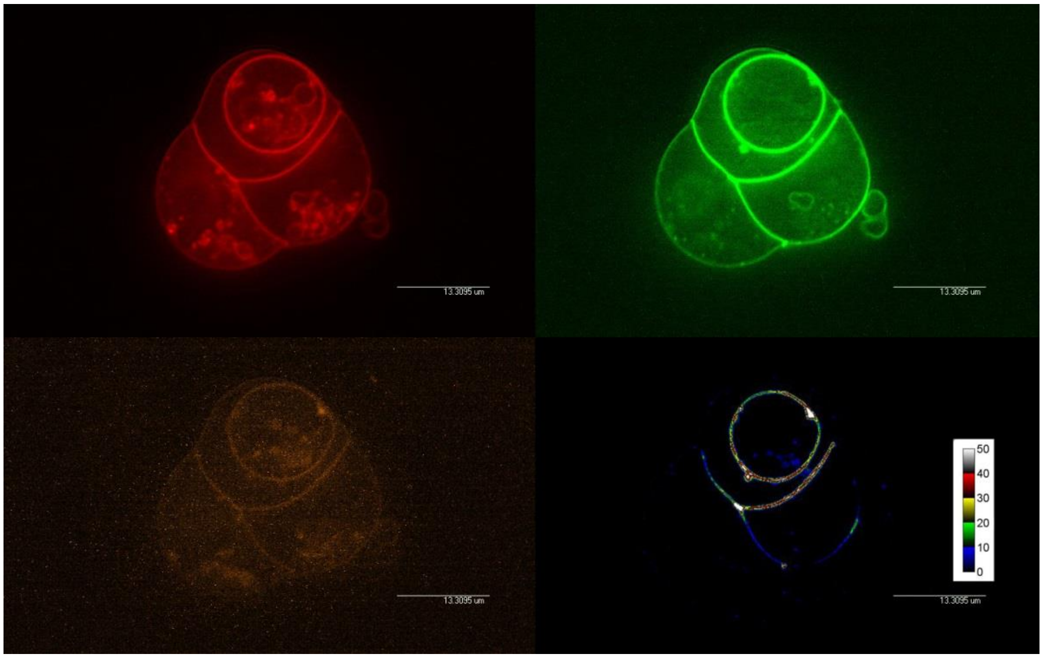

Figure 3.14 Spinning disc confocal fluorescent microscopy images of HEK293 cells co-transfected with 500 ng of D2R labeled with EGFP from its carboxyl end and GNAI3 labeled with mCherry from its 122nd aminoacid. (A) Demonstrates the localization of GNAI3 122 with mCherry channel excitation at 583 nm. (B) Demonstrates the localization of D2R with EGFP channel excitation at 482 nm. (C) FRET signal. (D) FRET signal efficiency. 63x. Color blue represents 0-10%, green 10-20%, yellow 20-30%, red 30-40%, and white 40-50% FRET efficiency.

Figure 3.14 shows successful labeling of D2R-EGFP, and GNAI3-122-mCherry as expected on the cell membrane as a thin line and for GNAI3, on the cytoplasm in the vesicles. Vesicles might be the result of over expression caused by the promoter of pcDNA3.1(-). On (D) part of Figure 3.14, pixels where FRET occurs were seen being mostly on cell membrane as a thin line, strengthening the 122nd position for labeling the Gα protein without interfering the positioning and interaction with each other.

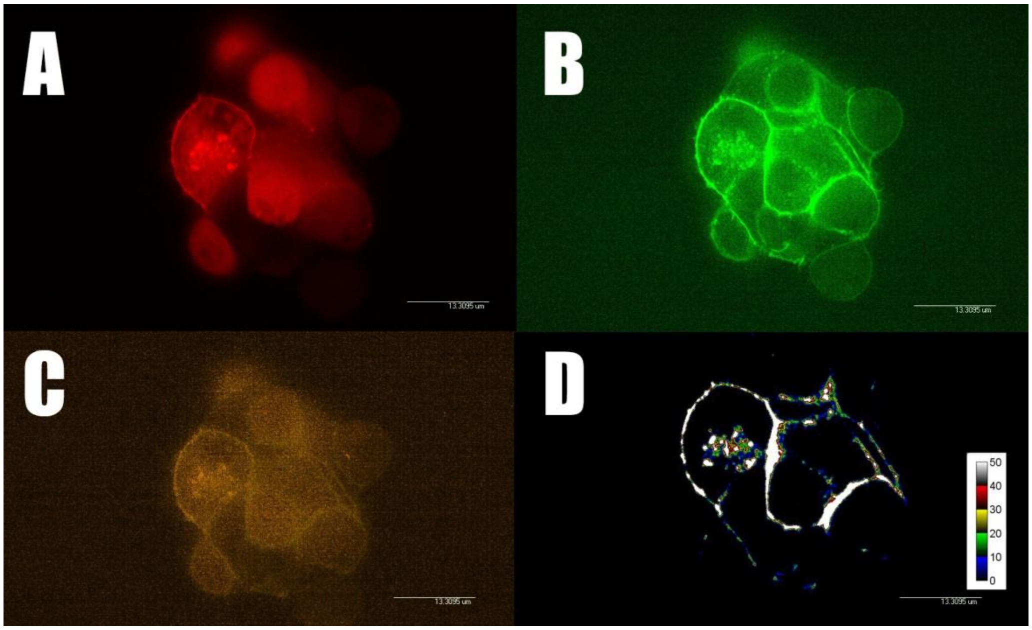

Figure 3.15 Spinning disc confocal fluorescent microscopy images of HEK293 cells co-transfected with 500 ng of D2R labeled with EGFP from its carboxyl end and GNAO1 labeled with mCherry from its 113th aminoacid. (A) Demonstrates the localization of GNAO1 113 with mCherry channel excitation at 583 nm. (B) Demonstrates the localization of D2R with EGFP channel excitation at 482 nm. (C) FRET signal. (D) FRET signal efficiency. 63x. Color blue represents 0-10%, green 10-20%, yellow 20-30%, red 30-40%, and white 40-50% FRET efficiency.

Figure 3.15 demonstrates labeling of D2R-EGFP, and GNAO1-113-mCherry. GNAO1-113-mCherry was again expressed across cytoplasm as it was when expressed in N2a. On (D) pixels where FRET occurs were better than when expressed in N2a cell line which strengthens the idea that the existence of internal D2R and G proteins in the N2a cells might be interfering with the positioning and targeting of modified proteins in the cell.

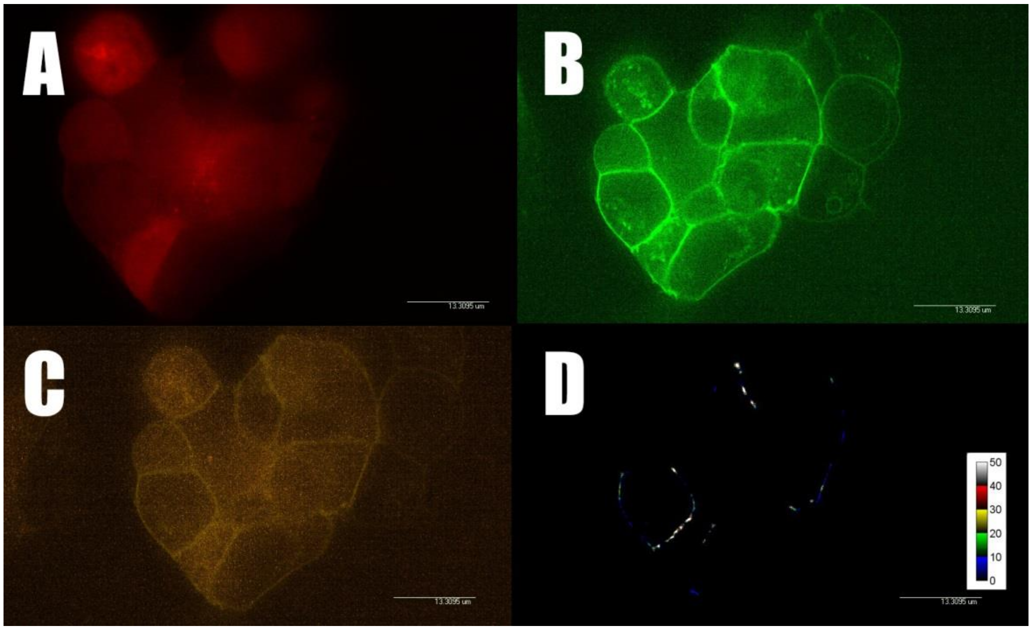

Figure 3.16 Spinning disc confocal fluorescent microscopy images of HEK293 cells co-transfected with 500 ng of D2R labeled with EGFP from its carboxyl end and GNAO1 labeled with mCherry from its 94th aminoacid. (A) Demonstrates the localization of GNAO1 94 with mCherry channel excitation at 583 nm (B) Demonstrates the localization of D2R with EGFP channel excitation at 482 nm. (C) FRET signal. (D) FRET signal efficiency. 63x. Color blue represents 0-10%, green 10-20%, yellow 20-30%, red 30-40%, and white 40-50% FRET efficiency.

On Figure 3.16 GNAO1-94-mCherry could be observed on part (A) as a cytosolic protein which was not expected and maybe caused by positioning of mCherry causing impairments in targeting. D2R-EGFP can be seen on part (B) as a smooth line on cell membrane, and On (D) pixels where FRET occurs are seen as with weak efficiency, on the other hand, far better than its efficiency on N2a cells as this time image shows coupling had occurred on the membrane as expected.

3.3. Functionality Assays

Effects of introduced fluorophore molecules to D2R, and 122nd position of GNAO1 and GNAI3 were tested as they were seemed to be the most proper positions for fluorophore tagging via cAMP-Glo™ assay. Assay determines the cAMP levels in the cells after activating D2R via its agonist quinpirole. Before assessing the test, cAMP levels were raised with forskolin.

EGFP labeled D2R from its carboxy end was tested in a study named "The Functional Assessment of Fluorescently Tagged Adenosine A_{2A} and Dopamine D_2 Receptors and Qualitative Analysis of Dimerization of Adenosine A_{2A} and Dopamine D_2 Receptors by Using FRET" by Selin Akkuzu and it was concluded that carboxy-end EGFP labeled D2R was equally functional as wild-type receptors.

3.3.1. Functionality Assays of 122nd Position Labeling of GNAI3 and GNAO1 with mCherry

Both GNAO1 and GNAI3 proteins labeled with mCherry from their 122nd positions were assessed for their effects on functionality of their receptors D2R over their wild type versions.

As D2R acts inhibitory over cAMP production, decrease in the cAMP levels is associated with the activity of the receptor. As Figure 3.17 shows, GNAI3 wild type and labeled with mCherry from 122nd aminoacid nearly as functional when there were only wildtype D2Rs present which were expressed by the cell line itself. However, when wild type D2R was also transfected to prevent the premature saturation of the D2Rs expressed by the cell line, cAMP levels reduced dramatically at the same ratio. Therefore, together with the results presented in the Figure H.1 (Appendix H), it can be concluded that GNAI3 labeled from 122nd amino acid with mCherry is as functional as its wild type, and their activity was increased proportional to the wild type D2R available for them to couple in the environment.

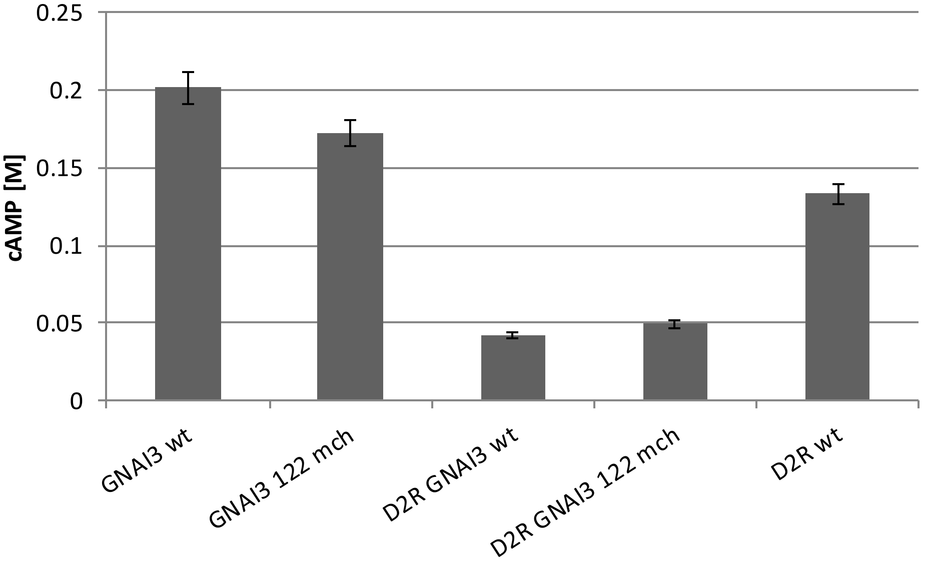

Figure 3.17 cAMP levels of N2a cells after transfecting or co-transfecting them with GNAI3 wt, GNAI3 122 mch, D2R wt + GNAI3 wt, D2R wt + GNAI3 122 mch, and D2R wt alone.

However, 122nd position mCherry labeled GNAO1 protein's results were not as expected as wild type and labeled ones once showed dramatic decrease in D2R activity when co-transfected with it (Figure H.2) and over activity of internal D2Rs when GNAO1 wild type transfected alone (Figure H.1). Detailed results were presented in Appendix H and it was concluded that more trials should have been done before reaching a certain conclusion.

CHAPTER 4

CONCLUSION AND FUTURE PERSPECTIVE

The aim of the present study was to optimize the labeling of inhibitory G protein α subunits GNAO1 (Go_1) and GNAI3 (Gi_3) for the first time in order to be able to detect and investigate molecular interactions between D2R and inhibitory G-proteins.

To accomplish labeling and detecting the signals and consequently investigate FRET signals, D2R was labeled with EGFP from its C-terminus and G protein α subunits were labeled and observed with mCherry from their three internal locations corresponding to places between alpha helices αB and αC, between alpha helices αA and αB, and to the linker between helical and GTPase domain of G protein α right after αA helix (122nd, 113th, and 94th positions for GNAO1; 122nd, 91st, and 60th positions for GNAI3 proteins, respectively) successfully.

To investigate FRET signals and their efficiencies, co-transfections of the labeled proteins to *Mus musculus* Neuro-2a (N2a) are done. To see whether cellular environment affects their expression and interaction or not, co-transfections to HEK293 cells are done. Imaging had been done via spinning disc confocal microscopy. The images of the cells were then analyzed by a computer application pixFRET for their FRET signal efficiencies.

Both N2a and HEK293 cell lines are mammalian and are chosen for comparison for two reasons. First, N2a line is derived from *Mus musculus* nerve cells and gives the correct environment for D2R and their G proteins. However, secondly, since they also contain internal D2Rs and G proteins, impairments in modified proteins' positioning and targeting might occur. Also, labeled proteins in this study may also couple with internal ones, resulting in decrease in FRET signal. HEK293 cells are derived from human embryonic kidney tissue and do not express D2R and their G proteins at their natural conditions.

When labeled GNAO1 and GNAI3 proteins' signals either in N2a investigated, 122nd position for both of the proteins were seemed to be targeted more properly (Figure 3.6, 3.7, 3.10, 3.11 and 3.14). Other positions were either totally expressed in cytosol or were giving more signal from vesicles instead of membrane. This is implying that tagging GNAO1 and GNAI3 from between αA-αB and between helical and GTPase domains (113th and 94th positions for GNAO1 and 91st and 60th positions for GNAI3) are causing impairments in positioning and targeting of the protein in the cell. GNAI3 protein's 122nd position labeling had been shown to be as functional as its wild type over the activity of their receptor D2R. GNAO1's 122nd position labeling and others' functionality predictions should be confirmed by assessing more functionality assays in future studies.

Also, signals investigated in HEK293 cells were more cleanly received from the membrane and in this cell line, signals coming from vesicles and cytoplasm were notably lower when compared to N2a cell line, which gives a hint that internal unlabeled D2Rs and G proteins are interfering with positioning, and targeting of these proteins. This should be analyzed and tested further by using organelle markers in future studies.

FRET signal efficiency was seemed to be higher when G protein α subunits are labeled from between αB-αC, and lowered dramatically when labeled from between αA-αB and between helical domain and GTPase domains. To make a statistically significant conclusion about labeled proteins' FRET efficiencies, it is obligatory to analyze more FRET set-ups.

Together with all of the results, this thesis gives an insight about how the behavior of G protein α subunits O1 and I3 differ and how their interactions with D2R is affected when these proteins are labeled from different positions and put under different conditions. This system can be used for analyzing interactions and behavior of various GPCRs with G-proteins. In addition, drug candidates and different agonists/antagonists can be applied to see the alterations in the behavior of the molecules. Moreover, Bimolecular Fluorescence Complementation (BiFC) assay can be applied to this system to study homo-/heterodimerizations and behaviors of various proteins in the presence of one another.

REFERENCES

Albertazzi, L., Arosio, D., Marchetti, L., Ricci, F., Beltram, F. (2009).Quantitative FRET analysis with the EGFP-mCherry fluorescent protein pair.*Photochemistry and Photobiology, 85,* 287-297. doi:10.1111/j.1751-1097.2008.00435.x

Alberts, B., Johnson, A., Lewis, J., *et al.* Molecular Biology of the Cell. 4th edition.(2002). Signaling through G-Protein-Linked Cell-Surface Receptors. *New York: Garland Science*. Available from: http://www.ncbi.nlm.nih.gov/books/NBK26912/ (last accessed on 10.04.2016)

Ballesteros, J. A., Shi, L., Javitch, J. A. (2001). Structural mimicry in G protein-coupled receptors: implications of the high-resolution structure of rhodopsin for structure-function analysis of rhodopsin-like receptors. *Mol Pharmacol, 60(1),* 1-19. doi:10.1124/mol.60.1.1

Beaulieu, J. M. & Gainetdinov, R. R. (2011).The Physiology, Signaling, and Pharmacology of Dopamine Receptors.*Pharmacol Rev, 63(1),* 182-217. doi:10.1124/pr.110.002642

Boute, N., Jockers, R., Issad, T. (2002). The use of resonance energy transfer in high-throughput screening: BRET versus FRET. *Trends Pharmacol Sci. 23(8),* 351-4.doi:10.1016/S0165-6147(02)02062-X

Bouvier, M. (2001).Oligomerization of G-protein-coupled transmitter receptors.*Nature Reviews. Neuroscience, 2,* 274-286. doi:10.1038/35067575

Brandt, D. R., Ross, E. M. (1985). GTPase activity of the stimulatory GTP-binding regulatory protein of adenylate cyclase, Gs. Accumulation and turnover of enzyme-nucleotide intermediates. *The Journal of Biological Chemistry 260 (1)*: 266–72.

Browne, M. (2010).Oprimizing Live Cell Confocal Imaging Webinar.*Andor*. http://www.andor.com/learning-academy/optimizing-live-cell-confocal-imaging-microscopy-and-analysis-webinar-by-dr-mark-browne

Catapano, L. A., Manji, H. K. (2007). G Protein-Coupled Receptor in Major Psychiatric Disorders.*Biochim Biophys Acta, 1768(4),* 976-993. doi: 10.1016/j.bbamem.2006.09.025

Chen, G., Li, X., He, G., Yu, Z., Luo, J., He, J., Huang, Z. (2015). Low expression of GNAI3 predicts poor prognosis in patients with HCC. *Int J Clin Exp Med, 8(11),* 21482-21486. ISSN:1940-5901/IJCEM0015465

Cherezov, V., Rosenbaum, D.M., Hanson, M.A., Rasmussen, S.G., Thian, F.S., Kobilka, T.S., Choi, H.J., Kuhn, P., Weis, W.I., Kobilka, B.K., Stevens, R.C. (2007). High-resolution crystal structure of an engineered human beta2-adrenergic G protein-coupled receptor.*Science,318*, 1258-1265.

Chung, K. Y., Rasmussen, S. G. F., Liu, T., Li, S., DeVree, B. T., Chae, P. S., Calinski, D., Kobilka, B. K., Woods Jr, V. L. & Sunahara R. K. (2011). Conformational changes in the G protein Gs induced by the β_2 adrenergic receptor. *Nature, 477,* 611-615. doi:10.1038/nature10488

Civelli O., Bunzow, J. R., Grandy, D. K. (1993). Molecular diversity of the dopamine receptors.*Annu. Rev. Pharmacol. Toxicol., 32*, 281-307.

Clegg, R. M. (1995). Fluorescence resonance energy transfer.*Current Opinion in Biotechnology*.doi:10.1016/0958-1669(95)80016-6

Denis, C., Sauliere, A., Galandrin, S., Senard, J. M., Gales, C. (2012).Probing heterotrimeric G protein activation: applications to biased ligands.*Curr Pharm Des 18(2),* 128-144. PMCID: PMC3389521

Dorsam, R. T. & Gutkind, J. S. (2007).G-protein-coupled receptors and cancer.*Nat Rev Cancer, 7(2),* 79-94. doi:10.1038/nrc2069

Feige, J., Sage, D., Wahli, W., Desvergne, B., Gelman, L. (2005). PixFRET, an ImageJ plug-in for FRET calculation that can accommodate variations in spectral bleed-throughs. *Microscopy Research and Technique, 68,* 51-58. doi:10.1002/jemt.20215

Förster, T. (1946).Energiewanderung und Fluoreszenz.*Naturwissenschaften, 33(6),* 166-175. doi:10.1007/BF00585226

Fredriksson, R., Lagerström, M. C., Lundin, L.-G., and Schlöth, H. B. (2003). The G-protein coupled receptors in the human genome form five main families. Phylogenetic analysis, paralogon groups, and fingerprints.*Mol. Pharmacol.* 63, 1256–1272

Gales, C., Van Durm, J. J., Schaak, S., Pontier, S., Percherancier, Y., Audet, M., Paris, H., Bouvier, M. (2006).Probing the activation-promoted structural rearrangements in preassembled receptor-G-protein complexes.*Nat. Struct. Mol. Biol., 13,* 778-786

Gentry, P. R., Sexton, P.M., and Christopoulos, A. (2015).Novel allosteric modulators of G protein-coupled receptors.*The Journal of Biological Chemistry, 290,* 19478-19488. doi: 10.1074/jbc.R115.662759

Gibson, S. K. and Gilman, A. G. (2006). Gia and Gb subunits both define selectivity of G protein activation by a2-adrenergic receptors. *Proc. Natl. Acad. Sci., 103*, 212-217

Gibson DG. (2011). Enzymatic assembly of overlapping DNA fragments.*Methods in Enzymology*. 498: 349–361. doi:10.1016/B978-0-12-385120-8.00015-2

Giulietti, M., Vivenzio, V., Piva, F., Principato, G., Bellantuono, C., Nardi, B. (2014). How much do we know about the coupling of G-proteins to serotonin receptors? *Molecular Brain, 49(7).*doi:10.1186/s13041-014-0049-y

Holz, G. G., Kream, R. M., Speiegel, A., Dunlap, K. (1989). G Proteins Couple α-Adrenergic and GABAb Receptors to Inhibition of Peptide Secretion from Peripheral Sensory Neurons.*J Neurosci 9(2),* 657-666. PMCID: PMC4516394

Kimple, M. E., Neuman, J. C., Linnemann, A. K., Casey P. J. (2014). Inhibitory G proteins and their receptors: emerging therapeutic targets for obesity and diabetes. *Experimental & Molecular Medicine, 46,* e102. doi:10.1038/emm.2014.40

Kobilka, B. K. (2007). G protein coupled receptor structure and activation. *Biochimica et Biophysica Acta, 1768,* 794-807. doi:10.1002/anie.201302116

Kobilka, B. K. (2013). The Structural Basis of G-Protein-Coupled Receptor Signaling (Nobel Lecture).*Angew Chem Int Ed Engl.,* 52(25): 6380–6388. doi:10.1002/anie.201302116

Kristiansen, K. (2004). Molecular mechanisms of ligand binding, signaling, and regulation within the superfamily of G-protein-coupled receptors: molecular modeling and mutagenesis approaches to receptor structure and function. *Pharmacology & Therapeutics 103,* 21-80. doi:10.1016/j.pharmthera.2004.05.002

Kulkarni, N., Tang, S., Bhardway, R., Bernes, S., Grebe T. A. (2015). Progressive Movement Disorder in Brothers Carrying a GNAO1 Mutation Responsive to Deep Brain Stimulation.*Journal of Child Neurology,* 1-4. doi: 10.1177/0883073815587945

Lagerstrom MC, Schioth HB. (2008) Structural diversity of G protein-coupled receptors and significance for drug discovery.*Nat Rev Drug Discov, 7,* 339-57. doi:10.1038/nrd2518

Lin, H. H. (2013). G-protein-coupled receptors and their (Bio) chemical significance win 2012 Nobel Prize in Chemistry. *Biodemical Journal, 36,* 118-24. doi:10.4103/2319-4170.113233

Milligan, G., Bouvier, M. (2005).Methods to monitor the quaternary structure of G protein-coupled receptors.*FEBS Journal.*doi: 10.1111/j.1742-4658.2005.04731.x

Mirzadegan, T., Benko, G., Filipek, S., Palczewski, K. (2003). Sequence Analyses of G-Protein-Coupled Receptors; Similarities to Rhodopsin. *Biochemistry, 42(10),* 2759-67. doi:10.1021/bi027224

Missale, C., Nash, S. R., Robinson, S. W., Jaber, M., Caron, M. G. (1998). Dopamine Receptors: From Structure to Function. *Physiological Reviews 78(1)* 0031-9333/98

Neve K. A., Neve R. L., Fidcl S., Janowsky A., and Higgins G. A. (1991) lncreased abundance of alternatively spliced forms of D_2 dopamine receptor niRNA after denervation. *Proi,.Natl. ilcad. Sci., 88,* 2802-2806.

Neve, K. A., Seamans, J. K., Trantham-Davidson, H. (2004). Dopamine Receptor Signaling. *Journal of Receptors and Signal Transduction, 24:3,* 165-205. doi: 10.1081/RRS-200029981

O'Dowd, B. F. (1993). Structures of Dopamine Receptors.*Journal of Neurochemistry, 60(3),* 804-816.

Palczewski, K.; Kumasaka, T.; Hori, T.; Behnke, C.A.; Motoshima, H.; Fox, B.A.; Le Trong, I.; Teller, D.C.; Okada, T.; Stenkamp, R.E.; Yamamoto, M.; Miyano, M. (2000). Crystal structure of rhodopsin: A G protein-coupled receptor. *Science, 289,* 739-745.

Rasmussen, S. G. F., DeVree, B. T., Zou, Y., Kruse, A. C., Chung, K. Y., Kobilka, T. S., Thian, F. S., Chae, P.S., Pardon, E., Calinski, D., Mathiesen, J. M., Shah, S. T. A., Lyons, J. A., Caffrey, M., Gellman, S. H., Steyaert, J., Skiniotis, G., Weis, W. I., Sunahara, R. K. & Kobilka, B. K. (2011). Crystal structure of the β_2 adrenergiv receptor-Gs protein complex.*Nature, 477,* 549-555. doi: 10.1038/nature10361

Shcacham, S., Topf, M., Avisar, N., Glaser, F., Marantz, Y., Bar-Haim, S., Noiman, S., Naor, Z., Becker, O. M. (2001). Modeling the 3D structure of GPCRs from sequence.*Med Res Rev, 21(5),* 472-83. doi:10.1002/med.1019

Shimomura, O., Johnson, H. F., Saiga, Y. (1962). Ectraction, Purification and Properties of Aequorin, a Bioluminescent Protein from the Luminous Hydromedusan, Aequora. *Journal of Cellular and Comparative Physiology, 59(3),* 223-229.

Schöneberg, T., Schulz, A., Biebermann, H., Hermsdorf, T., Römpler, H., & Sangkuhl, K. (2004).Mutant G-Protein-coupled receptors as a cause of human diseases. doi:10.1016/j.pharmthera.2004.08.008

Shultz, W. (2007).Multiple Dopamine Functions at Different Time Courses.*Annu. Rev. Neurosci., 30,* 259-88. doi:10.1146/annurev.neuro.28.061604.135722

Tavares, V. L. R., Gordon, C. T., Zechi-Ceide, R. M., Kokitsu-Nakata, N. M., Vousin, N., Tan, T. Y., Heggie, A. A., Vendramini-Pittoli, S., Propst, E. J., Papsin, B. C., Torres, T. T., Buermans, H., Capelo, L. P., den Dunnen, J. T., Guion-Almedia, M. L., Lyonnet, S., Amiel, J., Passos-Bueno, M. R. (2015). Novel variants in GNAI3 associated with auriculocondylar syndrome strengthen a common dominant negative effect. *European Journal of Human Genetics, 23,* 481-485. doi:10.1038/ejhg.2014.132

Tewson, P. H., Quinn, A. M., Hughes, T. E. (2013). A Multiplexed Fluorescent Assay for Independent Second-Messenger Systems: Decoding GPCR Activation in Living Cells. *Journal of Biomolecular Screening 18(7),* 797-806.doi:10.1177/1087057113485427

Trzaskowski, B., Latek, D., Yuan, S., Ghoshdastider U., Debinski, A., and Filipek S. (2012), Action of Molecular Switches in GPCRs – Theoretical and Experimental Studies.*Current Medicinal Chemistry, 19,* 1090-1109. doi: 10.2174/092986712799320556

Venkatakrishnan, A. J., Deupi, X., Lebon, G., Tate, C. G., Schertler, G. F., & Babu, M. M. (2013).Molecular signatures of G-protein-coupled receptors.*Nature, 494,* 185-194. doi:10.1038/nature11896

Wettschureck, N., Offermanns, S. (2005). Mammalian G Proteins and Their Cell Type Specific Functions. *Physiological Reviews, 85(4),* 1159-1204. doi: 10.1152/physrev.00003.2005

APPENDIX A

MEDIUMS, SOLUTIONS and BUFFERS

Table A.1 D-MEM high glucose with L-glutamine (Invitrogen, Cat#41966-029)

Component	Concentration (mg/mL)
Glycine	30
L-Arginine hydrochloride	84
L-Cysteine 2HCl	63
L-Glutamine	580
L-Histidine hydrochloride-H_2O	42
L-Isoleucine	105
L-Leucine	105
L-Lysine hydrochloride	146
L-Methionine	30
L-Phenylalanine	66
L-Serine	42
L-Threonine	95
L-Tryptophan	16
L-Tyrosine	72
L-Valine	94
Choline chloride	4
D-Calcium pantothenate	4
Folic acid	4
Niacinamide	4

Table A.1 (Continued)

Pyridoxine hydrochloride	4
Riboflavin	0.4
Thiamine hydrochloride	4
Inositol	7.2
Calcium chloride	264
Ferric nitrate	0.1
Magnesium sulfate	200
Potassium chloride	400
Sodium bicarbonate	3700
Sodium chloride	6400
Sodium phosphate monobasic	141
Glucose (Dextrose)	4500
Phenol Red	15
Sodium pyruvate	110

Table A.2 1X Phosphate Buffered Saline (PBS) Solution

Component	**Concentration (g/L)**
NaCl	8
KCl	0.2
Na_2HPO_4	1.44
KH_2PO_4	0.24

Solvent is distilled water. pH 7.4

Table A.3 Luria Bertani (LB) Medium

Component	**Concentration (g/L)**
Tryptone	10
Yeast Extract	5
NaCl	5

For solidification 15 g/L agar is added after sterilization. pH 7.0. Required amount of antibiotics is added after sterilization and maximum of 60°C.

1X TAE (Tris Base, Acetic acid, EDTA) Buffer

40mM Tris

20mM Acetic Acid

1mM EDTA

Dissolved in dH_2O.

Table A.4 Composition of TFBI and TFBII

TFBI	Solution Concentration	Prepared Stock (1M=1000mM)	for 100 mL Solution take from prepared stock
KOAc	30 mM	300 mM	10 mL
RbCl	100 mM	1000 mM	10 mL
CaCl2	10mM	1000 mM	1 mL
MnCl2	50 mM	1000 mM	5 mL
Glycerol	15%	87% Glycerol	17.2 mL
			Complete to 100 mL with distilled water
			Adjust pH to 5.8 with acetic acid (HOAc)
			0.45 mm filter or autoclave

TFBII	Solution Concentration	Prepared Stock (1M=1000mM)	for 10 mL Solution take from prepared stock
MOPS/PIPES	10 mM	1000 mM	0.1 mL
CaCl2	75 mM	1000 mM	0.75 mL
RbCl	10 mM	1000 mM	0.1 mL
Glycerol	15%	87% Glycerol	1.7 mL
			Complete to 10 mL with distilled water
			Adjust pH to 6.5 with KOH
			0.45 mm filter or autoclave (try not to autoclave but filter it)

APPENDIX B

PLASMIDS and PRIMERS

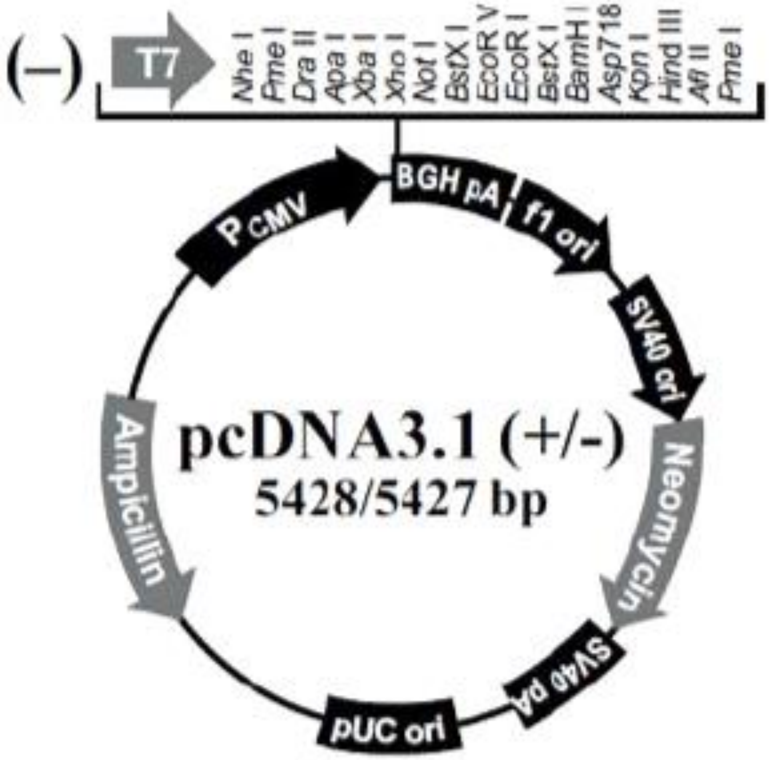
(–)
T7
Nhe I
Pme I
Dra II
Apa I
Xba I
Xho I
Not I
BstX I
EcoR V
EcoR I
BstX I
BamH I
Asp718 I
Kpn I
Hind III
Afl II
Pme I
PCMV
BGH pA
f1 ori
SV40 ori
pcDNA3.1 (+/-)
5428/5427 bp
Neomycin
SV40 pA
pUC ori
Ampicillin

Figure B.1 pcDNA3.1(-) specifications. (Invitrogen®)

Table B.1 Primer Sequences and Descriptions

Name	Sequence (5' - 3')	Description
D2R_C_EGFP_N_F	CGCAAGGCCTTCCTGAAGATCCTCCACTGCATGGTGAGCAAGGGCGAGGAG	D2R's last part and EGFP's first nucleotides
EGFP_C_pc3.1_R	GGCTGATCAGCGGTTTAAACTTAAGCTTCCTTACTTGTACAGCTCGTCCATGCCG	EGFP's last nucleotides plus pcDNA3.1(-) fragment immediately after where D2R is placed
GNAO1_EcoRI	TACTCAGAATTCATGGGATGTACTCTGAGCGCAGAG	EcoRI_GNAO1's first nucleotides
GNAO1_KpnI	TAGTATGGTACCTCAGTAGAGTCCACAGCCCC	GNAO1's last nucletodies_KpnI
GNAI3_EcoRI	GACAAGGAATTCATGGGCTGCACGTTGAGCG	EcoRI_GNAI3's first nucleotides
GNAI3_KpnI	AGGTCCGGTACCCTAATAAAGTCCACATTC	GNAI3's last nucletodies_KpnI
GO1_122A_F	GACACCGAGCCCTTCTCTGCAAGCGGAGGAGGAGGAAGCATGGTGAGCAAGGGCGA	GNAO1's region before A122 plus mCherry's first nucleotides
GO1_123E_R	CATCATGGCAGAAAGCAGCTCGCTTCCTCCTCCTCCGCTCTTGTACAGCTCGTCCAT	mCherry's last nucleotides plus GNAO1's region after E123
GO1_94E_F	GACACTTTGGGCATCGAAAGCGGAGGAGGAGGAAGCATGGTGAGCAAGGGCGAGGAG	GNAO1's region before E94 plus mCherry's first nucleotides
GO1_95Y_R	TCTCTCCTTATCACCATAGCTTCCTCCTCCTCCGCTCTTGTACAGCTCGTCCAT	mCherry's last nucleotides plus GNAO1's region after Y95
GO1_113R_F	TGTGATGTGGTGAGTCGGAGCGGAGGAGGAGGAAGCATGGTGAGCAAGGGCGAGGAG	GNAO1's region before R113 plus mCherry's first nucleotides
GO1_114M_R	GGGCTCGGTGTCTTCCATGCTTCCTCCTCCTCCGCTCTTGTACAGCTCGTCCAT	mCherry's last nucleotides plus GNAO1's region after M114

Color code: Green, EGFP and/or mCherry; Red, EcoRI; Orange, KpnI; Blue, linker.

Table B.1 (Continued)

Name	Sequence (5' - 3')	Description
GI3_122E_F	GAAGGAGTCATGACTCCAGAAAGCGGAGGAGGAGGAAGCATGGTGAGCAAGGGCGA	GNAI3's region before E122 plus mCherry's first nucleotides
GI3_123L_R	CCGTTTAATCACTCCTGCTAGGCTTCCTCCTCCTCCGCTCTTGTACAGCTCGTCCAT	mCherry's last nucleotides plus GNAI3's region after L123
GI3_60G_F	ATCATTCATGAGGATGGCAGCGGAGGAGGAGGAAGCATGGTGAGCAAGGGCGAGGAG	GNAI3's region before G60 plus mCherry's first nucleotides
GI3_61Y_R	ACATTCATCCTCTGAATAGCTTCCTCCTCCTCCGCTCTTGTACAGCTCGTCCAT	mCherry's last nucleotides plus GNAI3's region after Y61
GI3_91L_F	AGAGCCATGGGACGGCTAAGCGGAGGAGGAGGAAGCATGGTGAGCAAGGGCGAGGAG	GNAI3's region before L91 plus mCherry's first nucleotides
GI3_92K_R	TTCCCCAAAGTCAATCTTGCTTCCTCCTCCTCCGCTCTTGTACAGCTCGTCCAT	mCherry's last nucleotides plus GNAI3's region after K92
EGFP_416_Seq	GGGCACAAGCTGGAGTACA	To sequence after 416th nucleotide of EGFP
mCherry_426_Seq	GAAGAAGACCATGGGCTGG	To sequence after 426th nucleotide of mCherry
Pc3.1_MCS_F	ATCGAAATTAATACGACTCAC	Forwward primer to sequence multiple cloning site of pcDNA3.1(-)
Pc3.1_MCS_R	GCAACTAGAAGGCACAGTCGA	Reverse primer to sequence multiple cloning site of pcDNA3.1(-)

Color code: Green, EGFP and/or mCherry; Red, EcoRI; Orange, KpnI; Blue, linker.

APPENDIX C

pcDNA3.1(-) MCS, GNAO1 and GNAI3 CUT SITES

Table C.1 pcDNA3.1(-) MCS and GNAO1-GNAI3 gene cut site comparison

		GNAO1	GNAI3
pcDNA3.1(-) MCS	NheI	absent	absent
	PmeI*	absent	absent
	ApaI	absent	absent
	XbaI	absent	absent
	XhoI	present	absent
	NotI	absent	absent
	BstXI*	present	absent
	EcoRV	absent	absent
	EcoRI	absent	absent
	BstXI*	present	absent
	BamHI	present	absent
	Asp718I	absent	absent
	KpnI	absent	absent
	HindIII	present	present
	AflII	absent	absent
	PmeI*	absent	absent

* Plasmid has this cut site twice.

Absent: Gene does not have internal cut site for corresponding restriction enzyme.

Present: Gene does have internal cut site for corresponding restriction enzyme.

APPENDIX D

SIMILARITY SCORES OF GNAO1 AND GNAI3 GENES

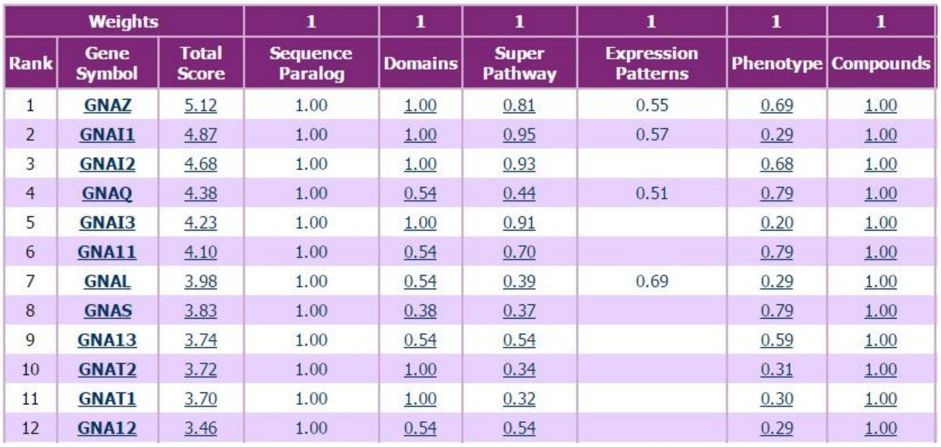

Weights			1	1	1	1	1	1
Rank	Gene Symbol	Total Score	Sequence Paralog	Domains	Super Pathway	Expression Patterns	Phenotype	Compounds
1	GNAZ	5.12	1.00	1.00	0.81	0.55	0.69	1.00
2	GNAI1	4.87	1.00	1.00	0.95	0.57	0.29	1.00
3	GNAI2	4.68	1.00	1.00	0.93		0.68	1.00
4	GNAQ	4.38	1.00	0.54	0.44	0.51	0.79	1.00
5	GNAI3	4.23	1.00	1.00	0.91		0.20	1.00
6	GNA11	4.10	1.00	0.54	0.70		0.79	1.00
7	GNAL	3.98	1.00	0.54	0.39	0.69	0.29	1.00
8	GNAS	3.83	1.00	0.38	0.37		0.79	1.00
9	GNA13	3.74	1.00	0.54	0.54		0.59	1.00
10	GNAT2	3.72	1.00	1.00	0.34		0.31	1.00
11	GNAT1	3.70	1.00	1.00	0.32		0.30	1.00
12	GNA12	3.46	1.00	0.54	0.54		0.29	1.00

Figure D.1 Similarity Scores of GNAO1 Gene

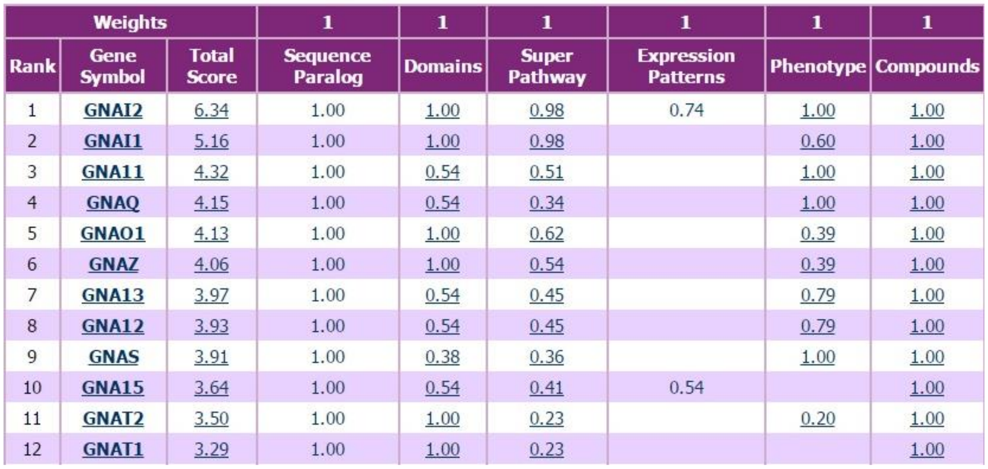

Weights			1	1	1	1	1	1
Rank	Gene Symbol	Total Score	Sequence Paralog	Domains	Super Pathway	Expression Patterns	Phenotype	Compounds
1	GNAI2	6.34	1.00	1.00	0.98	0.74	1.00	1.00
2	GNAI1	5.16	1.00	1.00	0.98		0.60	1.00
3	GNA11	4.32	1.00	0.54	0.51		1.00	1.00
4	GNAQ	4.15	1.00	0.54	0.34		1.00	1.00
5	GNAO1	4.13	1.00	1.00	0.62		0.39	1.00
6	GNAZ	4.06	1.00	1.00	0.54		0.39	1.00
7	GNA13	3.97	1.00	0.54	0.45		0.79	1.00
8	GNA12	3.93	1.00	0.54	0.45		0.79	1.00
9	GNAS	3.91	1.00	0.38	0.36		1.00	1.00
10	GNA15	3.64	1.00	0.54	0.41	0.54		1.00
11	GNAT2	3.50	1.00	1.00	0.23		0.20	1.00
12	GNAT1	3.29	1.00	1.00	0.23			1.00

Figure D.2 Similarity Scores of GNAI3 Gene

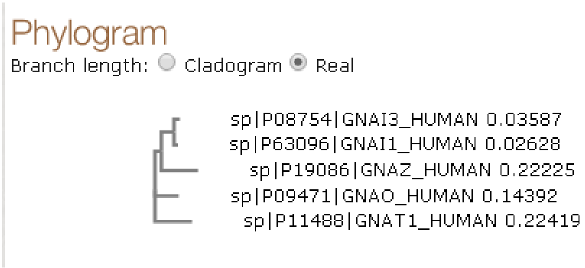

Phylogram

Branch length: ○ Cladogram ● Real

sp|P08754|GNAI3_HUMAN 0.03587
sp|P63096|GNAI1_HUMAN 0.02628
sp|P19086|GNAZ_HUMAN 0.22225
sp|P09471|GNAO_HUMAN 0.14392
sp|P11488|GNAT1_HUMAN 0.22419

Figure D.3 Philogenetic Tree Generated for GNAO1 and GNAI3 genes

APPENDIX E

FILTERS USED IN CONFOCAL FLUORESCENT MICROSCOPY

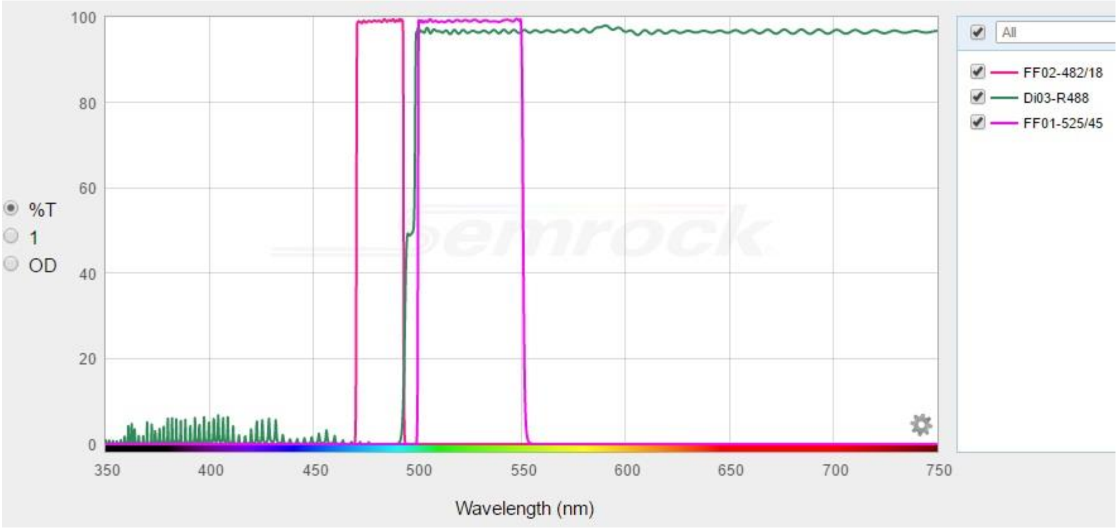

Figure E.1 Excitation and emission ranges of EGFP filter used in Leica DMI4000 B with Andor DSD2 Confocal device

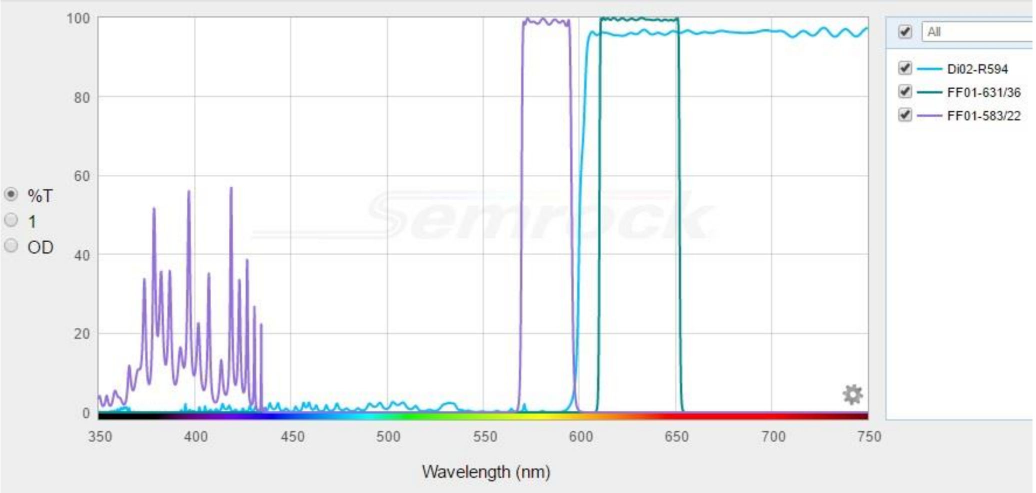

Figure E.2 Excitation and emission ranges of mCherry filter used in Leica DMI4000 B with Andor DSD2 Confocal device

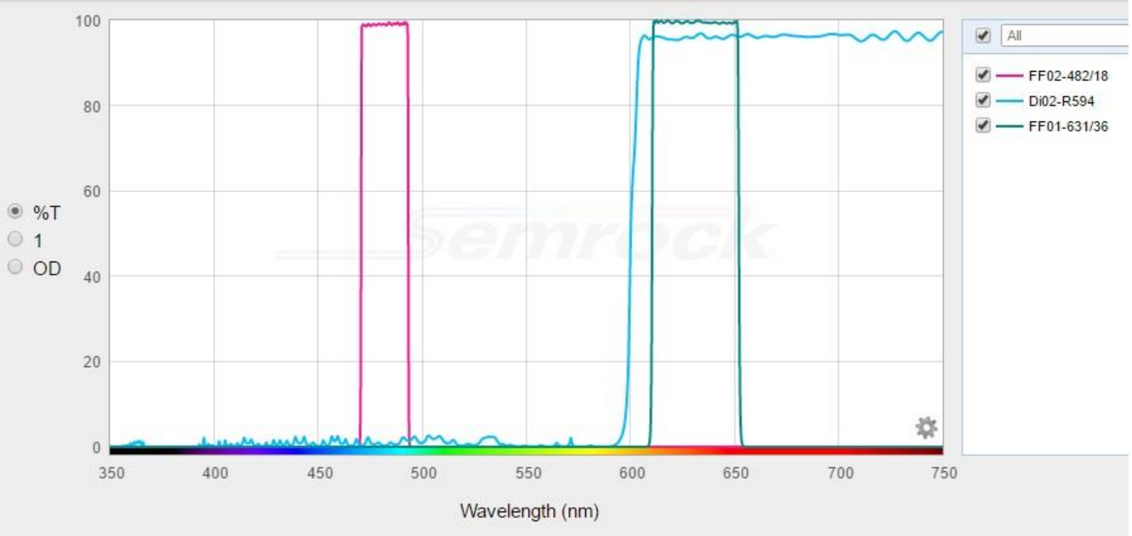

Figure E.3 Excitation and emission ranges of FRET configuration (EGFP excitation, mCherry emission) used in Leica DMI4000 B with Andor DSD2 Confocal device

APPENDIX F

SEQUENCES OF THE PROTEINS AND CONSTRUCTS

D2R in pcDNA3.1(-)

gctagcgtttaaacgggccctctagactcgagcggccgcataacttcgtatagcatacattatacgaagttatcagtcga
cATGGATCCACTGAATCTGTCCTGGTATGATGATGATCTGGAGAGGCAG
AACTGGAGCCGGCCCTTCAACGGGTCAGACGGGAAGGCGGACAGACCC
CACTACAACTACTATGCCACACTGCTCACCCTGCTCATCGCTGTCATCGT
CTTCGGCAACGTGCTGGTGTGCATGGCTGTGTCCCGCGAGAAGGCGCTG
CAGACCACCACCAACTACCTGATCGTCAGCCTCGCAGTGGCCGACCTCC
TCGTCGCCACACTGGTCATGCCCTGGGTTGTCTACCTGGAGGTGGTAGG
TGAGTGGAAATTCAGCAGGATTCACTGTGACATCTTCGTCACTCTGGAC
GTCATGATGTGCACGGCGAGCATCCTGAACTTGTGTGCCATCAGCATCG
ACAGGTACACAGCTGTGGCCATGCCCATGCTGTACAATACGCGCTACAG
CTCCAAGCGCCGGGTCACCGTCATGATCTCCATCGTCTGGGTCCTGTCC
TTCACCATCTCCTGCCCACTCCTCTTCGGACTCAATAACGCAGACCAGA
ACGAGTGCATCATTGCCAACCCGGCCTTCGTGGTCTACTCCTCCATCGT
CTCCTTCTACGTGCCCTTCATTGTCACCCTGCTGGTCTACATCAAGATCT
ACATTGTCCTCCGCAGACGCCGCAAGCGAGTCAACACCANACGCAGCA
GCCGAGCTTTCAGGGCCCACCTGAGGGCTCCACTAAAGGGCAACTGTA
CTCACCCCGAGGACATGAAACTCTGCACCGTTATCATGAAGTCTAATGG
GAGTTTCCCAGTGAACAGGCGGAGAGTGGAGGCTGCCCGGCGAGCCCA
GGAGCTGGAGATGGAGATGCTCTCCAGCACCAGCCCACCCGAGAGGAC
CCGGTACAGCCCCATCCCACCCAGCCACCACCAGCTGACTCTCCCCGAC
CCGTCCCACCATGGTCTCCACAGCACTCCCGACAGCCCCGCCAAACCAG
AGAAGAATGGGCATGCCAAAGACCACCCCAAGATTGCCAAGATCTTTG
AGATCCAGACCATGCCCAATGGCAAAACCCGGACCTCCCTCAAGACCA
TGAGCCGTAGGAAGCTCTCCCAGCAGAAGGAGAAGAAAGCCACTCAGA
TGCTCGCCATTGTTCTCGGCGTGTTCATCATCTGCTGGCTGCCCTTCTTC
ATCACACACATCCTGAACATACACTGTGACTGCAACATCCCGCCTGTCC
TGTACAGCGCCTTCACGTGGCTGGGCTATGTCAACAGCGCCGTGAACCC
CATCATCTACACCACCTTCAACATTGAGTTCCGCAAGGCCTTCCTGAAG
ATCCTCCACTGCggaagcttaagtttaaaccgctgatcagcctcgactgtgccttctagttgccagccatctgtt
gtt

Capital letters belong to D2R, lower case letters belong to pcDNA3.1(-)

D2R with EGFP fused to its C-Tail

Color Code: SalI,AflII,EGFP,**Bold** letters belong to pcDNA3.1(-)

GCTAGCGTTTAAACGGGCCCTCTAGACTCGAGCGGCCGCATAACTT
CGTATAGCATACATTATACGAAGTTATCAGTCGACATGGATCCACTG
AATCTGTCCTGGTATGATGATGATCTGGAGAGGCAGAACTGGAGCCGG
CCCTTCAACGGGTCAGACGGGAAGGCGGACAGACCCCACTACAACTAC
TATGCCACACTGCTCACCCTGCTCATCGCTGTCATCGTCTTCGGCAACGT
GCTGGTGTGCATGGCTGTGTCCCGCGAGAAGGCGCTGCAGACCACCAC
CAACTACCTGATCGTCAGCCTCGCAGTGGCCGACCTCCTCGTCGCCACA
CTGGTCATGCCCTGGGTTGTCTACCTGGAGGTGGTAGGTGAGTGGAAAT
TCAGCAGGATTCACTGTGACATCTTCGTCACTCTGGACGTCATGATGTG
CACGGCGAGCATCCTGAACTTGTGTGCCATCAGCATCGACAGGTACACA
GCTGTGGCCATGCCCATGCTGTACAATACGCGCTACAGCTCCAAGCGCC
GGGTCACCGTCATGATCTCCATCGTCTGGGTCCTGTCCTTCACCATCTCC
TGCCCACTCCTCTTCGGACTCAATAACGCAGACCAGAACGAGTGCATCA
TTGCCAACCCGGCCTTCGTGGTCTACTCCTCCATCGTCTCCTTCTACGTG
CCCTTCATTGTCACCCTGCTGGTCTACATCAAGATCTACATTGTCCTCCG
CAGACGCCGCAAGCGAGTCAACACCANACGCAGCAGCCGAGCTTTCAG
GGCCCACCTGAGGGCTCCACTAAAGGGCAACTGTACTCACCCCGAGGA
CATGAAACTCTGCACCGTTATCATGAAGTCTAATGGGAGTTTCCCAGTG
AACAGGCGGAGAGTGGAGGCTGCCCGGCGAGCCCAGGAGCTGGAGAT
GGAGATGCTCTCCAGCACCAGCCCACCCGAGAGGACCCGGTACAGCCC
CATCCCACCCAGCCACCACCAGCTGACTCTCCCCGACCCGTCCCACCAT
GGTCTCCACAGCACTCCCGACAGCCCCGCCAAACCAGAGAAGAATGGG
CATGCCAAAGACCACCCCAAGATTGCCAAGATCTTTGAGATCCAGACC
ATGCCCAATGGCAAAACCCGGACCTCCCTCAAGACCATGAGCCGTAGG
AAGCTCTCCCAGCAGAAGGAGAAGAAAGCCACTCAGATGCTCGCCATT
GTTCTCGGCGTGTTCATCATCTGCTGGCTGCCCTTCTTCATCACACACAT
CCTGAACATACACTGTGACTGCAACATCCCGCCTGTCCTGTACAGCGCC
TTCACGTGGCTGGGCTATGTCAACAGCGCCGTGAACCCCATCATCTACA
CCACCTTCAACATTGAGTTCCGCAAGGCCTTCCTGAAGATCCTCCACTG
CATGGTGAGCAAGGGCGAGGAGCTGTTCACCGGGGTGGTGCCCATCCT
GGTCGAGCTGGACGGCGACGTAAACGGCCACAAGTTCAGCGTGTCCGG
CGAGGGCGAGGGCGATGCCACCTACGGCAAGCTGACCCTGAAGTTCAT
CTGCACCACCGGCAAGCTGCCCGTGCCCTGGCCCACCCTCGTGACCACC
CTGACCTACGGCGTGCAGTGCTTCAGCCGCTACCCCGACCACATGAAGC
AGCACGACTTCTTCAAGTCCGCCATGCCCGAAGGCTACGTCCAGGAGCG
CACCATCTTCTTCAAGGACGACGGCAACTACAAGACCCGCGCCGAGGT
GAAGTTCGAGGGCGACACCCTGGTGAACCGCATCGAGCTGAAGGGCAT
CGACTTCAAGGAGGACGGCAACATCCTGGGGCACAAGCTGGAGTACAA

CTACAACAGCCACAACGTCTATATCATGGCCGACAAGCAGAAGAACGG
CATCAAGGTGAACTTCAAGATCCGCCACAACATCGAGGACGGCAGCGT
GCAGCTCGCCGACCACTACCAGCAGAACACCCCCATCGGCGACGGCCC
CGTGCTGCTGCCCGACAACCACTACCTGAGCACCCAGTCCAAGCTTAGC
AAAGACCCCAACGAGAAGCGCGATCACATGGTCCTGCTGGAGTTCGTG
ACCGCCGCCGGGATCACTCTCGGCATGGACGAGCTGTACAAGTAA**GGA**
AGCTTAAGTTTAAACCGCTGATCAGCCTCGACTGTGCCTTCTAGTT
GCCAGCCATCTGTTGTT

GNAI3 in pDONR-Dual

ATGGGCTGCACGTTGAGCGCCGAAGACAAGGCGGCAGTGGAGCGAAGC
AAGATGATCGACCGCAACTTACGGGAGGACGGGGAAAAAGCGGCCAA
AGAAGTGAAGCTGCTGCTACTCGGTGCTGGAGAATCTGGTAAAAGCAC
CATTGTGAAACAGATGAAAATCATTCATGAGGATGGCTATTCAGAGGA
TGAATGTAAACAATATAAAGTAGTTGTCTACAGCAATACTATACAGTCC
ATCATTGCAATCATAAGAGCCATGGGACGGCTAAAGATTGACTTTGGG
GAAGCTGCCAGGGCAGATGATGCCCGGCAATTATTTGTTTTAGCTGGCA
GTGCTGAAGAAGGAGTCATGACTCCAGAACTAGCAGGAGTGATTAAAC
GGTTATGGCGAGATGGTGGGGTACAAGCTTGCTTCAGCAGATCCAGGG
AATATCAGCTCAATGATTCTGCTTCATATTATCTAAATGATCTGGATAG
AATATCCCAGTCTAACTACATTCCAACTCAGCAAGATGTTCTTCGGACG
AGAGTGAAGACCACAGGCATTGTAGAAACACATTTCACCTTCAAAGAC
CTATACTTCAAGATGTTTGATGTAGGTGGCCAAAGATCAGAACGAAAA
AAGTGGATTCACTGTTTTGAGGGAGTGACAGCAATTATCTTCTGTGTGG
CCCTCAGTGATTATGACCTTGTTCTGGCTGAGGACGAGGAGATGAACCG
AATGCATGAAAGCATGAAACTGTTTGACAGCATTTGTAATAACAAATG
GTTTACAGAAACTTCAATCATTCTCTTCCTTAACAAGAAAGACCTTTTTG
AGGAAAAAATAAAGAGGAGTCCGTTAACTATCTGTTATCCAGAATACA
CAGGTTCCAATACATATGAAGAGGCAGCTGCCTATATTCAATGCCAGTT
TGAAGATCTGAACAGAAGAAAAGATACCAAGGAGATCTATACTCACTT
CACCTGTGCCACAGACACGAAGAATGTGCAGTTTGTTTTTGATGCTGTT
ACAGATGTCATCATTAAAAACAACTTAAAGGAATGTGGACTTTATTAG

GNAO1 in pDONR221

ATGGGATGTACTCTGAGCGCAGAGGAGAGAGCCGCCCTCGAGCGGAGC
AAGGCGATTGAGAAAAACCTCAAAGAGGATGGCATCAGCGCCGCCAAA
GACGTGAAATTACTCCTGCTCGGGGCTGGAGAATCAGGAAAAAGCACC
ATTGTGAAGCAGATGAAGATCATCCATGAAGATGGCTTCTCCGGAGAA
GACGTGAAACAGTACAAGCCTGTTGTCTACAGCAACACTATCCAGTCCC
TGGCAGCCATCGTCCGGGCCATGGACACTTTGGGCATCGAATATGGTGA
TAAGGAGAGAAAGGCTGACGCCAAGATGGTGTGTGATGTGGTGAGTCG
GATGGAAGACACCGAGCCCTTCTCTGCAGAGCTGCTTTCTGCCATGATG
CGGCTCTGGGGCGACTCAGGAATCCAAGAGTGCTTCAACCGGTCCCGG
GAGTATCAGCTCAACGACTCTGCCAAATACTACCTGGACAGCCTGGATC
GGATTGGGGCCGCCGACTACCAGCCCACCGAGCAGGACATCCTCCGAA
CCAGGGTCAAAACCACTGGCATCGTAGAAACCCACTTCACATTCAAGA
ACCTCCACTTCAGGCTGTTTGACGTCGGAGGCCAGCGATCTGAACGCAA
GAAGTGGATCCATTGCTTCGAGGACGTCACGGCCATCATTTTCTGTGTC
GCGCTCAGCGGCTATGACCAGGTGCTCCACGAAGACGAAACCACGAAC
CGCATGCACGAATCCCTGAAGCTTTTTGACAGCATCTGCAACAACAAAT
GGTTCACAGACACGTCCATCATCCTGTTTCTTAACAAGAAGGACATATT
TGAAGAGAAGATCAAGAAGTCCCCGCTCACCATCTGCTTTCCTGAATAT
ACAGGCCCCAGCGCCTTCACAGAAGCCGTGGCTTACATCCAGGCCCAGT
ACGAGAGCAAGAACAAGTCAGCCCACAAAGAGATCTACACCCACGTCA
CCTGCGCCACGGACACCAACAACATCCAGTTTGTCTTTGATGCTGTGAC
GGACGTCATCATCGCCAAAAACCTGCGGGGCTGTGGACTCTACTGAATC
CACCCAGCTTTCTTGTACTAG

GNAI3 with mCherry inserted between E122-L123 in pcDNA3.1(-)

ATGGGCTGCACGTTGAGCGCCGAAGACAAGGCGGCAGTGGAGCGAAGC
AAGATGATCGACCGCAACTTACGGGAGGACGGGGAAAAAGCGGCCAA
AGAAGTGAAGCTGCTGCTACTCGGTGCTGGAGAATCTGGTAAAAGCAC
CATTGTGAAACAGATGAAAATCATTCATGAGGATGGCTATTCAGAGGA
TGAATGTAAACAATATAAAGTAGTTGTCTACAGCAATACTATACAGTCC
ATCATTGCAATCATAAGAGCCATGGGACGGCTAAAGATTGACTTTGGG
GAAGCTGCCAGGGCAGATGATGCCCGGCAATTATTTGTTTTAGCTGGCA
GTGCTGAAGAAGGAGTCATGACTCCAGAA**AGCGGAGGAGGAGGAAG**
CATGGTGAGCAAGGGCGAGGAGGATAACATGGCCATCATCAAGGA
GTTCATGCGCTTCAAGGTGCACATGGAGGGCTCCGTGAACGGCCAC

GAGTTCGAGATCGAGGGCGAGGGCGAGGGCCGCCCCTACGAGGGC
ACCCAGACCGCCAAGCTGAAGGTGACCAAGGGTGGCCCCCTGCCC
TTCGCCTGGGACATCCTGTCCCCTCAGTTCATGTACGGCTCCAAGG
CCTACGTGAAGCACCCCGCCGACATCCCCGACTACTTGAAGCTGTC
CTTCCCCGAGGGCTTCAAGTGGGAGCGCGTGATGAACTTCGAGGA
CGGCGGCGTGGTGACCGTGACCCAGGACTCCTCCCTGCAGGACGG
CGAGTTCATCTACAAGGTGAAGCTGCGCGGCACCAACTTCCCCTCC
GACGGCCCCGTAATGCAGAAGAAGACCATGGGCTGGGAGGCCTCC
TCCGAGCGGATGTACCCCGAGGACGGCGCCCTGAAGGGCGAGATC
AAGCAGAGGCTGAAGCTGAAGGACGGCGGCCACTACGACGCTGAG
GTCAAGACCACCTACAAGGCCAAGAAGCCCGTGCAGCTGCCCGGC
GCCTACAATGTCAACATCAAGTTGGACATCACCTCCCACAACGAGG
ACTACACCATCGTGGAACAGTACGAACGCGCCGAGGGCCGCCACT
CCACCGGCGGCATGGACGAGCTGTACAAGAGCGGAGGAGGAGGAA
GCCTAGCAGGAGTGATTAAACGGTTATGGCGAGATGGTGGGGTACAAG
CTTGCTTCAGCAGATCCAGGGAATATCAGCTCAATGATTCTGCTTCATA
TTATCTAAATGATCTGGATAGAATATCCCAGTCTAACTACATTCCAACT
CAGCAAGATGTTCTTCGGACGAGAGTGAAGACCACAGGCATTGTAGAA
ACACATTTCACCTTCAAAGACCTATACTTCAAGATGTTTGATGTAGGTG
GCCAAAGATCAGAACGAAAAAAGTGGATTCACTGTTTTGAGGGAGTGA
CAGCAATTATCTTCTGTGTGGCCCTCAGTGATTATGACCTTGTTCTGGCT
GAGGACGAGGAGATGAACCGAATGCATGAAAGCATGAAACTGTTTGAC
AGCATTTGTAATAACAAATGGTTTACAGAAACTTCAATCATTCTCTTCCT
TAACAAGAAAGACCTTTTTGAGGAAAAAATAAAGAGGAGTCCGTTAAC
TATCTGTTATCCAGAATACACAGGTTCCAATACATATGAAGAGGCAGCT
GCCTATATTCAATGCCAGTTTGAAGATCTGAACAGAAGAAAAGATACC
AAGGAGATCTATACTCACTTCACCTGTGCCACAGACACGAAGAATGTGC
AGTTTGTTTTTGATGCTGTTACAGATGTCATCATTAAAAACAACTTAAA
GGAATGTGGACTTTATTAG

Red: mCherry Blue: Mutation at mCherry sequence 615 C>T Total sequence 981 C>T

GNAI3 with mCherry inserted between G60-Y61 in pcDNA3.1(-)

ATGGGCTGCACGTTGAGCGCCGAAGACAAGGCGGCAGTGGAGCGAAGC
AAGATGATCGACCGCAACTTACGGAGGACGGGGAAAAAGCGGCCAA
AGAAGTGAAGCTGCTGCTACTCGGTGCTGGAGAATCTGGTAAAAGCAC
CATTGTGAAACAGATGAAAATCATTCATGAGGATGGC**AGCGGAGGAG**
GAGGAAGCATGGTGAGCAAGGGCGAGGAGGATAACATGGCCATCA
TCAAGGAGTTCATGCGCTTCAAGGTGCACATGGAGGGCTCCGTGAA
CGGCCACGAGTTCGAGATCGAGGGCGAGGGCGAGGGCCGCCCCTA
CGAGGGCACCCAGACCGCCAAGCTGAAGGTGACCAAGGGTGGCCC
CCTGCCCTTCGCCTGGGACATCCTGTCCCCTCAGTTCATGTACGGC
TCCAAGGCCTACGTGAAGCACCCCGCCGACATCCCCGACTACTTGA
AGCTGTCCTTCCCCGAGGGCTTCAAGTGGGAGCGCGTGATGAACTT
CGAGGACGGCGGCGTGGTGACCGTGACCCAGGACTCCTCCCTGCA
GGACGGCGAGTTCATCTACAAGGTGAAGCTGCGCGGCACCAACTTC
CCCTCCGACGGCCCCGTAATGCAGAAGAAGACCATGGGCTGGGAG
GCCTCCTCCGAGCGGATGTACCCCGAGGACGGCGCCCTGAAGGGC
GAGATCAAGCAGAGGCTGAAGCTGAAGGACGGCGGCCACTACGAC
GCTGAGGTCAAGACCACCTACAAGGCCAAGAAGCCCGTGCAGCTG
CCCGGCGCCTACAACGTCAACATCAAGTTGGACATCACCTCCCACA
ACGAGGACTACACCATCGTGGAACAGTACGAACGCGCCGAGGGCC
GCCACTCCACCGGCGGCATGGACGAGCTGTACAAGAGCGGAGGAG
GAGGAAGCTATTCAGAGGATGAATGTAAACAATATAAAGTAGTTGTCT
ACAGCAATACTATACAGTCCATCATTGCAATCATAAGAGCCATGGGAC
GGCTAAAGATTGACTTTGGGGAAGCTGCCAGGGCAGATGATGCCCGGC
AATTATTTGTTTTAGCTGGCAGTGCTGAAGAAGGAGTCATGACTCCAGA
ACTAGCAGGAGTGATTAAACGGTTATGGCGAGATGGTGGGGTACAAGC
TTGCTTCAGCAGATCCAGGGAATATCAGCTCAATGATTCTGCTTCATAT
TATCTAAATGATCTGGATAGAATATCCCAGTCTAACTACATTCCAACTC
AGCAAGATGTTCTTCGGACGAGAGTGAAGACCACAGGCATTGTAGAAA
CACATTTCACCTTCAAAGACCTATACTTCAAGATGTTTGATGTAGGTGG
CCAAAGATCAGAACGAAAAAAGTGGATTCACTGTTTTGAGGGAGTGAC
AGCAATTATCTTCTGTGTGGCCCTCAGTGATTATGACCTTGTTCTGGCTG
AGGACGAGGAGATGAACCGAATGCATGAAAGCATGAAACTGTTTGACA
GCATTTGTAATAACAAATGGTTTACAGAAACTTCAATCATTCTCTTCCTT
AACAAGAAAGACCTTTTTGAGGAAAAAATAAAGAGGAGTCCGTTAACT
ATCTGTTATCCAGAATACACAGGTTCCAATACATATGAAGAGGCAGCTG
CCTATATTCAATGCCAGTTTGAAGATCTGAACAGAAGAAAAGATACCA
AGGAGATCTATACTCACTTCACCTGTGCCACAGACACGAAGAATGTGCA
GTTTGTTTTTGATGCTGTTACAGATGTCATCATTAAAAACAACTTAAAG
GAATGTGGACTTTATTAG

GNAI3 with mCherry inserted between L91-K92 in pcDNA3.1(-)

ATGGGCTGCACGTTGAGCGCCGAAGACAAGGCGGCAGTGGAGCGAAGC
AAGATGATCGACCGCAACTTACGGGAGGACGGGGAAAAAGCGGCCAA
AGAAGTGAAGCTGCTGCTACTCGGTGCTGGAGAATCTGGTAAAAGCAC
CATTGTGAAACAGATGAAAATCATTCATGAGGATGGCTATTCAGAGGA
TGAATGTAAACAATATAAAGTAGTTGTCTACAGCAATACTATACAGTCC
ATCATTGCAATCATAAGAGCCATGGGACGGCTA**AGCGGAGGAGGAGG**
AAGCATGGTGAGCAAGGGCGAGGAGGATAACATGGCCATCATCAA
GGAGTTCATGCGCTTCAAGGTGCACATGGAGGGCTCCGTGAACGG
CCACGAGTTCGAGATCGAGGGCGAGGGCGAGGGCCGCCCCTACGA
GGGCACCCAGACCGCCAAGCTGAAGGTGACCAAGGGTGGCCCCCT
GCCCTTCGCCTGGGACATCCTGTCCCCTCAGTTCATGTACGGCTCC
AAGGCCTACGTGAAGCACCCCGCCGACATCCCCGACTACTTGAAGC
TGTCCTTCCCCGAGGGCTTCAAGTGGGAGCGCGTGATGAACTTCGA
GGACGGCGGCGTGGTGACCGTGACCCAGGACTCCTCCCTGCAGGA
CGGCGAGTTCATCTACAAGGTGAAGCTGCGCGGCACCAACTTCCCC
TCCGACGGCCCCGTAATGCAGAAGAAGACCATGGGCTGGGAGGCC
TCCTCCGAGCGGATGTACCCCGAGGACGGCGCCCTGAAGGGCGAG
ATCAAGCAGAGGCTGAAGCTGAAGGACGGCGGCCACTACGACGCT
GAGGTCAAGACCACCTACAAGGCCAAGAAGCCCGTGCAGCTGCCC
GGCGCCTACAACGTCAACATCAAGTTGGACATCACCTCCCACAACG
AGGACTACACCATCGTGGAACAGTACGAACGCGCCGAGGGCCGCC
ACTCCACCGGCGGCATGGACGAGCTGTACAAGAGCGGAGGAGGAG
GAAGCAAGATTGACTTTGGGGAAGCTGCCAGGGCAGATGATGCCCGGC
AATTATTTGTTTTAGCTGGCAGTGCTGAAGAAGGAGTCATGACTCCAGA
ACTAGCAGGAGTGATTAAACGGTTATGGCGAGATGGTGGGGTACAAGC
TTGCTTCAGCAGATCCAGGGAATATCAGCTCAATGATTCTGCTTCATAT
TATCTAAATGATCTGGATAGAATATCCCAGTCTAACTACATTCCAACTC
AGCAAGATGTTCTTCGGACGAGAGTGAAGACCACAGGCATTGTAGAAA
CACATTTCACCTTCAAAGACCTATACTTCAAGATGTTTGATGTAGGTGG
CCAAAGATCAGAACGAAAAAAGTGGATTCACTGTTTTGAGGGAGTGAC
AGCAATTATCTTCTGTGTGGCCCTCAGTGATTATGACCTTGTTCTGGCTG
AGGACGAGGAGATGAACCGAATGCATGAAAGCATGAAACTGTTTGACA
GCATTTGTAATAACAAATGGTTTACAGAAACTTCAATCATTCTCTTCCTT
AACAAGAAAGACCTTTTTGAGGAAAAAATAAAGAGGAGTCCGTTAACT
ATCTGTTATCCAGAATACACAGGTTCCAATACATATGAAGAGGCAGCTG
CCTATATTCAATGCCAGTTTGAAGATCTGAACAGAAGAAAAGATACCA
AGGAGATCTATACTCACTTCACCTGTGCCACAGACACGAAGAATGTGCA
GTTTGTTTTTGATGCTGTTACAGATGTCATCATTAAAAACAACTTAAAG
GAATGTGGACTTTATTAG

GNAO1 with mCherry inserted between A122-E123 in pcDNA3.1(-)

ATGGGATGTACTCTGAGCGCAGAGGAGAGAGCCGCCCTCGAGCGGAGC
AAGGCGATTGAGAAAAACCTCAAAGAGGATGGCATCAGCGCCGCCAAA
GACGTGAAATTACTCCTGCTCGGGGCTGGAGAATCAGGAAAAAGCACC
ATTGTGAAGCAGATGAAGATCATCCATGAAGATGGCTTCTCCGGAGAA
GACGTGAAACAGTACAAGCCTGTTGTCTACAGCAACACTATCCAGTCCC
TGGCAGCCATCGTCCGGGCCATGGACACTTTGGGCATCGAATATGGTGA
TAAGGAGAGAAAGGCTGACGCCAAGATGGTGTGTGATGTGGTGAGTCG
GATGGAAGACACCGAGCCCTTCTCTGCA**AGCGGAGGAGGAGGAAGCA**
TGGTGAGCAAGGGCGAGGAGGATAACATGGCCATCATCAAGGAGT
TCATGCGCTTCAAGGTGCACATGGAGGGCTCCGTGAACGGCCACG
AGTTCGAGATCGAGGGCGAGGGCGAGGGCCGCCCCTACGAGGGCA
CCCAGACCGCCAAGCTGAAGGTGACCAAGGGTGGCCCCCTGCCCT
TCGCCTGGGACATCCTGTCCCCTCAGTTCATGTACGGCTCCAAGGC
CTACGTGAAGCACCCCGCCGACATCCCCGACTACTTGAAGCTGTCC
TTCCCCGAGGGCTTCAAGTGGGAGCGCGTGATGAACTTCGAGGAC
GGCGGCGTGGTGACCGTGACCCAGGACTCCTCCCTGCAGGACGGC
GAGTTCATCTACAAGGTGAAGCTGCGCGGCACCAACTTCCCCTCCG
ACGGCCCCGTAATGCAGAAGAAGACCATGGGCTGGGAGGCCTCCT
CCGAGCGGATGTACCCCGAGGACGGCGCCCTGAAGGGCGAGATCA
AGCAGAGGCTGAAGCTGAAGGACGGCGGCCACTACGACGCTGAGG
TCAAGACCACCTACAAGGCCAAGAAGCCCGTGCAGCTGCCCGGCG
CCTACAACGTCAACATCAAGTTGGACATCACCTCCCACAACGAGGA
CTACACCATCGTGGAACAGTACGAACGCGCCGAGGGCCGCCACTC
CACCGGCGGCATGGACGAGCTGTACAAGAGCGGAGGAGGAGGAAG
CGAGCTGCTTTCTGCCATGATGCGGCTCTGGGGCGACTCAGGAATCCAA
GAGTGCTTCAACCGGTCCCGGGAGTATCAGCTCAACGACTCTGCCAAAT
ACTACCTGGACAGCCTGGATCGGATTGGGGCCGCCGACTACCAGCCCA
CCGAGCAGGACATCCTCCGAACCAGGGTCAAAACCACTGGCATCGTAG
AAACCCACTTCACATTCAAGAACCTCCACTTCAGGCTGTTTGACGTCGG
AGGCCAGCGATCTGAACGCAAGAAGTGGATCCATTGCTTCGAGGACGT
CACGGCCATCATTTTCTGTGTCGCGCTCAGCGGCTATGACCAGGTGCTC
CACGAAGACGAAACCACGAACCGCATGCACGAATCCCTGAAGCTTTTT
GACAGCATCTGCAACAACAAATGGTTCACAGACACGTCCATCATCCTGT
TTCTTAACAAGAAGGACATATTTGAAGAGAAGATCAAGAAGTCCCCGC
TCACCATCTGCTTTCCTGAATATACAGGCCCCAGCGCCTTCACAGAAGC
CGTGGCTTACATCCAGGCCCAGTACGAGAGCAAGAACAAGTCAGCCCA
CAAAGAGATCTACACCCACGTCACCTGCGCCACGGACACCAACAACAT
CCAGTTTGTCTTTGATGCTGTGACGGACGTCATCATCGCCAAAAACCTG
CGGGGCTGTGGACTCTACTGAATCCACCCAGCTTTCTTGTACTAG

GNAO1 with mCherry inserted between E94-Y95 in pcDNA3.1(-)

ATGGGATGTACTCTGAGCGCAGAGGAGAGAGCCGCCCTCGAGCGGAGC
AAGGCGATTGAGAAAAACCTCAAAGAGGATGGCATCAGCGCCGCCAAA
GACGTGAAATTACTCCTGCTCGGGGCTGGAGAATCAGGAAAAAGCACC
ATTGTGAAGCAGATGAAGATCATCCATGAAGATGGCTTCTCCGGAGAA
GACGTGAAACAGTACAAGCCTGTTGTCTACAGCAACACTATCCAGTCCC
TGGCAGCCATCGTCCGGGCCATGGACACTTTGGGCATCGAA**AGCGGAG**
GAGGAGGAAGCATGGTGAGCAAGGGCGAGGAGGATAACATGGCCA
TCATCAAGGAGTTCATGCGCTTCAAGGTGCACATGGAGGGCTCCGT
GAACGGCCACGAGTTCGAGATCGAGGGCGAGGGCGAGGGCCGCCC
CTACGAGGGCACCCAGACCGCCAAGCTGAAGGTGACCAAGGGTGG
CCCCCTGCCCTTCGCCTGGGACATCCTGTCCCCTCAGTTCATGTAC
GGCTCCAAGGCCTACGTGAAGCACCCCGCCGACATCCCCGACTACT
TGAAGCTGTCCTTCCCCGAGGGCTTCAAGTGGGAGCGCGTGATGAA
CTTCGAGGACGGCGGCGTGGTGACCGTGACCCAGGACTCCTCCCT
GCAGGACGGCGAGTTCATCTACAAGGTGAAGCTGCGCGGCACCAA
CTTCCCCTCCGACGGCCCCGTAATGCAGAAGAAGACCATGGGCTGG
GAGGCCTCCTCCGAGCGGATGTACCCCGAGGACGGCGCCCTGAAG
GGCGAGATCAAGCAGAGGCTGAAGCTGAAGGACGGCGGCCACTAC
GACGCTGAGGTCAAGACCACCTACAAGGCCAAGAAGCCCGTGCAG
CTGCCCGGCGCCTACAACGTCAACATCAAGTTGGACATCACCTCCC
ACAACGAGGACTACACCATCGTGGAACAGTACGAACGCGCCGAGG
GCCGCCACTCCACCGGCGGCATGGACGAGCTGTACAAGAGCGGAG
GAGGAGGAAGCTATGGTGATAAGGAGAGAAAGGCTGACGCCAAGATG
GTGTGTGATGTGGTGAGTCGGATGGAAGACACCGAGCCCTTCTCTGCAG
AGCTGCTTTCTGCCATGATGCGGCTCTGGGGCGACTCAGGAATCCAAGA
GTGCTTCAACCGGTCCCGGGAGTATCAGCTCAACGACTCTGCCAAATAC
TACCTGGACAGCCTGGATCGGATTGGGGCCGCCGACTACCAGCCCACC
GAGCAGGACATCCTCCGAACCAGGGTCAAAACCACTGGCATCGTAGAA
ACCCACTTCACATTCAAGAACCTCCACTTCAGGCTGTTTGACGTCGGAG
GCCAGCGATCTGAACGCAAGAAGTGGATCCATTGCTTCGAGGACGTCA
CGGCCATCATTTTCTGTGTCGCGCTCAGCGGCTATGACCAGGTGCTCCA
CGAAGACGAAACCACGAACCGCATGCACGAATCCCTGAAGCTTTTTGA
CAGCATCTGCAACAACAAATGGTTCACAGACACGTCCATCATCCTGTTT
CTTAACAAGAAGGACATATTTGAAGAGAAGATCAAGAAGTCCCCGCTC
ACCATCTGCTTTCCTGAATATACAGGCCCCAGCGCCTTCACAGAAGCCG
TGGCTTACATCCAGGCCCAGTACGAGAGCAAGAACAAGTCAGCCCACA
AAGAGATCTACACCCACGTCACCTGCGCCACGGACACCAACAACATCC
AGTTTGTCTTTGATGCTGTGACGGACGTCATCATCGCCAAAAACCTGCG
GGGCTGTGGACTCTACTGAATCCACCCAGCTTTCTTGTACTAG

GNAO1 with mCherry inserted between R113-M114 in pcDNA3.1(-)

ATGGGATGTACTCTGAGCGCAGAGGAGAGAGCCGCCCTCGAGCGGAGC
AAGGCGATTGAGAAAAACCTCAAAGAGGATGGCATCAGCGCCGCCAAA
GACGTGAAATTACTCCTGCTCGGGGCTGGAGAATCAGGAAAAAGCACC
ATTGTGAAGCAGATGAAGATCATCCATGAAGATGGCTTCTCCGGAGAA
GACGTGAAACAGTACAAGCCTGTTGTCTACAGCAACACTATCCAGTCCC
TGGCAGCCATCGTCCGGGCCATGGACACTTTGGGCATCGAATATGGTGA
TAAGGAGAGAAAGGCTGACGCCAAGATGGTGTGTGATGTGGTGAGTCG
G**AGCGGAGGAGGAGGAAGCATGGTGAGCAAGGGCGAGGAGGATAA**
CATGGCCATCATCAAGGAGTTCATGCGCTTCAAGGTGCACATGGAG
GGCTCCGTGAACGGCCACGAGTTCGAGATCGAGGGCGAGGGCGAG
GGCCGCCCCTACGAGGGCACCCAGACCGCCAAGCTGAAGGTGACC
AAGGGTGGCCCCCTGCCCTTCGCCTGGGACATCCTGTCCCCTCAGT
TCATGTACGGCTCCAAGGCCTACGTGAAGCACCCCGCCGACATCCC
CGACTACTTGAAGCTGTCCTTCCCCGAGGGCTTCAAGTGGGAGCGC
GTGATGAACTTCGAGGACGGCGGCGTGGTGACCGTGACCCAGGAC
TCCTCCCTGCAGGACGGCGAGTTCATCTACAAGGTGAAGCTGCGCG
GCACCAACTTCCCCTCCGACGGCCCCGTAATGCAGAAGAAGACCAT
GGGCTGGGAGGCCTCCTCCGAGCGGATGTACCCCGAGGACGGCGC
CCTGAAGGGCGAGATCAAGCAGAGGCTGAAGCTGAAGGACGGCGG
CCACTACGACGCTGAGGTCAAGACCACCTACAAGGCCAAGAAGCCC
GTGCAGCTGCCCGGCGCCTACAACGTCAACATCAAGTTGGACATCA
CCTCCCACAACGAGGACTACACCATCGTGGAACAGTACGAACGCGC
CGAGGGCCGCCACTCCACCGGCGGCATGGACGAGCTGTACAAGAG
CGGAGGAGGAGGAAGCATGGAAGACACCGAGCCCTTCTCTGCAGAGC
TGCTTTCTGCCATGATGCGGCTCTGGGGCGACTCAGGAATCCAAGAGTG
CTTCAACCGGTCCCGGGAGTATCAGCTCAACGACTCTGCCAAATACTAC
CTGGACAGCCTGGATCGGATTGGGGCCGCCGACTACCAGCCCACCGAG
CAGGACATCCTCCGAACCAGGGTCAAAACCACTGGCATCGTAGAAACC
CACTTCACATTCAAGAACCTCCACTTCAGGCTGTTTGACGTCGGAGGCC
AGCGATCTGAACGCAAGAAGTGGATCCATTGCTTCGAGGACGTCACGG
CCATCATTTTCTGTGTCGCGCTCAGCGGCTATGACCAGGTGCTCCACGA
AGACGAAACCACGAACCGCATGCACGAATCCCTGAAGCTTTTTGACAG
CATCTGCAACAACAAATGGTTCACAGACACGTCCATCATCCTGTTTCTT
AACAAGAAGGACATATTTGAAGAGAAGATCAAGAAGTCCCCGCTCACC
ATCTGCTTTCCTGAATATACAGGCCCCAGCGCCTTCACAGAAGCCGTGG
CTTACATCCAGGCCCAGTACGAGAGCAAGAACAAGTCAGCCCACAAAG
AGATCTACACCCACGTCACCTGCGCCACGGACACCAACAACATCCAGTT
TGTCTTTGATGCTGTGACGGACGTCATCATCGCCAAAAACCTGCGGGGC
TGTGGACTCTACTGAATCCACCCAGCTTTCTTGTACTAG

APPENDIX G

CROSS-TALK and BACKGROUND ELIMINATION

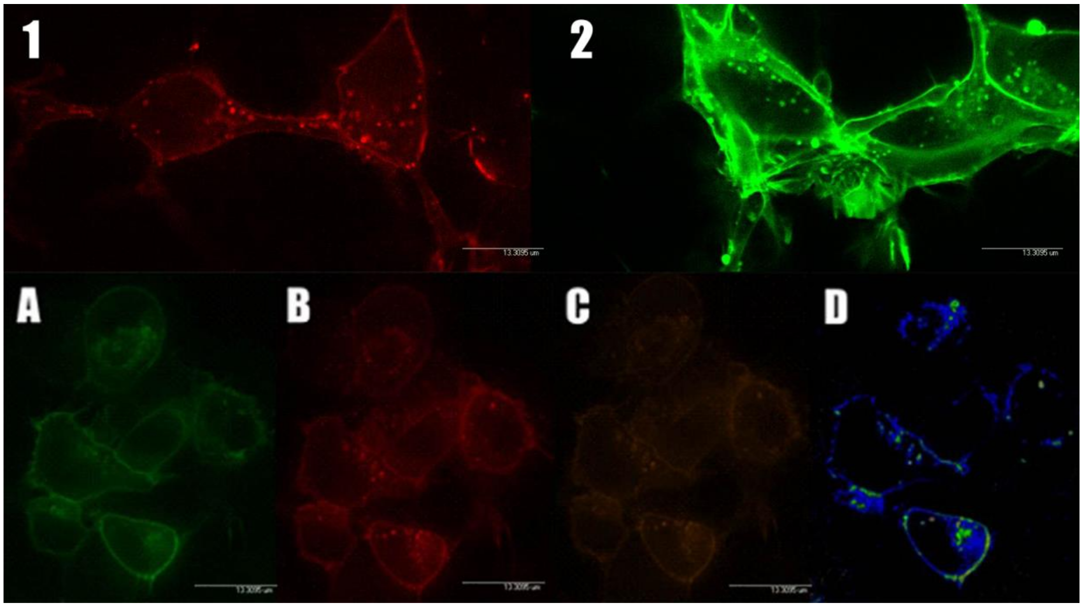

Figure G.1 A sample FRET experiment set up and the FRET signal effciency. (1) GNAI3 tagged with mCherry from its 122nd aminoacid transfected to N2a cells alone. (2) D2R tagged with EGFP transfected to N2a cells alone. (A) N2a cells co-transfected with GNAI3-122-mCherry and D2R-EGFP. Excitation was done with 482 nm (EGFP excitation). Emmision coming from EGFP was collected. (B) N2a cells co-transfected with GNAI3-122-mCherry and D2R-EGFP. Excitation was done with 583 nm (mCherry excitation). Emmision coming from EGFP was collected. (C) FRET Signal. N2a cells co-transfected with GNAI3-122-mCherry and D2R-EGFP. Excitation was done with 482 nm (EGFP exciatiton). Emmision coming from mCherry was collected. (D) FRET signal efficiency.

To get a FRET signal from a co-transfected experiment set-up without background signal, without signals coming from acceptor channel (mCherry) when cells are excited with donor (EGFP) excitation wavelength (i.e. spectral bleed-through - SBT) or vice-versa, different imaging set ups should be used to gather the interfering data and cut them out from the resulting FRET image.

To get the necessary data that causes cross-talk, a FRET experiment set up for investigating two constructs should be prepared as follows: a plate with donor construct which was transfected with the same amount of DNA with the FRET plate (1), another plate with the acceptor construct which was transfected with the same amount of DNA with the FRET plate (2), and a plate with two of the constructs co-transfected to collect FRET signal (A, B, C, and D).

From the 1st and 2nd constructs, the spectral bleed-through amounts and background signals from their own emission channels were calculated by getting two images from each of them which are including;

- (1) donor excitation & donor emission – donor excitation & acceptor emission (overlap between emission spectra of the molecules would cause FRET signal cross-talk when there was no acceptor transfected) for the plate containing the construct with donor molecule to calculate donor's SBT and cancel it out from its normal emission. Background signal coming from these images were also calculated and cancelled.

- (2) acceptor excitation & acceptor emission – donor excitation & acceptor emission (overlap between excitation spectra of the molecules would cause FRET signal cross-talk when there was no donor transfected) for the plate containing the construct with acceptor molecule to calculate acceptor's SBT and cancel it out from its emission. Background signal coming from these images were also calculated and cancelled out.

After these donor and acceptor signal normalizations were done, three images from FRET set-up are gathered, which are including;

- (A) donor (EGFP) excitation and donor emission
- (B) acceptor (mCherry) excitation and acceptor emission
- (C) donor excitation and acceptor emission (FRET signal)

The data gathered from set ups 1 and 2 were aligned with the signals gathered from A and B cases and finally normalized and optimized FRET signal image was output. This image was then processed to see its energy transfer energy as in (D).

APPENDIX H

FURTHER RESULTS OF FUNCTIONALITY ASSAYS

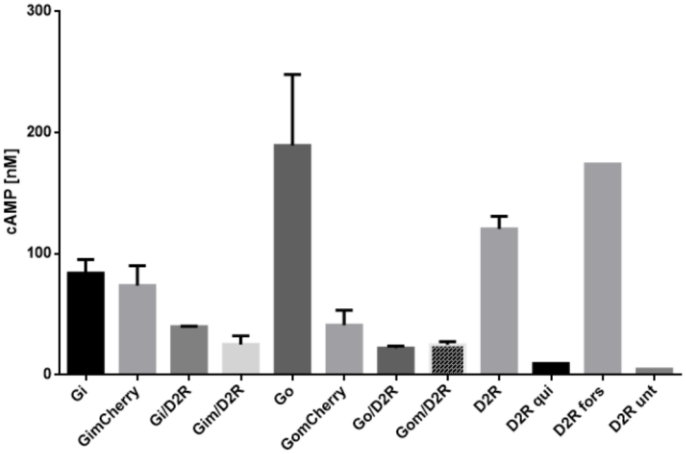

Figure H.1 cAMP levels of N2a cells after transfecting or co-transfecting them with GNAI3 wt, GNAI3 122 mch, D2R wt + GNAI3 wt, D2R wt + GNAI3 122 mch, GNAO1 wt, GNAO1 122 mch, D2R wt + GNAO1 wt, D2R wt + GNAO1 122 mch and D2R wt alone, treated only with quinpirole, forskolin or untreated. (Presented in 3rd term report of TÜBİTAK Project 113Z639)

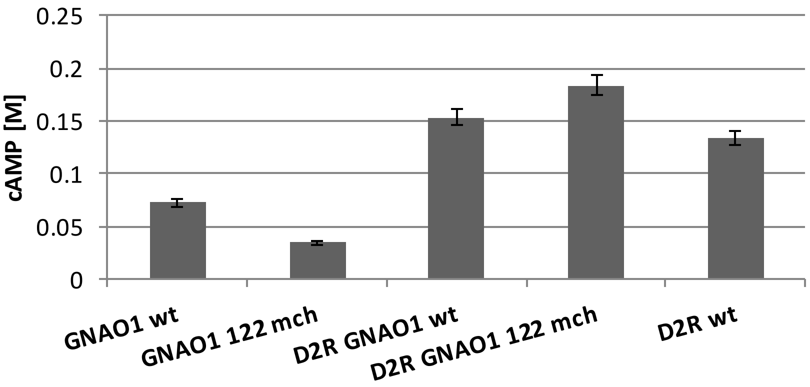

Figure H.2 cAMP levels of N2a cells after transfecting or co-transfecting them with GNAO1 wt, GNAO1 122 mch, D2R wt + GNAO1 wt, D2R wt + GNAO1 122 mch and D2R wt alone.